NOTE TO USERS

This reproduction is the best copy available.

UMI®

DYNAMIC MODELLING AND SIMULATION OF ROTATING BIOLOGICAL CONTACTORS

By

HAFIZ M. ABDULLAH

BSc Chemical Engineering, University of the Punjab, Pakistan 1995
MSc Chemical Engineering, University of the Punjab, Pakistan 1997

A Thesis

presented to Ryerson University

in partial fulfillment of the

requirement for the degree of

Master of Applied Science

in the program of

Chemical Engineering

Toronto, Ontario, Canada, 2004

Borrower's Page

Ryerson University requires the signatures of all persons using or photocopying this thesis. Please sign below, and give address and date.

1.....

2.....

3.....

4.....

5.....

6.....

7.....

8.....

9.....

10.....

11.....

12.....

13.....

14.....

15.....

DYNAMIC MODELING AND SIMULATION OF ROTATING BIOLOGICAL CONTACTORS

MASc Chemical Engineering 2004

Hafiz Muhammad Abdullah

Department of Chemical Engineering

RYERSON UNIVERSITY

ABSTRACT

Rotating Biological Contactor is a remediation technology used in the secondary treatment of wastewater (domestic and biodegradable industrial wastes). In this work, a mathematical model for rotating biological contactors (RBC) is presented, which encapsulates the consumption of soluble substrate in the developed bio-film attached to the disk of a rotating biological contactor. The model describes the consumption of the substrate and oxygen in the bio-film, and in the trough assuming the liquid in the trough is completely mixed, and the rates of substrate and oxygen utilization within the bio-film follow Monod kinetics. The numerical solution of the model agrees with the experimental data reported by other workers. The simulation also predicts the performance of RBCs in the event of any fluctuations in the flow rate and concentration of the soluble BOD_5 in the influent wastewater stream. The developed model can be used in the future to aid in the optimization of the performance of RBCs.

Acknowledgements

My sincere appreciation goes to Dr. Manuel Alvarez Cuenca, and Dr. Simant R. Upreti, my advisors, who made this technological and scientific challenge a reality. My gratitude also goes to Dr. Manuel Alvarez Cuenca and Dr. Simant R. Upreti for the supervision, support and the time that they afforded to the success of this work. Their academic guidance is invaluable. My deep gratitude also goes to Dr. Ali Lohi for providing the partial financial support during the course of my study.

My thanks also go to the faculty members and staff of the Department of Chemical Engineering for their contribution to my career development during my program in the University.

I deeply thank my colleagues Sajjad Yasin, Baranitharan Sundraram, Zafar Khan, Adnan Khan and Mujahid Shah for their friendship and emotional encouragement.

I especially owe to my mother, brothers and sisters for their true understanding of my time who always support me with their love to spur my spirits up in return.

Dedicated to

Muhammad Akhtar Khawaja

A tribute to my father, who is ever alive in my heart as he used to be before, a comforting shoulder to rest my head in the long summer afternoons

TABLE OF CONTENTS **PAGE**

LIST OF TABLES

LIST OF ILLUSTRATIONS

NOMENCLATURE

A	Disk surface area (m^2)
$C_{sbod,BF}$	Concentration of soluble substrate in the bio-film (g/m^3)
$C_{O2,BF}$	Concentration of oxygen in the bio-film (g/m^3)
$C_{sbod,in}$	Concentration of soluble substrate in the influent wastewater (g/m^3)
$C_{sbod,T}$	Concentration of soluble substrate in the trough (g/m^3)
$C_{O2,T}$	Concentration of oxygen in the trough (g/m^3)
$C_{O2,in}$	Concentration of oxygen in the liquid film (g/m^3)
F	Volumetric flow rate of the influent wastewater (m^3/hr)
k_{sbod}	Mass transfer coefficient of substrate from liquid to bio-film (m/hr)
K_{sbod}	Substrate half saturation constant (g/m^3)
k_{O2}	Mass transfer coefficient of oxygen from liquid to bio-film (m/hr)
K_{O2}	Oxygen half saturation constant (g/m^3)
M_{sbod}	Mass of the soluble substrate transferred (g/hr)
M_{O2}	Mass of oxygen transferred (g/hr)
RBC	Rotating biological contactor
r_{sbod}	Rate of substrate consumption in the bio-film ($g/m^3.hr$)
r_{O2}	Rate of oxygen consumption in the bio-film ($g/m^3.hr$)
μ	Specific growth rate of attached biomass (1/hr)
μ_{max}	Maximum specific growth rate (1/hr)

V	Volume of the trough (m^3)
X	Specific concentration of attached biomass (g/m^3)
Y	Yield coefficient for attached biomass (g cells produced/g cells consumed)

CHAPTER 1 INTRODUCTION

1.1 Brief history of the rotating biological contactors

In the last two decades, Rotating Biological Contactors (RBCs) have been consolidated as one of the most remarkable technologies in domestic and industrial wastewater treatment. Thousands of installations in North America, Europe, and Japan show the extraordinary interest that this process has attracted among wastewater treatment professionals and equipment manufacturers [1].

In 1975, the Comptroller General of the United States issued a report to the Congress entitled "*Potential of Value Analysis for Reducing Waste Treatment Plant Costs*". This report, prepared by several teams of experts from the U.S. Environmental Protection Agency, focused on new advanced technologies and identified RBCs as: "The major development most often mentioned... in light of recent technical progress, the teams foresaw few problems with use of this treatment process in lieu of activated sludge and recommended strong consideration of this process" [1].

Rotating biological contactors (RBCs) were first installed in West Germany in 1960 and later introduced in the United States. Hundreds of RBC installations were installed in the 1970s, and the process has been reviewed in a number of reports [2].

The history of RBC installations has been troublesome due to inadequate mechanical design and lack of understanding of the biological process. Structural failure of shafts, disks, and disk support systems has occurred in some installations. Development of excessive growth and sloughing problems has also led to mechanical shaft, bearing, and

disk failures. Many of these problems were related to a lack of conservatism in design and scale-up issues from pilot-plant to full-scale units [3].

The development of RBC technology in Canada has applications in the following areas:

1. Treatment of industrial wastewater
2. Municipal wastewater treatment
3. Landfill leachate treatment.

In 1973, the Ministry of the Environment of Ontario undertook the evaluation of an RBC to treat municipal wastewater. The design basis for such evaluation was the production of a secondary quality effluent i.e. 15 mg/l BOD_5 and suspended solids. A literature survey carried out by the Ministry of the Environment of Ontario report indicated that a secondary effluent quality could not be expected from a Rotating Biological system, treating domestic waste, when organic loading exceeds 1 lb/day/1000 ft^2 BOD_5. The results of the study concluded that secondary quality effluent could only be achieved when the organic load is limited to about 1 lb/day/1000 ft^2 disk area. Present RBCs can achieve that secondary effluent quality with organic loads well above 2.5lb/day/1000 ft^2 [3].

1.2 Role of the RBC technology

The emergence of RBC technology in the last thirty years comes as a result of comparative evaluations with respect to other biological treatment systems. This technology involves allowing wastewater to come in contact with a biological medium in order to facilitate the removal of contaminants. In its simplest form, disks or media blocks mounted on a horizontal shaft of a rotating biological contactor are driven so that the media rotates to the flow of sewage.

A biological slime grows on the media when conditions are suitable. The slime is rotated into the settled wastewater, and then into the atmosphere to provide oxygen for the organisms. The wastewater being treated either flows parallel or perpendicular to the shaft as it flows from one stage to another. As the drum rotates, the media pick up a thin layer of wastewater, which flows over the biological slimes on the disks. Organisms living in the slimes use organic matter from the wastewater as substrate and dissolved oxygen from the air, thus removing organic content from the water being treated. As the attached slimes pass through the wastewater, some of the slimes are sloughed from the media. The effluent with the sloughed slimes flows to the secondary clarifier where the slimes are removed from the effluent by gravity settling.

The RBC process is usually divided into four different stages. Staging is used in order to maximize the effectiveness of a given amount of media surface area. Organisms on the first stage media are exposed to high levels of BOD_5 and reduce the BOD_5 at a high rate. As the BOD_5 levels decrease from stage to stage, the rate at which the organisms can remove BOD_5 decreases and nitrification starts. Rotating biological contactor units are usually covered for the following reasons [3]:

1. To protect biological slime growths from freezing
2. To prevent intense rains from washing off some of the slime growths
3. To stop exposure of media to direct sunlight to prevent growth of algae, and which may cause the media to become brittle
4. To provide protection for operators from sun, rain, snow or wind while maintaining equipment.

1.3 Advantages of the RBC process

RBC process has some major advantages over other more conventional water treatment processes. These advantages are [3]:

1. Low energy consumption up to 20% of that used by activated sludge for the same application.
2. Easy maintenance and mechanical simplicity, hence lower operating costs.
3. Good recovery from organic and hydraulic surges because of its micro fauna diversity.
4. Low floor space requirement and because of its modular configuration, greater design flexibility.
5. Low sludge production
6. Faster recovery from toxic shocks is achieved in RBC than in slurry reactors or activated sludge processes because of its biomass short residence time.
7. No need for biomass control.
9. Low noise and odour emissions.

1.4 Limitations of the RBC process

RBC process failure have resulted due to the following [3]:

1. Structural failure of the shaft, media, or media support systems.
2. Less than anticipated treatment performance.
3. Excessive development of nuisance organisms.
4. Development of excessive or uneven biomass growth, and
5. Inadequate performance of air-drive systems for shaft rotation.

Primarily, these process failures have been attributed to [4]:

a. Misapplication of the process or use of inadequate design criteria.
b. Original designs for shafts and media support systems that were inadequate.
c. Inadequate upstream treatment.
d. Failure to consider the effect of side stream loadings in the process design.
e. Lack of a thorough understanding of the long-term performance efficiency and characteristics of the process in full-scale use.
f. The development of design standards and criteria on the basis of limited data, much of which was developed using small scale systems, and
g. The general lack of a conservative approach in developing design relationships for the process.

For the successful application of the process, proper sizing and process design, a conservative and flexible design approach, and careful consideration to the specification of materials and components are necessary [4].

1.5 Physical description

An RBC consists of series of circular plastic disks as media, attached to and supported by a horizontal rotating shaft and placed in a trough. The circular disks made of styrofoam or polyethylene are partly submerged in wastewater [5]. The shaft is rotated by drive equipment that consists of a motor, gear reducer, and chain drive. The main shaft is supported by two main bearings. Since the RBC has few moving parts, it requires relatively minor amount of maintenance. All that is required is to keep the chain, reducer,

shaft bearings, and motor well lubricated, and the chain and belt drive systems well aligned and with proper amount of tension. Maintenance procedures that are in accordance with the manufacturer's recommendations should be adopted for maintenance and lubrication.

1.6 Functional description

Figure 1.1 shows the flow chart of the biological treatment process and figure 1.2 provides a graphic representation of the process. During rotation, the disk of the Rotating Biological Contactor carries the biomass and a film of wastewater into the air where oxygen is absorbed. The dissolved oxygen and organic materials in the wastewater diffuse into the biomass, and are then metabolized into additional biomass, carbon dioxide and water. During this process, either oxygen or the substrate could be the limiting reagent, which can limit the rate of reaction. The supply of food and nutrients in appropriate concentrations is necessary for cell syntheses to increase the rate of substrate consumption. Excess biomass shears off at a steady rate as the media rotates. These solids are carried through the RBC process for subsequent removal in a conventional clarifier. An inter-stage baffle is used to separate the shaft into different stages. RBCs are covered to protect biomass from freezing as the reduction of biological activity, and a decrease in BOD_5 removal occurs at low temperatures.

The RBC process is typically configured with several stages arranged in series, with one or more shafts composing each stage and with one or more parallel trains of shaft stages

Figure 1.1: Flow chart of the biological treatment process

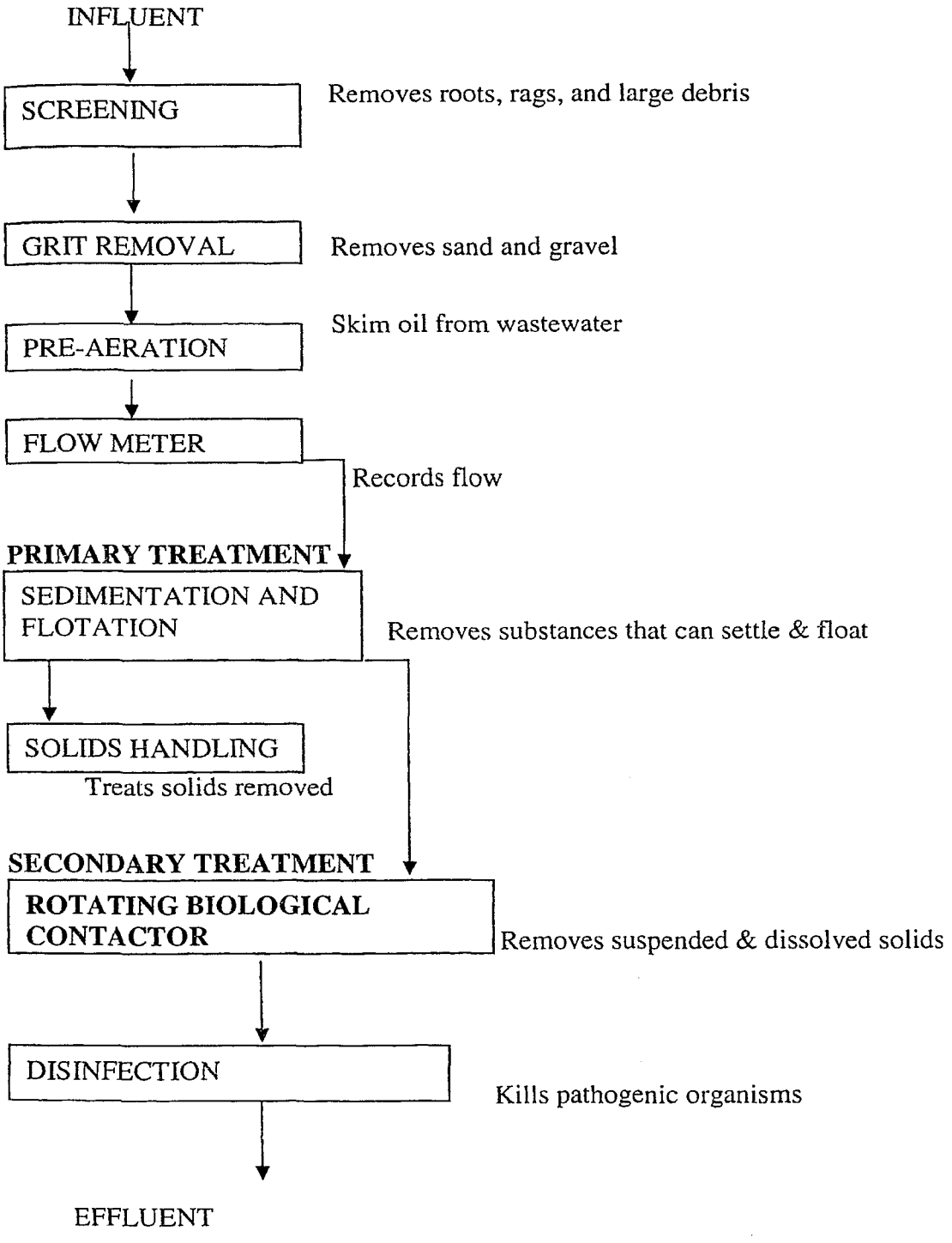

Figure 1.2 General representation of RBC process [4]

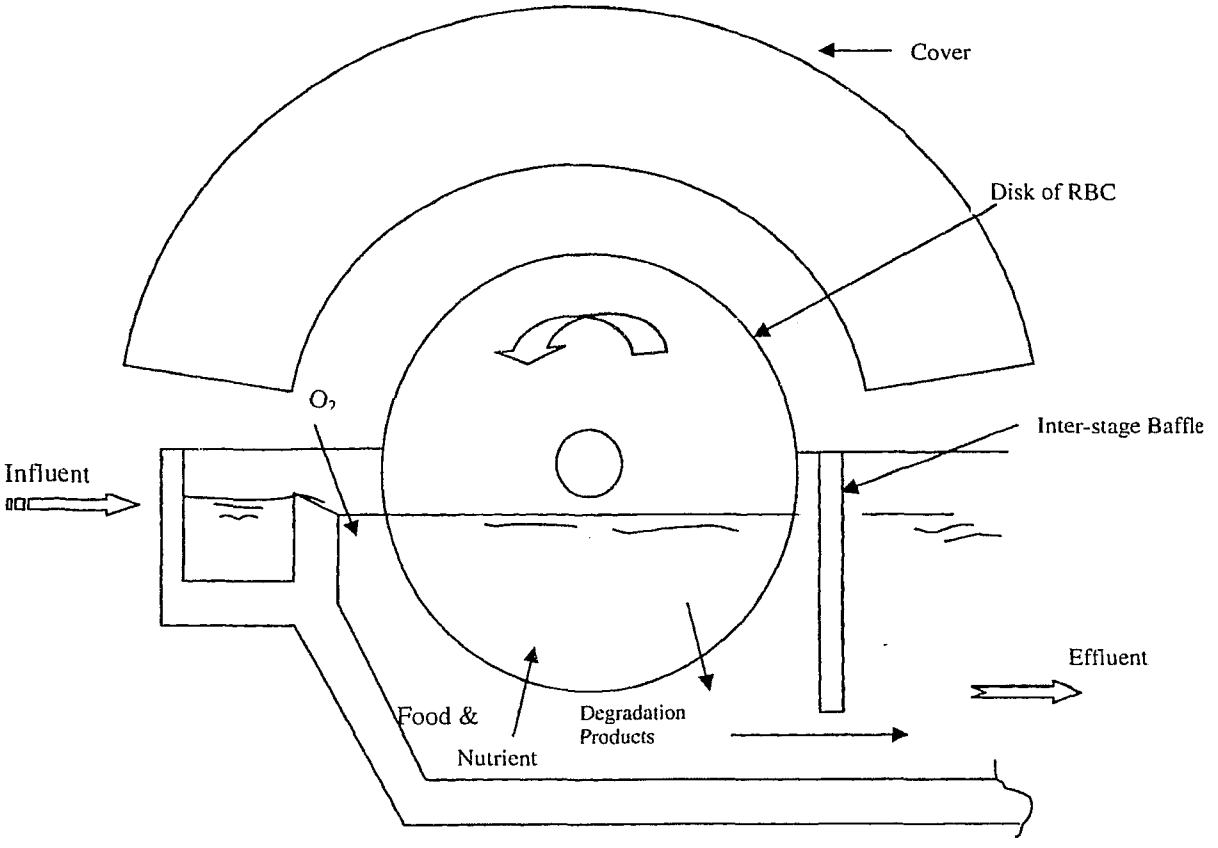

to provide the needed surface area. The number of stages required depends on the degree of treatment desired, with one or two stages provided for roughing applications, two to four stages for BOD_5 removal and six or more stages provided where advanced treatment with nitrification is necessary. Figure 1.3 shows the general arrangements typically used for the RBC process [2].

RBC shafts are placed parallel to the direction of the flow path with each stage separated by baffles as shown in Figure 1.3 (a). In larger installations, shafts are mounted perpendicular to flow with several stages in series to form a process train. Figure 1.3 (b) represents this type of arrangement. To handle the loading on the initial units of the RBCs in larger installations, the step feed arrangement as shown in Figure 1.3 (c) is used. For situations in which upsets in the initial units of RBCs are more likely, a tapered system as shown in Figure 1.3 (d) is used. This flow arrangement helps maintain hydraulic fluctuations in larger installations. Also, the units can be isolated for shutdown or maintenance purposes. Treatment systems applying RBC technology have been used for BOD_5 removal, pretreatment of industrial wastewater, combined BOD_5 removal and nitrification, tertiary nitrification, and de-nitrification [2].

1.7 The biodegradation process

The use of bacteria to consume carbonaceous material has been a method of water purification for a very long time. Scientists have learned which operating conditions must be set to increase the efficiency of this process. Advancements in industrial processes have led to the production of complex organic and inorganic molecules.

Figure 1.3 RBC process general flow arrangements

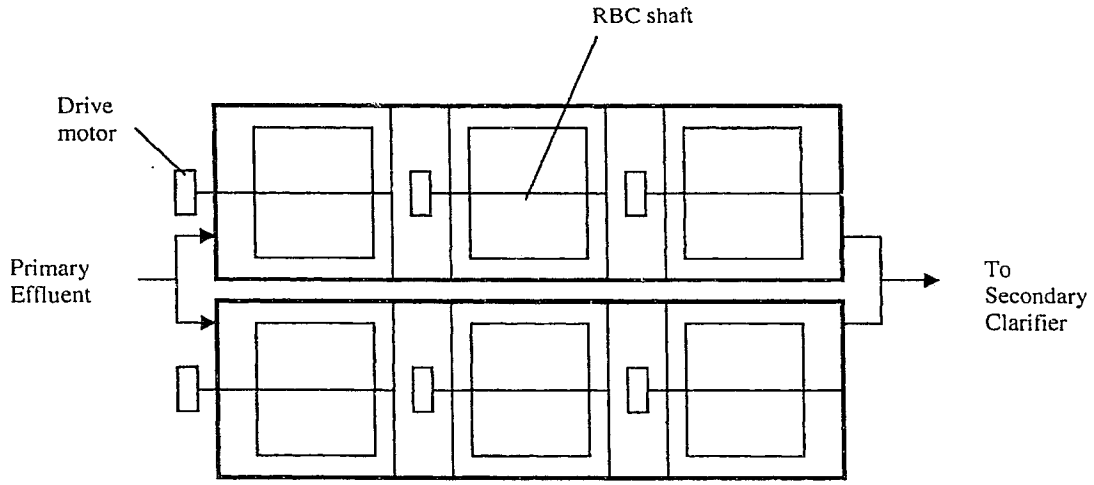

Figure 1.3 (a) Flow parallel to the shaft [2]

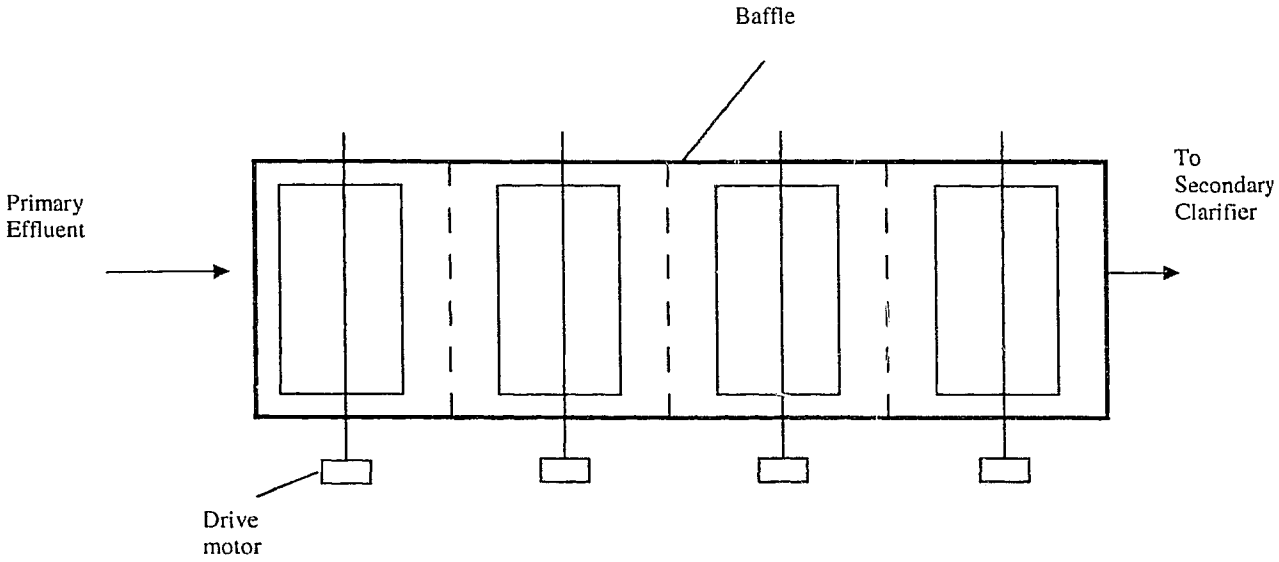

Figure 1.3 (b) Flow perpendicular to the shaft [2]

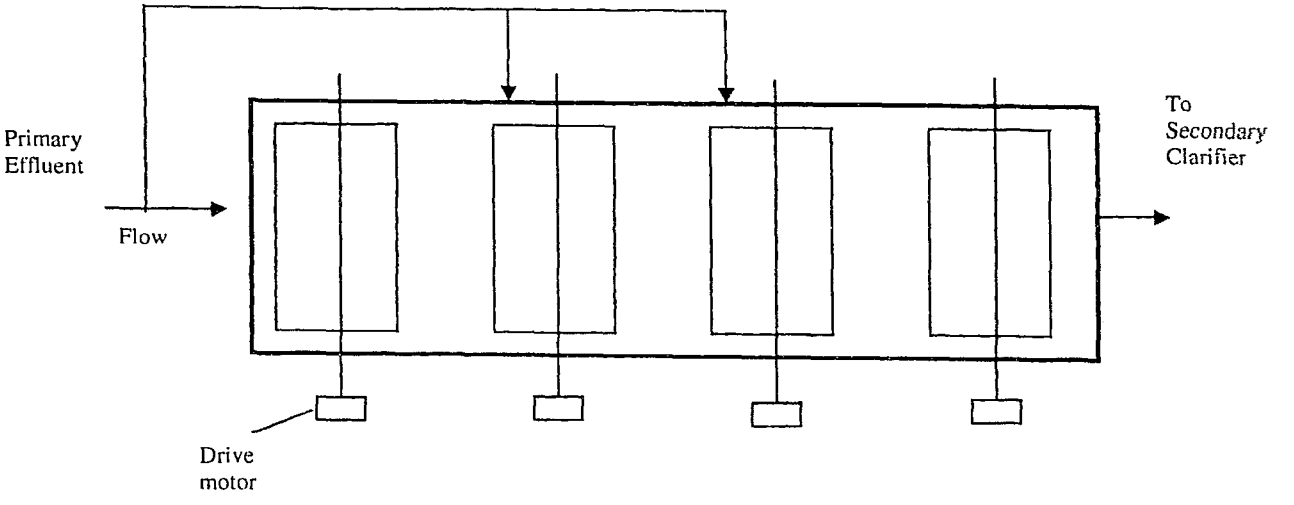

Figure 1.3 (c) Step feed flow [2]

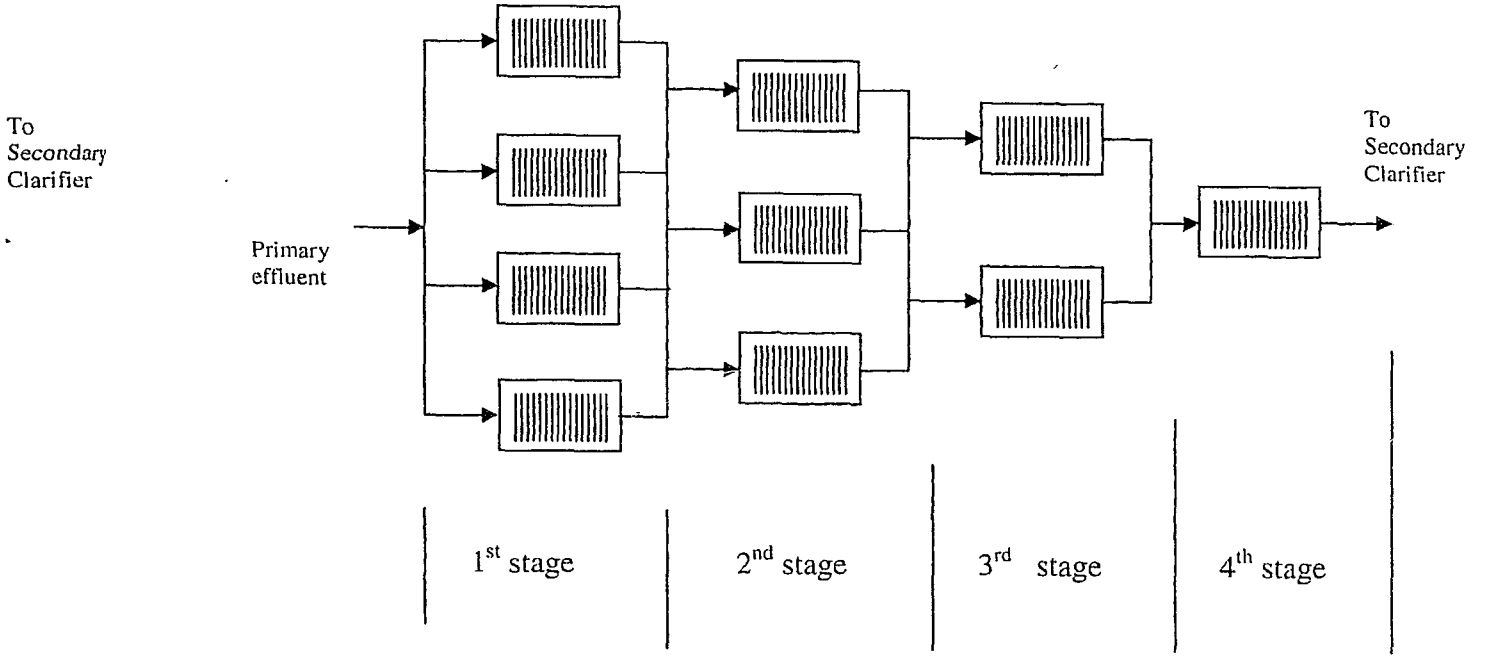

Figure **1.3 (d) Tapered feed flow parallel to the shaft [2]**

The size of these molecules, coupled with their strong bonds, allows them to pass through conventional biological treatment. This section will discuss the important concept of biological degradation, which is an inexpensive alternative process in the wastewater and water treatment industry.

1.7.1 Microorganisms

Microorganisms can be found almost anywhere, provided there is a food source and water to sustain life. Reproduction occurs mainly through binary fission, although some cases of sexual reproduction and budding have been noted. Since there are thousands of bacterial species, they have been subdivided into three categories based on their shape [6]. These are:

1. Spherical (0.5 – 1 μ in diameter)
2. Cylindrical (0.5 – 1 μ in diameter by 1-3 μ in length)
3. Helical (0.5–5 μ in width by 6 – 15 μ in length)

The temperature ranges at which they thrive, are given by

1. Cryophilic bacteria live in environments between –2 to 30 °C
2. Mesophilic live in environments between 20 to 45 °C
3. Thermophilic live in environments between 45 to 75 °C

1.7.2 Nutrient requirements

It is a well-established fact that chemical reactions are limited by the lack of one reactant, the limiting reagent. In the case of aerobic biodegradation, it is easy to assume that the limiting reagent is either oxygen or the substrate. However, cell syntheses also require

inorganic nutrients, which are often lacking in industrial effluents. This requirement limits the rate of cell growth and substrate removal. As such, it is often necessary to supply these nutrients in appropriate concentrations in order to maximize the rate of biological degradation [7].

CHAPTER 2 PROCESS DESIGN CONSIDERATION

2.1 Design and operating parameters

Soluble and particulate carbonaceous BOD_5 components of wastewater are reduced in an RBC process by a combination of oxidation by the attached bio-film and synthesis into new cell mass. While designing RBCs, it must be ensured that soluble waste components, nutrients, and oxygen should be transferred to the bio-film from the bulk liquid, and degradation products should be transferred from the bio-film to the bulk liquid. Furthermore, particulate waste components must be enmeshed by the bio-film and hydrolyzed before degradation can occur. For the overall process to work successfully, the proper environmental and process conditions must be present [4].

Some disadvantages observed in the past, like shaft failure of biomass overload, have largely been overcome by better control and operation. At the same time, kinetics, microbial growth, oxygen mass transfer mechanisms, and fluid flow behaviour in RBCs are not well known. Thus, the impact and nature of operating and design parameters are often qualitative. Following are the most related variables [3]:

1. Nature of the influent

- Biochemical Oxygen Demand, BOD_5.
- Chemical Oxygen Demand COD.
- Dissolved Oxygen, DO.
- pH
- Total suspended solids, TSS.

- Total volatile suspended solids, TVSS.
- Temperature [3].

2. Wastewater flow rate

- Residence Time
- Type of reactor (Plug flow, CSTR, Dispersion) [3].

3. RBC: Operation and design

- Disk surface area and geometry.
- Disk submergence, spacing, and rotational speed.
- Feeders' configuration.
- Staging.
- Recirculation [3].

4. Nature of microbial population

- Distribution of the micro fauna.
- Pathogens removal [3].

2.2 Principal process design parameters

Water Environment Federation [4] lays out the following RBC process design considerations:

2.2.1 Media surface area

Adequate media surface area is essential to the RBC process to provide sufficient bio-film for the effective treatment of the biodegradable waste, and produce specific substrate

use rate (for example, the mass of BOD_5/unit time/unit media surface area). This rate must be matched by the oxygen transfer capability of the system, because the concentration of substrate, oxygen or both can limit the substrate removal rate. Sufficient media, and proper operational modes, like rotation of disk and additional oxygen supply through diffusers, are necessary to reduce the potential for nuisance organism development and to limit excessive bio-film buildup that could lead to structural damage to the shaft or media [4].

The selection of the media surface area to meet design objectives is a balance between a conservative assessment of the capability of the process and economics. Because higher specific substrate consumption rates occur at higher bulk wastewater substrate concentrations, staging the process can provide the same degree of treatment that could be provided by a single stage system having a larger surface area. Care should be taken, however, so that loading to the first stage is not high enough to cause inadequate oxygen transfer, nuisance organism development, overweight shafts, and associated process problems [4].

2.2.2 pH and nutrient balance

As with any biological treatment process a proper pH and nutrient balance must be provided for effective treatment by the RBC process. Where nitrification is required, optimum performance has been observed at a slightly alkaline pH, with the optimum pH being 7.5 to 8.5 for suspended growth systems [8]. For RBC systems, nitrification rates have been reported to fall off rapidly, with decreasing pH from 7.0 to 6.0 [9]. Well-acclimated RBC systems, where pH is maintained in a narrow range, may be able to

tolerate pH values somewhat below 7.0. However, with the minimal buffering at this pH, a stable pH is difficult to maintain.

As microorganisms providing treatment require nutrients for cell growth, an adequate supply of available nutrients is necessary for the proper performance of the RBC process. A minimum mass ratio of 100:5:1 (BOD_5: nitrogen: phosphorus) is typically used [4].

2.2.3 Toxic and inhibitory substances

Toxic and inhibitory substances, for example, nickel, iron, etc., if present in sufficient concentration in plant influent, have a negative effect on wastewater treatment. In addition, excessive quantities of such substances may have a deleterious effect on solids management and effluent quality because of pass-through. The review of design data from current technical literature is helpful, for information on such substances, if they are suspected of being present in concentrations that are deleterious to biological systems [4].

2.2.4 Oxygen transfer

The rate of oxygen transfer must be sufficient to maintain fully aerobic conditions in the RBC process. Organic loadings above the oxygen transfer capability of the system could result in reduced performance, odors, and development of nuisance organisms. Maximum oxygen transfer rates of 6.8 to 7.3 g oxygen/m^2.d (1.4 to 1.5 lb/d/1000ft^2) have been reported [10] based on tests conducted with full scale, mechanical-drive systems. Studies of supplemental aeration applied to a mechanical-drive RBCs indicate an oxygen-transfer efficiency of 2 to 2.5% for applied air [11].

Historically, pilot testing of the RBC process was performed using small-scale units operating at the same media peripheral velocity (approx. 18 m/min [60ft/min]) as full-scale units [4]. Data on process performance collected on small diameter units can be misleading because of the higher oxygen-transfer capability of the smaller units compared to full scale units. In one study [12] it was estimated that a 0.5 m diameter test unit provided an oxygen transfer rate 1.6 times that of a 3.2 m diameter unit that was also tested. Other researchers noted similar scale-up problems as well [9]. For these reasons, data collected on small-scale systems can only be used for treat-ability considerations, and not to establish sizing criteria [4].

2.2.5 Flows and loading variability

Manufacturers of RBC equipment have recommended maximum organic loadings to the first stage of RBC systems of approximately 20 g soluble $BOD_5/m^2.d$ (4 $lb/d/1000ft^2$) of media. This equates to the organic loading of 39 g $BOD_5/m^2.d$ (8 $lb/d/1000ft^2$) on a total BOD_5 basis for a typical domestic wastewater with 50% soluble BOD_5/BOD_5 in the primary effluent [4]. However, a survey of 23 plants indicated nuisance organism development because of oxygen limiting conditions for first stage loadings in excess of approximately 31.2 g $BOD_5/m^2.d$ (6.4 $lb/d/1000ft^2$) of media [13]. Another manufacturer [14] recommends maximum first stage loadings of 12 to 20 g soluble $BOD_5/m^2.d$ (2.5–4.0 $lb/d/1000ft^2$). The designers considered limiting organic loading to approximately 29 g $BOD_5/m^2.d$ (6 $lb/d/1000ft^2$ total BOD_5 basis) to any RBC stage. These criteria limited loadings to levels within the oxygen transfer capability of the system and the growth of nuisance organisms [4].

Typically, higher effluent concentrations during the higher loading periods of the day are counterbalanced by lower effluent values during low loading periods. A high degree of variability in influent flow or organic loading, however, may disrupt the RBC process. The designer should be aware of the variability in organic loadings, including the effect of recycle loads from solids processing unit operations. Providing flow equalization may compensate for both flow and loading variability and eliminate the requirement for additional RBC tank-age and media [4].

2.2.6 Solids production

The estimation of excess solids production is necessary for the sizing of the solids-handling facilities of the plant. Solids production in the RBC process is a function of synthesis of new cell mass, cell mass decay caused by endogenous respiration and solids loss from the system caused by total suspended solids in the process clarified effluent. In general, solids production from the RBC process is expected to be similar to fixed film processes [4].

CHAPTER 3 REVIEW OF THE MATHEMATICAL MODELS OF THE RBC

3.1 RBC models: state of the art

A number of mathematical models have been developed to describe the kinetics of substrate utilization in RBC units. These models can be divided into four categories according to the criteria on which they are based [15]:

3.1.1 Models based exclusively on empirical observations

The manufacturers of bio-disk plants have themselves developed empirical design methods based on curves derived from data gathered in their plants. These curves are used for plants designed to treat domestic wastewater or common industrial wastewater. These curves cannot predict the behaviour of other plants or even of the same plant in different operative conditions from those experimentally studied. If the feed, temperature, number of stages, type of disk, and other operative characteristics fall within the specified parameters, these curves are to be regarded as reliable [15].

3.1.2 Models based on reaction order and substrate diffusion through bio-film

In the simplest models of these types, it is assumed that the substrate removal follows an experimentally determined kinetic order. The more developed models also take into account the transport of nutrients and oxygen within the layer of attached biomass, thus modifying the constants, and the order of reaction. The procedure established for these models [7,16] is as follows:

- Define the order of reaction within the layer of biomass,

- Identify the limiting substrate,
- Determine whether the bio-film is wholly or partially active,
- Modify the order of reaction accordingly.

These models actually are semi-empirical, and not widely used because they can predict the behavior of the reactor only within the ranges of data calibration, and hence only for highly specific operating conditions [15].

3.1.3 Models based on microbial growth kinetics

In these types of model, the substrate removal is described by correlating its concentration in the reactor with the microorganism growth rate [17]. A Monod-type expression is adopted and inserted into the substrate mass balance. This means that such models can be used for any limiting substrate, and hence for both carbon removal and nitrification. It also means, however, that the kinetic constants must be separately determined for each individual stage and each individual substrate. The models of this type were developed to describe the removal of substrate by attached-biomass systems [18,19]. Experimental testing of these models demonstrated their validity, and confirmed their capacity to use data obtained in a wide range of organic loading rates [20].

The greatest limitation of these types of models lies in the underlying assumption that the only limiting factor for microbial growth is substrate concentration itself. The availability of required oxygen is thus taken for granted, which makes the result uncertain when organic loading rate is comparatively high and oxygen supply to the microorganisms may become insufficient and hence limiting, as often occurs in the first disks of a large RBC treatment unit. These models are therefore unreliable for high organic loading rate or in any case for the concentrations of dissolved oxygen lower than 1–2 mg/l [15].

3.1.4 Models based on micro organisms kinetic growth and mass transport in the bio-film

Far more complex models have been developed with a view to solving the problems of insufficient oxygen transport, and the simultaneous utilization of more than one substrate [21,22]. These models take into account the different conditions in the several layers of attached biomass and the diffusion of all the substrates through them, the mechanisms of oxygen transport, the various phenomena underway in the different areas of the disk during its phases of immersion and emersion, the layer of liquid film, and thus the disk rotational speed [15].

Another model [20] developed from and by simplifying previous model [23], provides a good example. The laboratory-scale application of this model may be particularly useful with a view to predicting the organic loading rate at which limitation in oxygen transfer occurs. Such information is very useful in the scale-up process of constructing a treatment plant, usually by means of a pilot plant of intermediate size. Its actual use appears awkward due to both the complex mathematical operation involved and the quantity of experimental tests and data required [15]. Some of the important research contributions that have been reviewed are as follows:

Williamson & McCarty [17,24] presented and verified a model of substrate utilization by attached microorganisms that considers the effects of substrate diffusion to the bio-film from the bulk liquid and, subsequently, through the bio-film to the reaction site. The fundamental principles of substrate transport and reaction described in their model have served as the basis for a number of more complex models of substrate utilization by attached microorganisms. Also, bio-film models have become more advanced [17,20,24,25], and can be used to calculate the unsteady state utilization of multiple

substrates by several types of microorganisms growing on the same media. Few of these models have been applied specifically to a particular attached growth wastewater treatment such as the RBC processes. This is because the bio-film models incorporate a large number of parameters, many of which are difficult to measure [26,27].

It should be noted that numerous empirical models have been proposed that predict the steady state removal of substrate in a rotating biological disk reactor in terms of the operating variables [28,29]. In these models, the removal of substrate per stage is written as a power function of operating and design variables such as feed rate, feed concentration, retention time, disk area, disk diameter, disk speed, and temperature. The removal rate constant, and the coefficients in the models are obtained by the regression analysis of experimental data.

Finally, several researchers have studied the physical transfer mechanism of oxygen from air to water in RBCs. Some researchers [30–32] suggested that the oxygen transfer process in the water film on the RBC disk affects the overall performance of the process because the treatment efficiency depends on the oxygen capacity of water.

3.2 Summary of different mathematical models:

3.2.1 Kornegay model

This model [33] ignored the aerated and submerged sectors, and assumed that the entire bio-film was exposed to the substrate concentration in the bulk liquid. It also assumed that the rate of substrate removal by suspended cells in the trough of the RBC was negligible. The effects of mass transfer were accounted for by assuming that the Monod

half-saturation coefficient was a function of the rotational speed of the disks. This was equivalent to making the overall effectiveness factor dependent on the substrate concentration, and half-saturation coefficient [34].

3.2.2 Gujer model

Gujer and Boller [22] developed a model that incorporated carbon oxidation, nitrification and denitrification. Surface shear of the bio-film was also included, allowing the bio-film thickness to be an output from the model. The rotating biological contactor was modeled as a series of CSTRs with the reactions occurring only in the submerged sector. The model was able to predict the effect of organic substrate biodegradation on nitrification, and represents a significant step in the modeling of all possible events in RBC, though it did not include the effects of disk rotational speed [34].

Gujer and Boller [22] considered two surface reactions, flocculation and shear, which they thought to be important in RBC systems. They chose simple mathematical rate equations due to the lack of detailed understanding of these processes. Flocculation was modeled as a first order process; the flux of particulate material from the reactor bulk liquid to the surface of the bio-film was considered. Shear from the bio-film surface to the reactor bulk liquid was modeled as a process dependent on the bio-film thickness and the concentration of the particulate component at the surface of the bio-film [34].

3.2.3 Watanabe model

Watanabe [27] developed a mathematical model for carbon oxidation, nitrification and denitrification providing a number of empirical relationships. While a direct solution technique was used, the kinetics were simplified, with zero order intrinsic kinetics being

assumed for both nitrification and denitrification, giving overall half order reaction rates when substrate transport was considered. In addition, an empirical relationship was employed to estimate the distribution of heterotrophic and autotrophic biomass in the bio-films. The model also assumed that the oxygen flux into the bio-film was independent of the composition of the microbial community, so that the use of oxygen by the microbial community would depend upon their distribution in the bio-film [34]. The biofilm kinetic was developed under the following assumptions:

1. The bulk liquid is completely mixed.
2. Molecular diffusion of substrates occurs through the diffusion layer
3. Molecular diffusion of substrates with a simultaneous zero order biochemical reaction occurs within the biofilm.

The substrate flux through the diffusion layer was given by the following equation.

$$F_b = \left(\frac{D_w}{L_d}\right)(C_b - C_s) \qquad (1)$$

In this equation, F_b is the substrate flux ($g/m^2.h$), D_w is the molecular diffusion coefficient of the substrate (m^2/h), L_d is the diffusion layer thickness (m), and C_b, C_s are the concentrations of the substrate in the bulk liquid and at the biofilm surface respectively (g/m^3).

3.2.4 Hansford model

Hansford [35] developed both dynamic and steady state models for the rotating biological contactor. It had many similarities to the model of Grady and Lim [36]. Hansford model recognized two sectors, submerged and aerated, and that a rotating disk carries a liquid film from the trough into the aerated sector as it turns. The major difference between this

model and one of Grady and Lim [36] was, Hansford model assumed that the substrate concentration in the bio-film was independent of depth. Further Hansford model assumed that the reaction takes place only in the bio-film rather than in both the bio-film and bulk liquid, and the thickness of the liquid film in the aerated sector was assumed to be constant [34].

Hansford provided the dynamic equations for the substrate removal considering an elemental volume ΔV_L fixed in space at position θ. Mass balance of substrate in the liquid film is given by

$$\frac{dc_1}{d\theta} = -\frac{k_L}{2\pi N\delta_L}(c_1 - c_2) \qquad (2)$$

In this equation, c_1 is the substrate concentration in liquid film (g/m^3), c_2 is the substrate concentration in the biofilm (g/m^3), k_L is mass transfer coefficient between liquid film and biofilm (m/h), N is the disk rotational speed (h^{-1}), δ_L is the thickness of liquid film (m), and $\Delta\theta$ is the elemental angle.

Mass balance of substrate in the biofilm on the exposed portion of the disk at steady state is given by

$$\frac{dc_2}{d\theta} = \frac{k_L}{2\pi N\delta_B}c_1 - \left[\frac{k_L}{2\pi N\delta_B} + \frac{\hat{\mu}X}{2\pi NY(K_c + c_2)}\right]c_2 \qquad (3)$$

In this equation, X is the specific microorganism concentration attached to the biofilm (g/m^3), δ_B is the thickness of the biofilm (m), $\hat{\mu}$ is the maximum specific growth rate constant (h^{-1}), Y is the yield constant (g/g), and K_c is the half saturation constant (g/m^3).

The mass balance of substrate in the biofilm on the submerged portion of the disk at steady state is given by

$$\frac{k_L}{\delta_B}(c_B - c_s) - \frac{\hat{\mu} X c_s}{Y(K_c + c_s)} = 0 \qquad (4)$$

In this equation, c_B is the substrate concentration in biofilm on the submerged portion of disk (g/m^3), and c_s is the substrate concentration in the bulk of liquid in the trough (g/m^3).

Mass balance of substrate in the trough at steady state is given by

$$c_B = \frac{Fc_o + F_f c_l(\beta)}{F + F_f + k_L A_s (k_l / 1 + K_l)} \qquad (5)$$

In this equation, F is the volumetric flow rate of feed (m^3/hr), c_o is the concentration of substrate in feed (g/m^3), F_f is the volumetric flow rate of liquid film (m^3/hr), $c_l(\beta)$ is concentration of substrate in the liquid film on disk re-entering the trough (g/m^3), K_l is the coefficient of biological parameters.

3.2.5 Spengel and Dzombak model

Spengel and Dzombak [20] developed a very complete model, based on another work [23], which considered both carbon oxidation and nitrification with competition for

oxygen in the bio-film. Their substrate utilization terms were double Monod expressions. However, the bio-film thickness and density had to be provided as input to the model. Two simplifications were made to facilitate their solution. First, the disk was divided into four sectors, two in the submerged region and two in the aerated region and the substrate removal rates were calculated for each sector. Second, the bio-film was divided into four layers, with each being considered as a mixed zone [34]. The model employed following mass balance equations for the trough and liquid film:

$$V\frac{dS^T}{dt} = Q(S^I - S^T) + Q_L(S_2^L - S^T) - K_M A_S \sum_{j=3}^{4} S^T - S_j^{BLi}) + K_{MT} A_{al}(S^* - S^T) \qquad (6)$$

In this equation, t is time (days), V is the mixed liquid volume in stage (L), S^T is the substrate concentration in mixed liquid (mg/L), S^I is the substrate concentration of stage influent (mg/L), S^L is the substrate concentration in attached liquid film (mg/L), S^* is the saturated liquid substrate concentration for oxygen (mg/L), S^{BLi} is the substrate concentration at biofilm-liquid interface (mg/L), Q is the volumetric flow rate of influent/effluent (L/d), K_M is the mass transfer coefficient from liquid to bio-film, (m/d), K_{MT} is the oxygen transfer coefficient from air to the mixed liquid, (m/d), Q_L is the volumetric flow rate of attached liquid layer (L/d), A_s is the surface area of submerged sector (m^2) and A_{al} is the surface area at air and mixed liquid interface (m^2). The liquid film substrate mass balance equation for oxygen employed was:

$$A_a \delta_L (\frac{dS^L}{dt}) = Q_L(S_{j-1}^L - S_j^L) - K_M A_a (S_j^L - S_j^{BLi}) + K_{ML} A_a (S^* - S_j^L) \qquad (7)$$

In this equiation, A_a is surface of aerated sector (m^2), δ_L is the thickness of attached liquid layer (m), S^L_{j-1} is the substrate concentration in liquid film; subscript denotes sector number (mg/L), and K_{ML} is the oxygen transfer coefficient from air to liquid film (m/d).

The rate of substrate utilization equation was:

$$R_s = \frac{dS}{dt} = \frac{\mu_{max} X_a}{Y \delta_B} \frac{S}{K_S + S} \frac{S_O}{K_{S.O} + S_O} \qquad (8)$$

In this equation, R_s is the substrate utilization rate (mg/L.d), μ_{max} is the maximum specific growth rate of microorganisms (day^{-1}), X_a is the surface concentration of microorganisms in region (one layer in one sector) (g/m^2), A is the surface area of attached microorganisms in sector (m^2), S is the substrate concentration in region (mg/L), S_O is the oxygen concentration in region , Y is the organism yield coefficient (g biomass produced/g substrate used), K_S and $K_{S.O}$ are the substrate and oxygen half saturation constants (mg/L).

Spengel and Dzombak model [20] was useful in identifying the trough dissolved oxygen concentration at which RBC performance started to decline as a result of oxygen limitation. They proposed that the radial variation of biomass thickness and density would improve the utility of the model for scale up [34].

CHAPTER 4 SIMULATION MODEL FOR RBCs

4.1 Objective

The primary objective of this study is to use mathematical models developed by previous researchers, Spengel et al. [20], Watanabe [21], and Hansford et al. [35], and as a general direction to develop a simplified model and to compare the predicted values from the developed model with the experimental data obtained by Alvarez-Cuenca [5] and Paolini [37]. These researchers [5,37] have determined the soluble BOD_5 concentration at different organic loadings, and the overall removal rate for dissolved organic carbon. The particular model used in this study is taken from Spengel et al. [20]. Another objective of the study is to predict any process changes due to the upsets in the influent wastewater flow, and the soluble BOD_5 loadings from the model used in this study. This model describes the phenomenon of degradation of the substrate by considering the two regions for analysis, which are, the bio-film and the trough.

The model is based on the approach of earlier researchers [20,21,35], and considers the mass transport of the substrate from the liquid film, and the reaction within the bio-film on the exposed and the submerged portion of the rotating disk. The simulated model calculates the concentration and the overall removal rates of the dissolved organic carbon and oxygen in the bulk liquid in the trough.

The model assumes that a liquid film is attached on the bio-film of the rotating disk as it emerges from the mixed liquid and remains stationary on the disk. When the disk reenters the trough, the stationary liquid attached to the disk strips off, and mixes completely with the liquid in the trough. The liquid and bio-film layers are considered to be well mixed.

The model considers that the concentration, and the activity of the suspended biomass in the RBC unit are far lower than that of the attached biomass, and can be regarded as negligible [15]. Grady and Lim, for their model [36], also assumed that both the attached and detached microorganisms contribute to substrate removal. The simulated model assumes that 0–2% substrate consumption takes place in the submerged portion of the disk, and the liquid in the trough.

4.2 Model parameters for a 4-stage RBC pilot plant [5]:

The approach adopted for the parameter selection is to use the best estimate of the values of maximum growth rate, microorganism concentration and yield constant available in the literature. The parameter selection for the Case I of this study is described below:

The active thickness of the bio-film has been shown to be less than the total thickness of bio-film in several forms of fixed film reactor having well-established biofilms [35]. Kornegay and Andrews [38] reported values ranging from 70 to 200 μm for the active depth of the biofilms. A value of 200 μm has been chosen for the simulation of the model.

The value for the mass transfer coefficient is taken from the work by Grieves [39]who found the values for mass transfer coefficient ranging from 0.3 to 1.0 m/hr for his dynamic model of the rotating biological disk. A value of 0.4 m/hr has been used for this study. Kornegay [40] reported a value of 95000 g/m^3 for the concentration of the microorganism for the entire film, while Heohn [41] showed that the concentration of the

microorganism varied from 20000 to 105000 g/m^3, which is dependent on several factors including overall film thickness. A value of 26400 g/m^3 has been used for this study.

The values for the maximum growth rate constant, the yield constant, and the saturation constant reported in the literature for disperse cultures vary widely depending on the substrate and the growth conditions [42]. The values for these parameters have been taken from Clark et al. [19] for this study.

4.3 Model parameters for a 3-stage RBC lab scale unit [37]:

The values of biofilms thickness, mass transfer coefficient, microorganism concentration, and half saturation constant for Case II study have been taken from the work done by Paoilini [37], and are provided in Table 6.

4.4 Assumptions of the process model

The mass balance equations of the simulated model for the bio-film and the trough are based on the following assumptions.

1. The liquid in the trough is completely mixed.
2. The wastewater in trough has uniform compositions at any given time.
3. The biofilms are fully grown and have uniform compositions.
4. Oxygen consumption in bio-film is directly proportional to substrate consumption
5. The concentration of microorganisms is constant throughout the bio-film.
6. Substrate and oxygen concentrations are independent of radial and tangential positions within the liquid and bio-films.

7. The liquid film on the exposed portion of the disk is assumed to be of constant thickness, which is dependent on the disk rotational speed and diameter.
8. It is assumed that the liquid film mixes immediately with the bulk of the liquid when it passes through the submerged portion of the trough.
9. The growth limiting substrates are
    (i) The soluble substrate in the exposed portion of the rotating disk and
    (ii) The dissolved oxygen in the submerged portion of the disk.
10. Rates of substrate and oxygen utilization within the bio-film and the liquid in the trough follow Monod kinetics.
11. Rate of substrate utilization and microbial activity are confined to bio-film on the disk, and do not occur in the liquid film on the exposed portion of the disk. In the bulk liquid in the trough, the rate is 0–2 % of that in the bio-film [36].

4.5 Dynamic model equations

Consider a rotating disk about its axis parallel to the surface of the liquid in a trough as shown in Fig1.2. When the disk rotates and passes through trough and air, a thin liquid layer of wastewater is formed on the bio-film developed on disk. The organic material in wastewater is removed by microbial metabolism in bio-film. The dynamic equations are written by applying mass balances for substrate and oxygen in the following two areas:

1. The bio-film
2. The trough

4.5.1 The bio-film

Mass balance equation for concentration of substrate in the bio-film is given by

$$\frac{dC_{sbod,BF}}{dt} = k_{sbod} A(C_{sbod,T} - C_{sbod,BF}) / V_b - r_{sbod} \quad (9)$$

which is the equation for the change in concentration of the soluble BOD_5 in the bio-film. In this equation, $C_{sbod,BF}$ is the concentration of the soluble substrate in bio-film (g/m^3), $C_{sbod,T}$ is the concentration of the substrate in the trough (g/m^3), r_{sbod} is the rate of substrate consumption in the bio-film ($g/m^3.hr$), A is the disk surface area (m^2), k_{sbod} is the mass transfer coefficient of substrate from liquid to bio-film (m/hr) and V_b is the volume of the biofilms (m^3).

4.5.2 Equation for rate of substrate consumption

Assuming soluble carbonaceous substrate is the only limiting substrate, during the aeration phase, provided that the liquid film adhering to the layer of biomass is constantly oxygenated and attains quickly oxygen saturation conditions, the following Monod expression is used for the growth of the biomass

$$\mu = \mu_{max} \frac{C_{sbod,BF}}{K_{sbod} + C_{sbod,BF}} \quad (10)$$

In this equation, K_{sbod} is the half saturation constant (g/m^3) and μ_{max} is the maximum specific growth rate (1/hr).

Rate of substrate consumption can be calculated from the expression is given by [34]:

$$r_{sbod} = \frac{\mu}{Y} X \quad (11)$$

In this equation, X is the specific concentration of attached biomass (g/m^3), μ is the specific growth rate of attached biomass (1/hr), and Y is the yield coefficient for attached biomass (g cells produced/g substrate consumed).

Writing mass balance equation for consumption of oxygen in the bio-film, we get

$$\frac{dC_{O_2,BF}}{dt} = k_{O_2} A(C_{O_2,in} - C_{O_2,BF})/V_b - r_{O_2} \quad (12)$$

In this equation, $C_{O_2,BF}$ is the concentration of oxygen in the bio-film (g/m^3), $C_{O_2,in}$ is the saturated concentration of oxygen in the liquid film (g/m^3), k_{O_2} is the mass transfer coefficient of oxygen from liquid to bio-film (m/hr), and r_{O_2} is the rate of oxygen consumption in the bio-film (g/m^3.hr).

Rate of oxygen consumption is calculated from the Monod expression, which is given by

$$r_{O_2} = \frac{\mu}{Y} X \quad (13)$$

$$\mu = \mu_{max} \frac{C_{O_2,BF}}{K_{O_2} + C_{O_2,BF}} \quad (14)$$

In this equation, K_{O_2} is the oxygen half saturation constant (g/m^3).

4.5.3 The trough

For the attached biomass in the trough, assuming 0–2% of the soluble substrate is consumed in the trough for residence times of more than an hour, under higher oxygen concentrations in the trough. Writing the mass balance equation for the concentration of the soluble substrate in the trough, we get

$$\frac{dC_{sbod,T}}{dt} = \frac{F}{V_t}(C_{sbod,in} - C_{sbod,T}) + \frac{M_{sbod}}{V_t} - fr_{sbod} \quad (15)$$

In this equation $C_{sbod,in}$ is the concentration of the soluble substrate in the influent stream (g/m^3), F is the volumetric flow rate of the influent stream (m^3/hr), V_t is the volume of

the trough and M_{sbod} is the mass of substrate transferred in the trough (g/hr). The factor f is the percent consumption of the substrate in the attached bio-film in the submerged portion of the rotating disk in the trough, and the value of 0.015 was used in the computer program for simulation.

The mass of soluble substrate transferred in the trough is given by the following equation.

$$M_{sbod} = k_{sbod} A\left(C_{sbod,BF} - C_{sbod,T}\right) \tag{16}$$

4.5.4 Mass balance equation for concentration of oxygen in the trough

$$\frac{dC_{O_2,T}}{dt} = \frac{F}{V}\left(C_{O_2,in} - C_{O_2,T}\right) + \frac{M_{O_2}}{V} - r_{O_2} \tag{17}$$

In this equation, r_{O_2} is the rate of oxygen consumption in trough (g/m^3.hr), and is given by equation (5).

The mass of oxygen transferred in the trough is given by

$$M_{O_2} = k_{O_2} A\left(C_{O_2,BF} - C_{O_2,T}\right) \tag{18}$$

4.5.5 Equation for rate of oxygen consumption in trough

The rate of oxygen utilization follows Modified Monod (Double Monod Model) in this case. In the trough, the wastewater in contact with the biomass has a dissolved oxygen concentration that may prove lower than the required level, as there are no oxygen saturation conditions in the liquid film attached to biomass in the submerged portion of the disk in the trough. Oxygen concentration then comes to influence the substrate removal kinetics [20], if no additional oxygen supply is maintained in the trough. The following Monod expression is used in this phase.

$$\mu = \mu_{max} \frac{C_{sbod}}{K_{sbod}+C_{sbod}} \cdot \left(\frac{C_{O_2}}{K_{O_2}+C_{O_2}} \right) \quad (19)$$

In this equation, K_{O_2} is the Monod half saturation constant for oxygen (g/m^3), and K_{sbod} is the substrate half saturation constant (g/m^3).

The above model equations were solved using the Runge Kutta Fehlberg and adaptive step size control algorithm such that the exit concentration of the soluble BOD of the 1st stage is the inlet to the 2nd stage and the concentration of soluble BOD at the exit of the second stage is the inlet concentration of soluble BOD to the 3rd stage.

Chapter 5 SIMULATION

5.1 Model validation

The dynamic model described in the previous chapter is validated from the experimental results of two studies [5,37], herein described as Case I and Case II. Case I study is of a 4-stage RBC pilot plant operation for the treatment of raw sewage from Toronto Metroworks main plant whereas Case II is a 3-stage lab scale RBC unit used for the treatment of an industrial effluent. The wastewater used in the tests was diluted with tap water when the BOD exceeded the established high value in the influent wastewater stream. The ratio between the values of the soluble BOD and of the COD was practically independent of the strength of the wastewater and was equal to 0.88-0.90,which is the required one for readily biodegradable waste.

5.2 Runge kutta fehlberg method [43]:

The differential equations were solved using the 5^{th} order Runge-Kutta-Fehlberg method, and adaptive step size control with Cash-Karp parameters.

The integration methods such as this one automatically avoid unnecessary and excessive calculations compared to constant step size methods. These methods require the estimate of the local truncation error at each step. This error estimate serves as a basis for lengthening or decreasing the step size. There are two approaches to incorporate adaptive step size control into one-step methods.

1. The error is estimated as the difference between two predictions using the same order RK method but with different step sizes.
2. Local truncation error is estimated as the difference between two predictions using different order RK methods.

The 5^{th} order Runge-Kutta-Fehlberg method uses the approach for obtaining an error estimate that involves computing two RK predictions of different order. The results can then be subtracted to obtain an estimate of the local truncation error.

The fourth and fifth order prediction amount to a total of 10 derivative evaluations per step while the Runge-Kutta Fehlberg prediction amounts to 6 derivative evaluations per step.

5.3 Case I

In this case study, the dynamic model is examined by applying the experimental results obtained in the treatment of raw sewage from the main plant of Metroworks in Ashbridges Bay (Toronto) [5]. The pilot plant unit consisted of six stages; the first four stages were aerobic. The characteristics of the pilot plant unit, and the characteristics of the raw sewage studied are provided in Table 1. The various parameters for this case study are provided in Table 1[35]. The values of half saturation constant and maximum specific growth rates are taken from the estimated kinetic coefficients for a 4-stage RBC pilot plant [19], operated under varying organic loadings. Table 2 provides the experimental data for the concentration of soluble BOD_5 for case I [5].

The computer program with the 5th order Runge-Kutta-Fehlberg method [43] using the Cash-Karp approach was run for these different organic loadings, assuming 0–2% of the rate of soluble BOD_5 consumption in the trough. Table 3 shows the results obtained from the computer program run for the dynamic model at the organic loadings chosen by Alvarez-Cuenca M [5]. The simulation results of % BOD_5 removal calculated from the dynamic model are provided in Table 4. Table 5 shows the comparison of the model predictions and the experimental results in terms of % BOD_5 removal obtained by Alvarez-Cuenca, M [5].

Table 1: Pilot plant unit specifications, wastewater characteristics and model input parameters for Case I, Alvarez-Cuenca [5].

	Parameter	Value
Pilot plant unit specifications	No. of biological stages	4
	Total number of disks	47
	Disk diameter, m	0.88
	Net volume per stage, m^3	0.18
	Total surface area of the disks, m^2	57.15
Wastewater characteristics	COD, g/m^3	850
	Soluble BOD_5, g/m^3	243
	Nitrate-N, g/m^3	9.2
	Dissolved Oxygen	9.7
	Nitrite-N, g/m^3	0.86
	Total suspended solids, g/m^3	598
	pH value	9.7, 5.2
Values of parameters used in model for the simulation [38]	Mean thickness of bio-films, m	$2x10^{-4}$
	Mass transfer coefficient, m/h	0.4
	Microorganism concentration, g/m^3	26400
	Yield constant, g cells/g substrate	0.96

Table 2: Experimental data for the concentration of soluble BOD_5 for Case I, Alvarez-Cuenca [5]:

Organic load ($g/m^2.d$)	Organic load ($g/m^2.hr$)	BOD_5 removal exiting the 4^{th} stage of the RBC (%)
1.9	0.079	99
4.5	0.1875	92
8.4	0.35	94
12.7	0.53	90
20.5	0.85	97
21.1	0.88	79
26.0	1.08	88

Table 3: Soluble BOD_5 concentration in wastewater predicted by the model for Case I, Alvarez-Cuenca [5]:

Organic load ($g/m^2.d$)	Steady-state Concentration of soluble BOD_5 at the exit of 1^{st} stage (g/m^3)	Steady-state Concentration of soluble BOD_5 at the exit of 2^{nd} stage (g/m^3)	Steady-state Concentration of soluble BOD_5 at the exit of 3^{rd} stage (g/m^3)	Steady-state Concentration of soluble BOD_5 at the exit of 4^{th} stage (g/m^3)
1.9	27.7	4.43	0.066	0.0026
4.5	60.4	19.3	0.693	0.062
8.4	96.7	46.2	3.21	0.525
12.7	124	73.5	8.41	2.19
20.5	156	111	25.3	13.9
21.1	158	114	27.5	15.9
26.0	170	130	42.6	31.3

Table 4: Simulation results of soluble BOD_5 concentration in terms of percent removal predicted by the model for Case I, Alvarez-Cuenca [5]:

Organic load ($g/m^2.d$)	Organic load ($g/m^2.hr$)	BOD_5 removal exiting the 4^{th} stage of the RBC (%)
1.9	0.079	99.99
4.5	0.1875	99.97
8.4	0.35	99.78
12.7	0.53	99.10
20.5	0.85	94.27
21.1	0.88	93.43
26.0	1.08	87.1

Table 5: Comparison of the experimental data for the concentration of soluble BOD_5, and the simulation results of soluble BOD_5 concentration in terms of percent removal predicted by the model for Case I, Alvarez-Cuenca [5]:

Organic load ($g/m^2.d$)	% BOD_5 removal (Experimental)	% BOD_5 removal (Simulated)	% Deviation = [1 – (%BOD_5 simulated/ %BOD_5 Experimental)] 100
1.9	99	99.99	1
4.5	92	99.97	8
8.4	94	99.78	6
12.7	90	99.10	10
20.5	97	94.27	3
21.1	79	93.43	18
26.0	88	87.10	2

The data from Table 3 show that the concentration of soluble BOD_5 at the fourth stage increases with an increase in the organic load. The model's predicted results of percent BOD_5 removal lie within close proximity to the experimental results as shown in Table 4. The model predictions agree with the observed experimental values at organic loads from 1.9 to 26.0 $g/m^2.d$. The percent deviation of simulated model results, as shown in Table 5, ranges from 1% to 18 % from that of the experimental results.

The simulation results for the concentration of soluble BOD_5, and the concentration of oxygen in the trough at different organic loadings, for Case I [5], are provided in Figure 5.1 to Figure 5.7. The comparison of the model and the experimental results is shown in Figure 5.8. These figures show the substrate (expressed as soluble BOD_5), and oxygen consumption profiles with respect to time at different organic loadings, plotted for the four stages of the RBC. The data show a decrease in concentration of soluble BOD_5 with each stage, and is in agreement with the experimental results of Case I study [5].

From Figures 5.1(a)–5.4(a), it is observed that at organic loadings (less than 12.7 $g/m^2.d$), low substrate concentration levels (less than 10 g/m^3) are achieved in the third stage of RBC, and concentration levels less than 5 g/m^3 are obtained in the fourth stage. Figures 5.5(a)–5.7(a) show that the concentration of the substrate, in each stage, starts increasing at a higher organic loading. At the loading of 21.1 $g/m^2.d$, the concentration of the substrate in the trough is less than 20 g/m^3 in the fourth stage of the RBC, and at the maximum loading of 26 $g/m^2.d$, the substrate concentration in the trough is greater than 20 g/m^3 in the fourth stage. Further, the drop in the third stage is steeper than expected. This is due to the fact that the value for the half saturation constant for soluble BOD_5 in

the third stage is much less compared to the 1st and 2nd stage half saturation constant values, used in the program, taken from the experimental observations [19], for Case I study. The values of these estimated kinetics constants for the four stage RBC pilot plant [19], show that due to less concentration of soluble BOD_5 in the third stage, the maximum specific growth rate for the biomass is less, giving low value of half saturation constant. The oxygen consumption profiles with respect to time in the trough, in 4-stages are shown in Figures 5.1(b)–5.7(b) at different organic loadings.

5.3.1 Initial conditions:

The initial conditions for the four-stage pilot plant RBC are given by

At time t = 0

$C_{sbod,\,T} = 243\ g/m^3$

$C_{O2,\,T} = 9.7\ g/m^3$

$C_{sbod,\,BF} = 243\ g/m^3$

$C_{O2,\,BF} = 9.5\ g/m^3$

The trends for the oxygen consumption with respect to time in figures 5.1 (b)–5.7 (b) show a drastic decrease in oxygen concentration initially in each stage, and achieve steady state in 5–20 hours. The simulation profiles with respect to time for the consumption of the soluble BOD_5 and oxygen, in the bio-film, are provided in Figure 5.9, at the organic loading of 26 $g/m^2.d$. In the bio-film, the consumption of the substrate, as shown in Figure 5.9 (a) follows the same trend as that observed for the consumption of the substrate in the trough as shown in Figure 5.7 (a). The concentration of oxygen in the bio-film is drastically decreased in each stage, as shown in Figure 5.9 (b).

Figure 5.1 (a): Predicted $C_{sbod,T}$ in a 4-stage RBC at Organic Loading = 1.9 g/m^2.d for Case I, Alvarez-Cuenca [5]
Steady state concentration at the exit of RBC = 0.0026 g/m^3

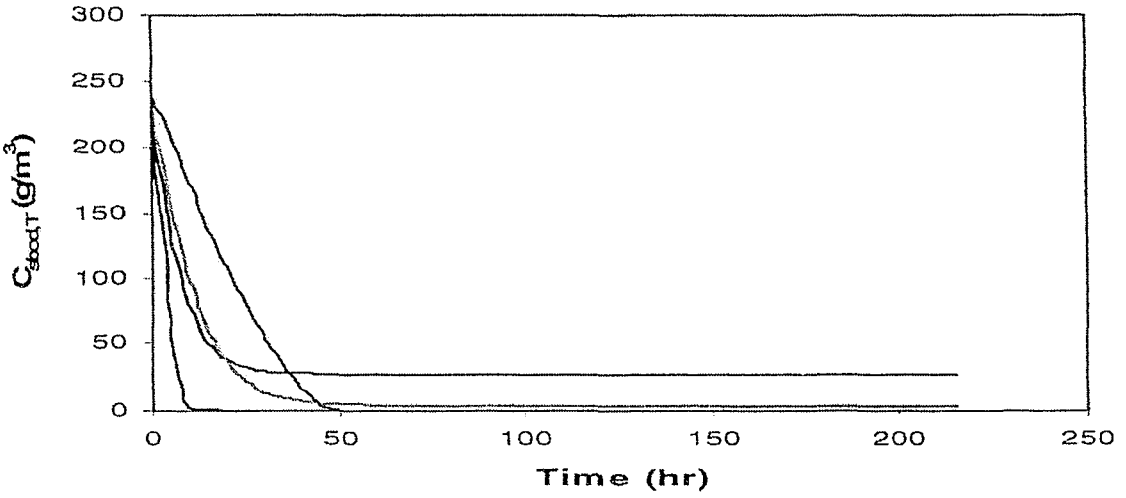

Figure 5.1 (b): Predicted $C_{O2,T}$ in a 4-stage RBC at Organic Loading = 1.9 g/m^2.d for Case I
Steady state concentration at the exit of RBC = 2.35x10^{-13} g/m^3

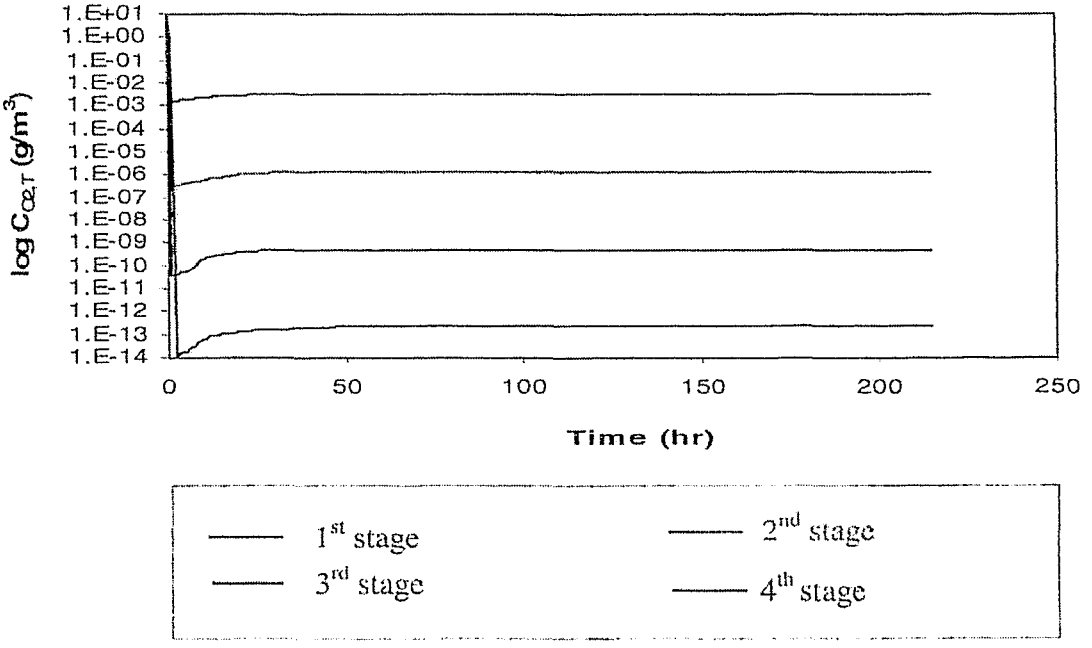

Figure 5.2 (a): Predicted $C_{sbod,\,T}$ in a 4-stage RBC at Organic Loading = 4.5 g/m^2.d for Case I, Alvarez-Cuenca [5]

Steady state concentration at the exit of RBC = 0.062 g/m^3

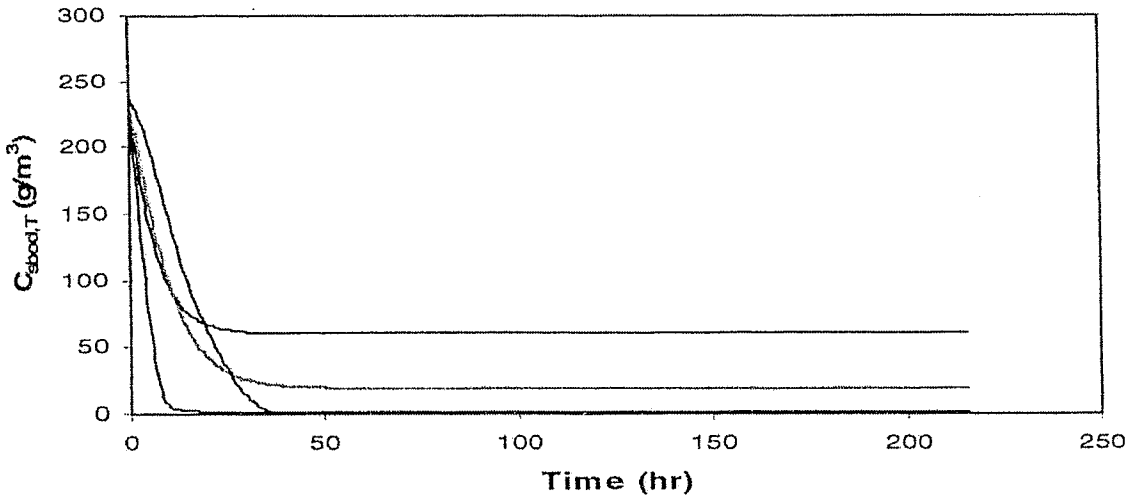

Figure 5.2 (b): Predicted $C_{O2,\,T}$ in a 4-stage RBC at Organic Loading = 4.5 g/m^2.d for Case I

Steady state concentration at the exit of RBC = 0.0026 g/m^3

Steady state concentration at the exit of RBC = 5.38x10^{-12} g/m^3

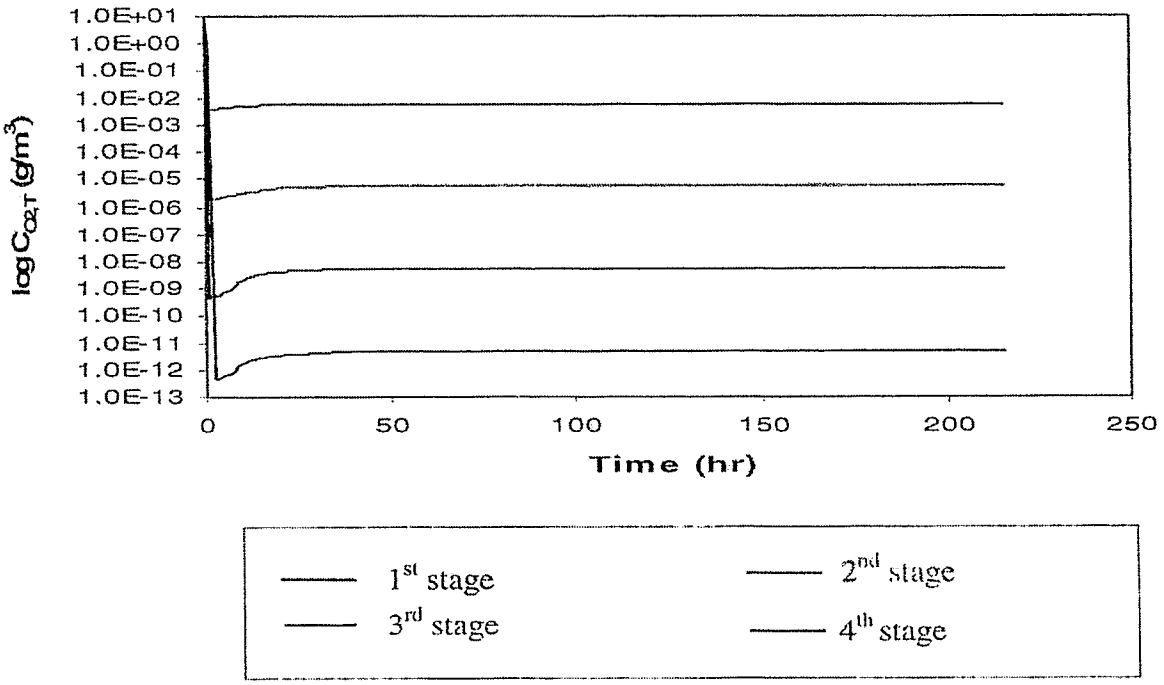

Figure 5.3 (a): Predicted $C_{sbod,T}$ in a 4-stage RBC at Organic Loading = 8.4 g/m^2.d for Case I, Alvarez-Cuenca [5]
Steady state concentration at the exit of RBC = 0.525 g/m^3

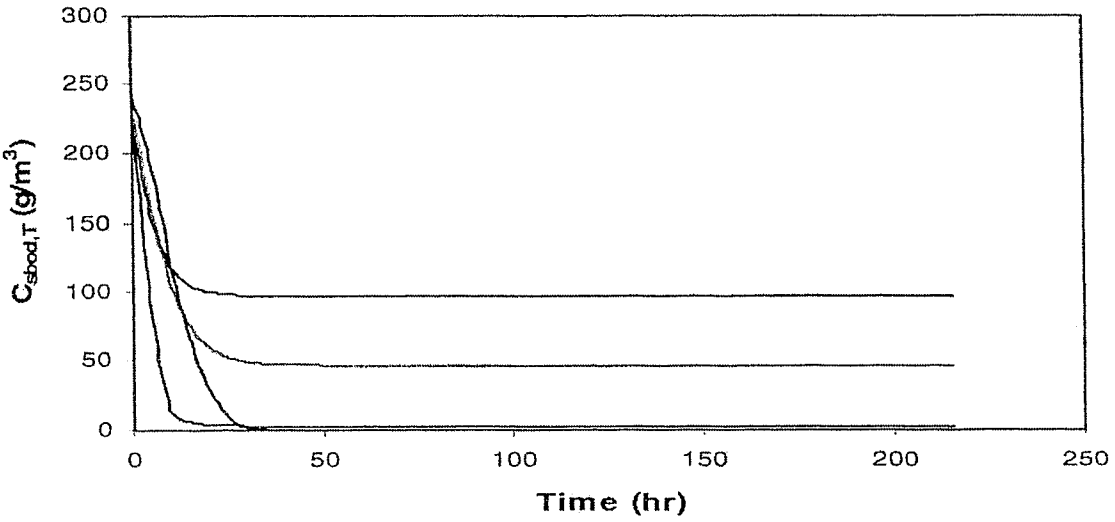

Figure 5.3 (b): Predicted $C_{O2,T}$ in a 4-stage RBC at Organic Loading = 8.4 g/m^2.d for Case I
Steady state concentration at the exit of RBC = 3.87x10^{-11} g/m^3

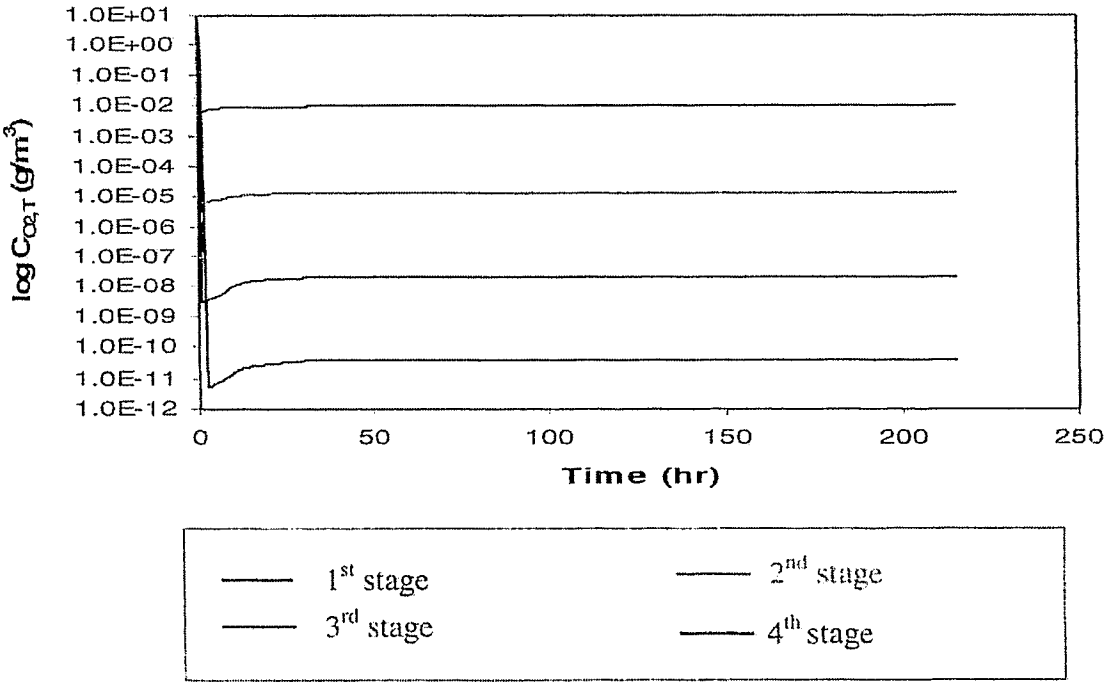

Figure 5.4 (a): Predicted $C_{sbod,T}$ in a 4-stage RBC at Organic Loading = 12.7 g/m^2.d for Case I, Alvarez-Cuenca [5]
Steady state concentration at the exit of RBC = 2.19 g/m^3

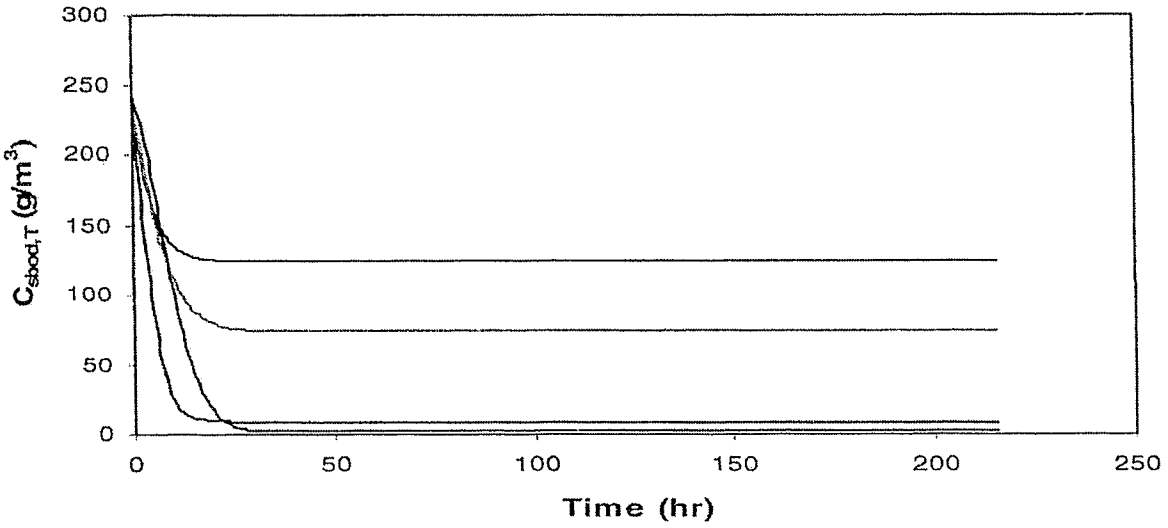

Figure 5.4 (b): Predicted $C_{O2,T}$ in a 4-stage RBC at Organic Loading = 12.7 g/m^2.d for Case I
Steady state concentration at the exit of RBC = 1.21x10^{-10} g/m^3

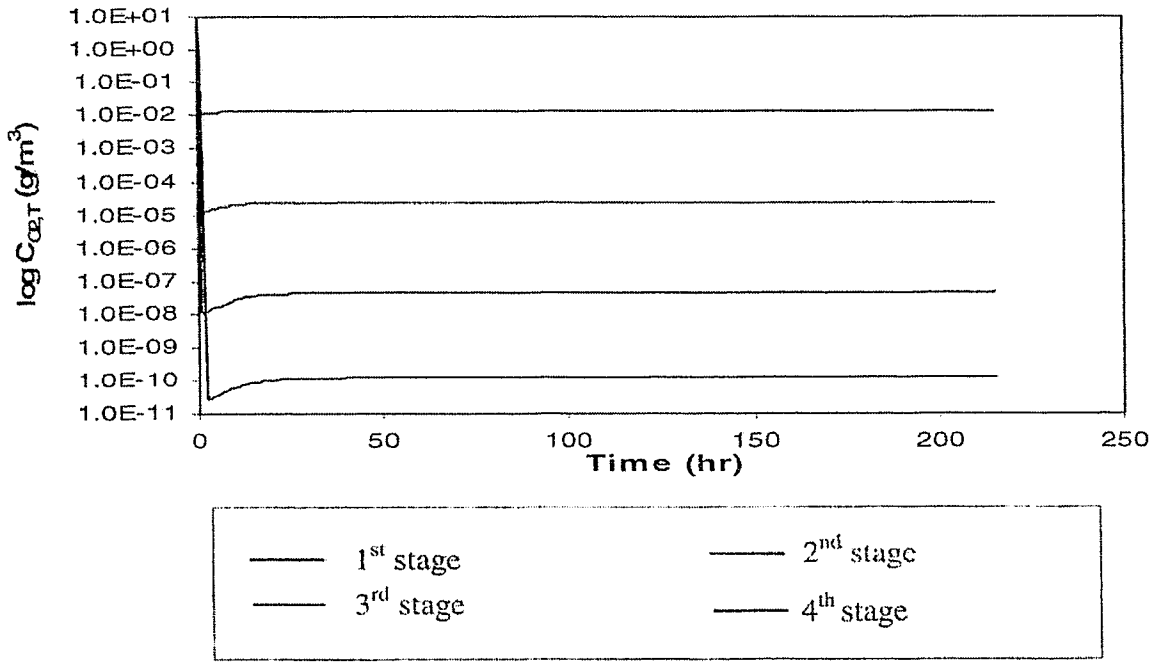

Figure 5.5 (a): Predicted $C_{sbod,\,T}$ in a 4-stage RBC at Organic Loading = 20.5 g/m^2.d for Case I, Alvarez-Cuenca [5]

Steady state concentration at the exit of RBC = 13.9 g/m^3

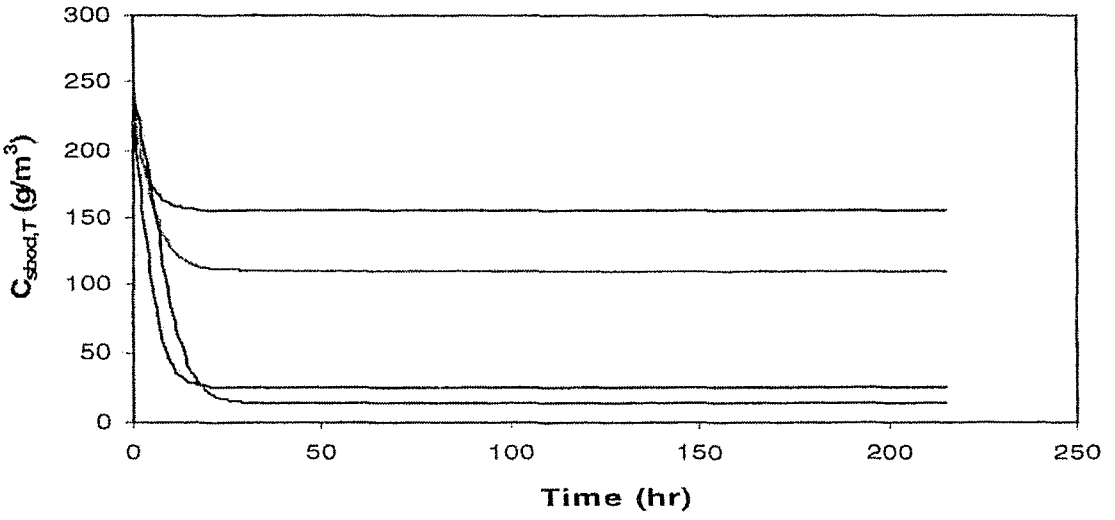

Figure 5.5 (b): Predicted $C_{O2,\,T}$ in a 4-stage RBC at Organic Loading = 20.5 g/m^2.d for Case I

Steady state concentration at the exit of RBC = 4.18x10^{-10} g/m^3

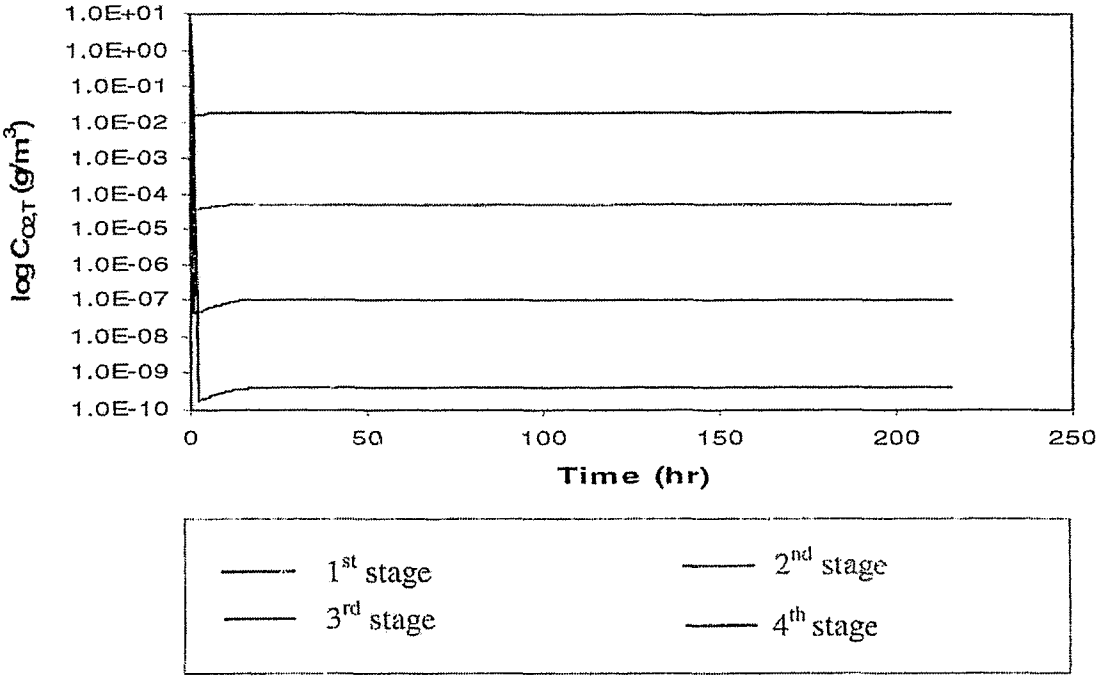

Figure 5.6 (a): Predicted $C_{sbod,T}$ in a 4-stage RBC at Organic Loading = 21.1 g/m^2.d for Case I, Alvarez-Cuenca [5]
Steady state concentration at the exit of RBC = 15.9 g/m^3

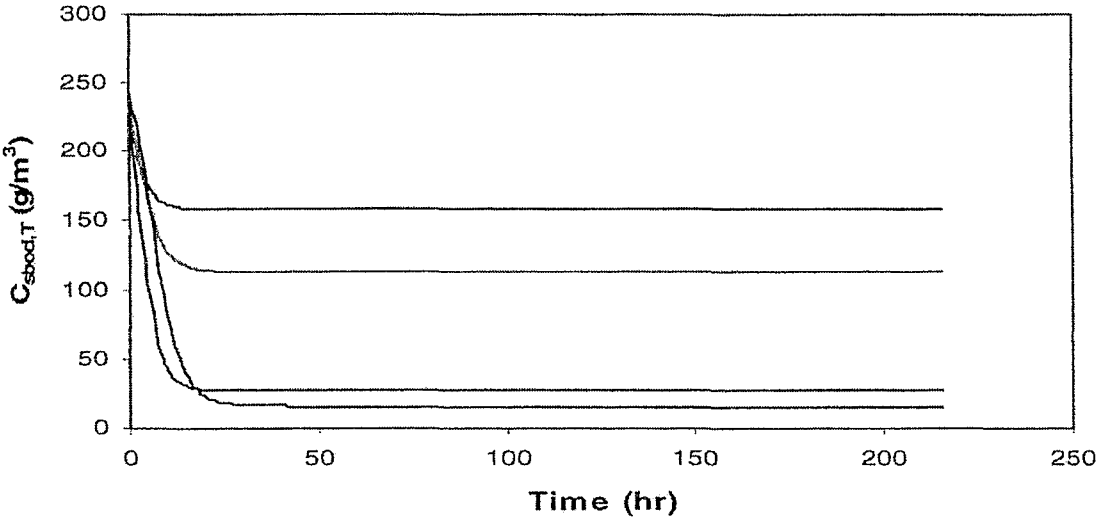

Figure 5.6 (b): Predicted $C_{O2,T}$ in a 4-stage RBC at Organic Loading = 21.1 g/m^2.d for Case I
Steady state concentration at the exit of RBC = 4.61x10^{-10} g/m^3

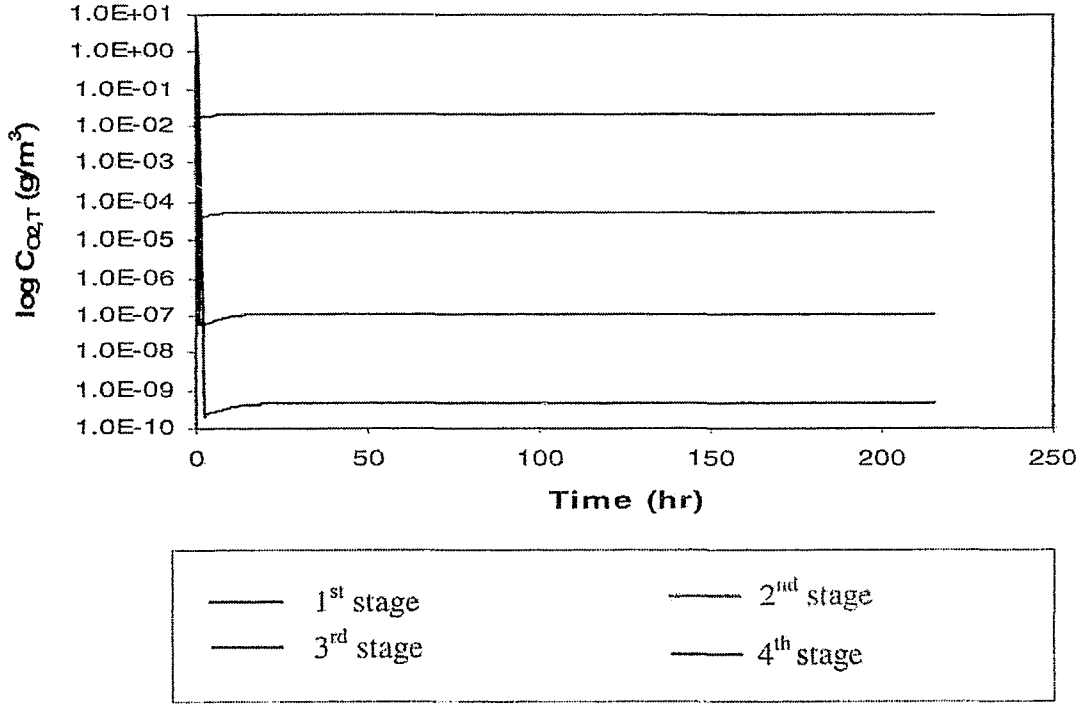

Figure 5.7 (a): Predicted $C_{sbod,T}$ in a 4-stage RBC at Organic Loading = 26.0 g/m^2.d for Case I, Alvarez-Cuenca [5]
Steady state concentration at the exit of RBC = 31.3 g/m^3

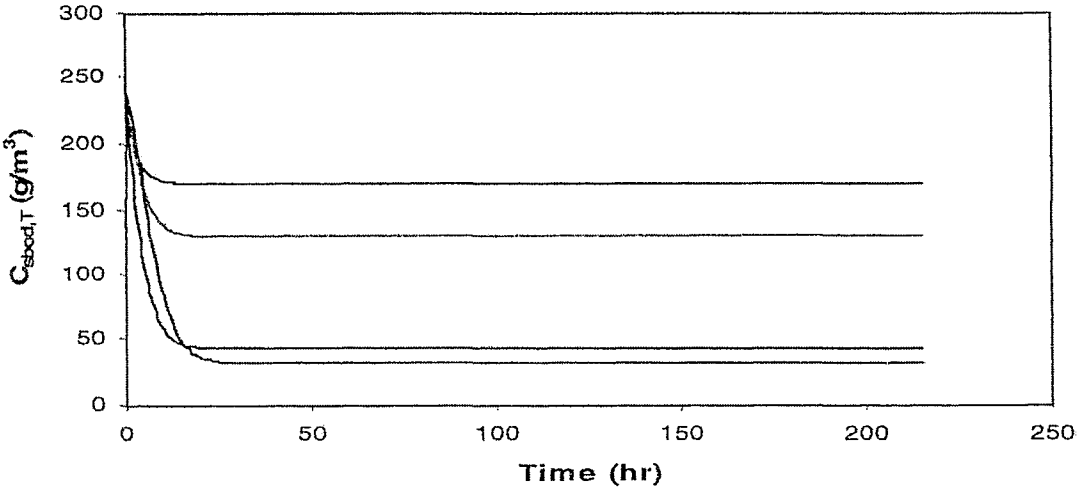

Figure 5.7 (b): Predicted $C_{O2,T}$ in a 4-stage RBC at Organic Loading = 26.0 g/m^2.d for Case I
Steady state concentration at the exit of RBC = 8.24x10^{-10} g/m^3

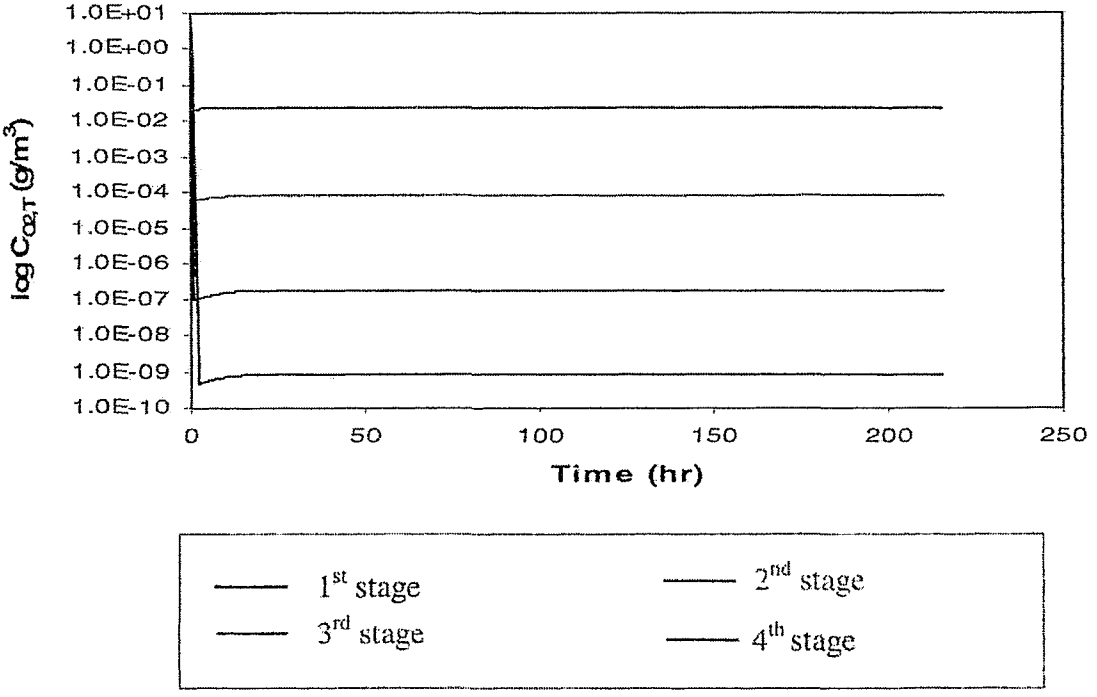

Figure 5.8: Comparison of simulated model results and the experimental results of a 4-stage RBC for Case I, Alvarez-Cuenca [5]

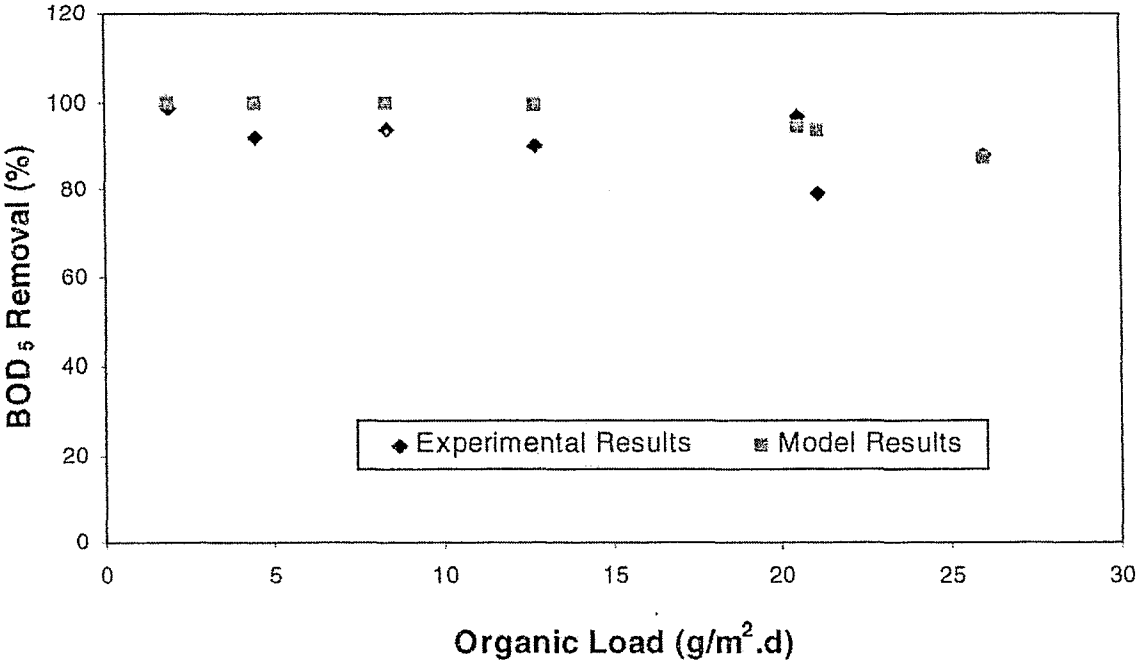

Figure 5.9 (a): Predicted $C_{sbod,\,BF}$ in a 4-stage RBC at Organic Loading = 26.0 g/m^2.d for Case I, Alvarez-Cuenca [5]
Steady state concentration at the exit of RBC = 31.3 g/m^3

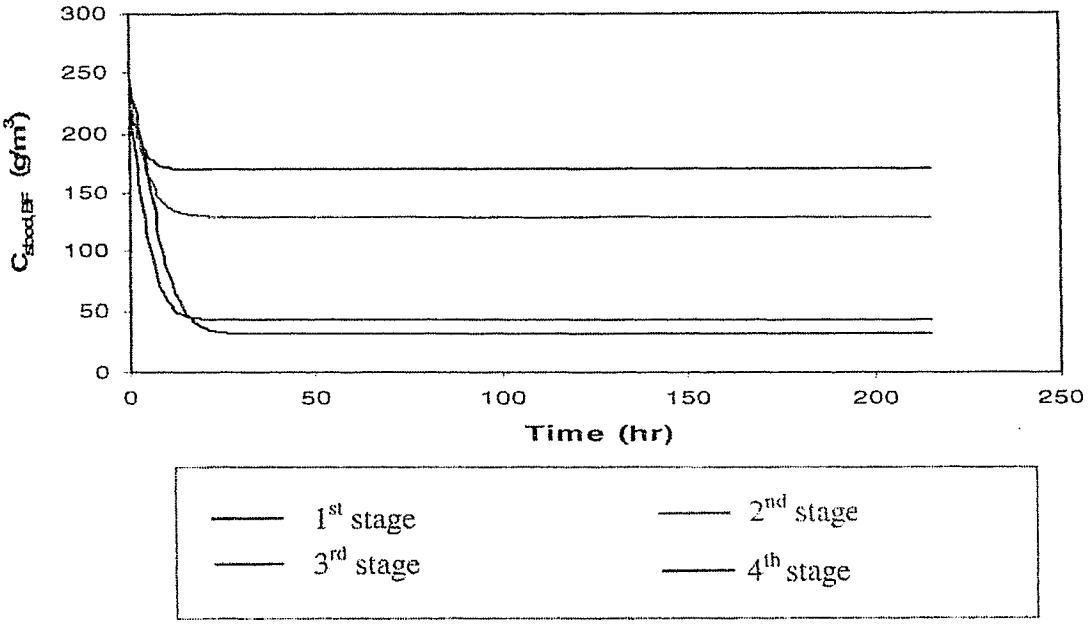

Figure 5.9 (b): Predicted $C_{O2,\,BF}$ in a 4-stage RBC at Organic Loading = 26.0 g/m^2.d for Case I

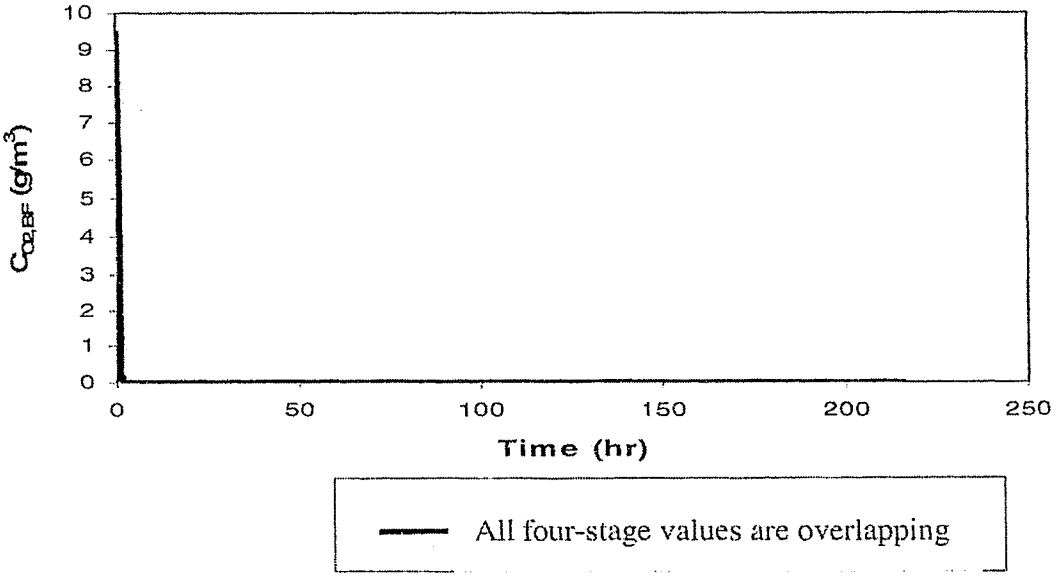

5.3.2 Effect of upsets for Case I:

Another effort is done to check the behaviour of the system under any organic or hydraulic shock loadings. The computer program was run for variations in the influent wastewater flow rate, the influent concentration of the soluble BOD_5, and with changes in both the variables. This upset was introduced in the computer program by defining a function called ChangeVariable. This function was provided with data to introduce the upsets in flow and concentration of soluble BOD_5 when the system reaches the steady state. For example, considering the upsets at an organic load of 12.7 $g/m^2.d$, Figure 5.4(a) represents the situation where there is no variation in the influent parameters at this load, and the system reaches a steady state in 35 hours. The following upsets are applied to find the variation in the concentration of soluble BOD_5 in each stage of RBC:

1. When the influent flow rate is doubled.
2. When the concentration of soluble BOD_5 is doubled.
3. When the flow rate is increased one and a half times, and soluble BOD_5 is doubled.
4. When both the flow rate and the soluble BOD_5 is doubled.

The simulation results of Case I [5], for the upsets in the system, show variations in the behaviour of the system. These variations incur, when a change is introduced in the influent flow and the concentration of the soluble BOD_5 at $12.7g/m^2.d$ organic load. These simulation results are provided in Figures 5.10–5.12. Figure 5.10 (a) shows an increase in the concentration of the soluble substrate, in each stage, when the influent flow rate is doubled. The concentration of soluble substrate in the fourth stage after the second steady state achieved, is 29.1 g/m^3 due to the upset in the flow rate. The trend for

Figure 5.10 (a): Predicted $C_{sbod,\,T}$ in a 4-stage RBC at Organic Loading = 12.7 g/m^2.d, for Case I, Alvarez-Cuenca [5], when the influent flow rate is doubled.
Steady state achieved after upset = 63 hours
Steady state concentration at the exit of RBC = 29.1 g/m^3

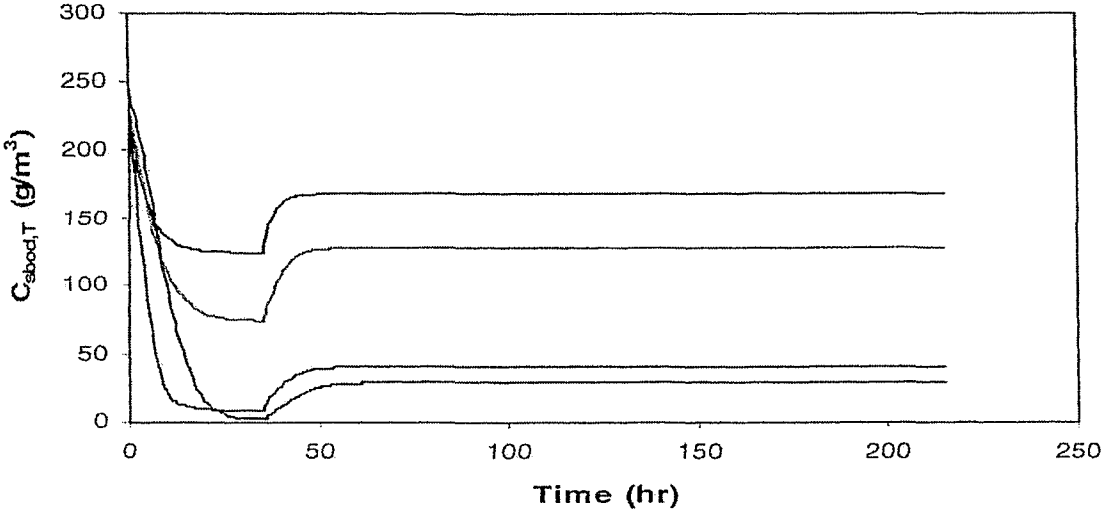

Figure 5.10 (b): Predicted $C_{O2,\,T}$ in a 4-stage RBC at Organic Loading = 12.7 g/m^2.d, for Case I [5], when the influent flow rate is doubled.
Steady state concentration at the exit of RBC = 7.6×10^{-10} g/m^3

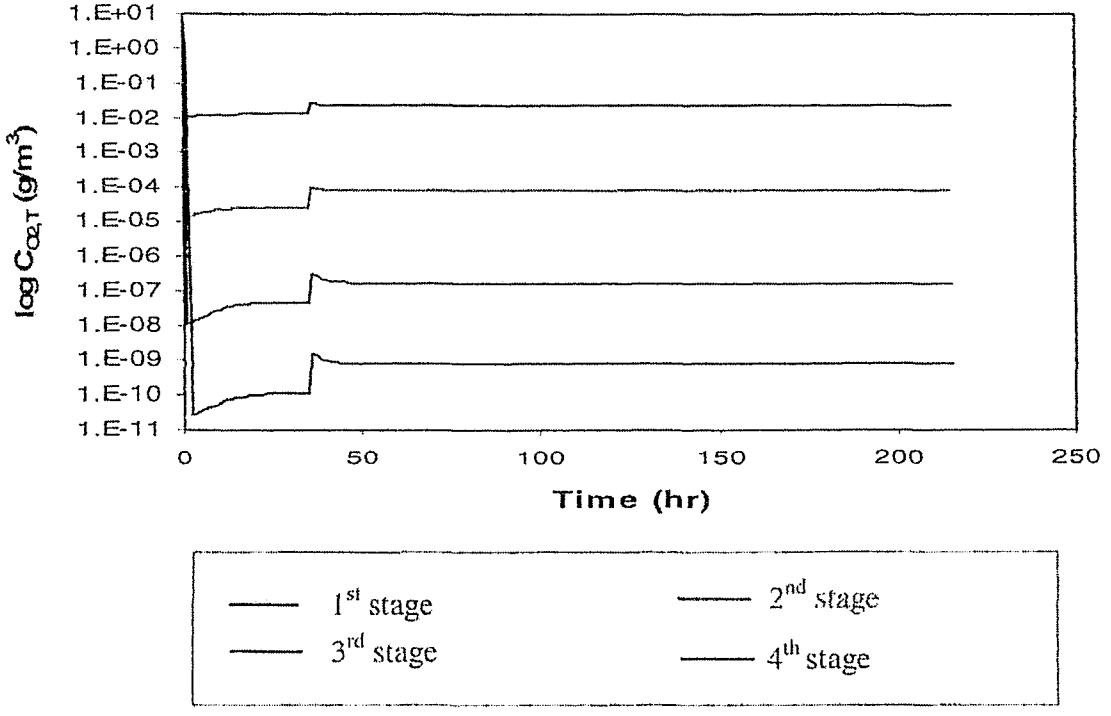

Figure 5.11 (a): Predicted $C_{sbod,\,T}$ in a 4-stage RBC at Organic Loading = 12.7 g/m^2.d, for Case I, Alvarez-Cuenca [5], when concentration of soluble BOD_5 is doubled.

Steady state achieved after upset = 79 hours

Steady state concentration at the exit of RBC = 11.2 g/m^3

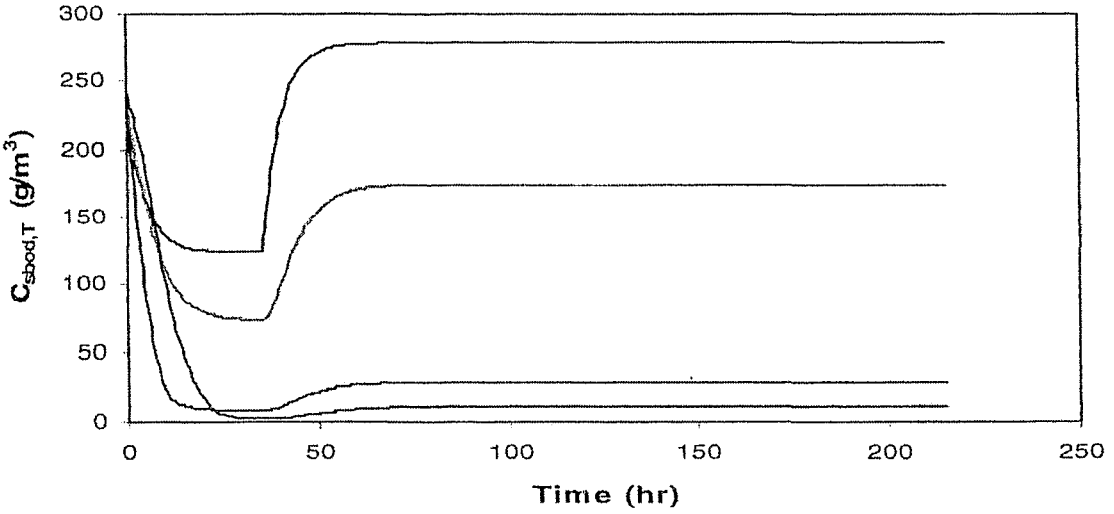

Figure 5.11 (b): Predicted $C_{O2,\,T}$ in a 4-stage RBC at Organic Loading = 12.7 g/m^2.d, for Case I [5], when concentration of soluble BOD_5 is doubled.

Steady state concentration at the exit of RBC = 3.98x10^{-11} g/m^3

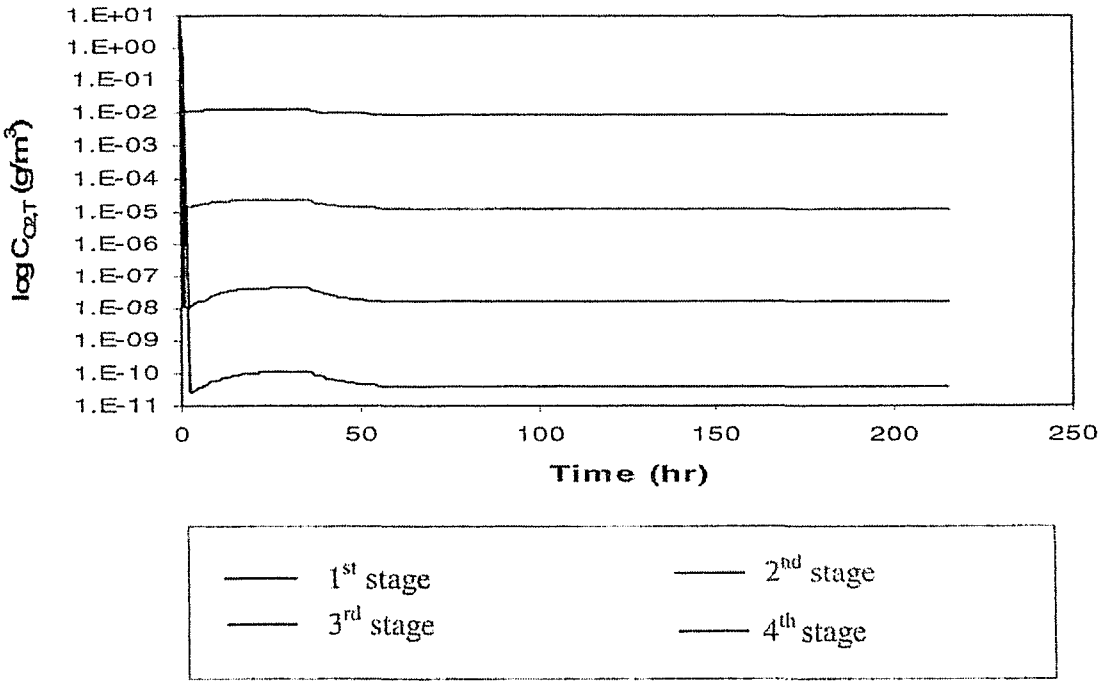

Figure 5.12 (a): Predicted $C_{sbod,\,T}$ in a 4-stage RBC at Organic Loading = 12.7 g/m^2.d, for Case I, Alvarez-Cuenca [5], when the influent flow rate is increased one and half times and the concentration of the soluble BOD_5 is doubled.
Steady state achieved after upset = 82 hours
Steady state concentration at the exit of RBC = 72.7 g/m^3

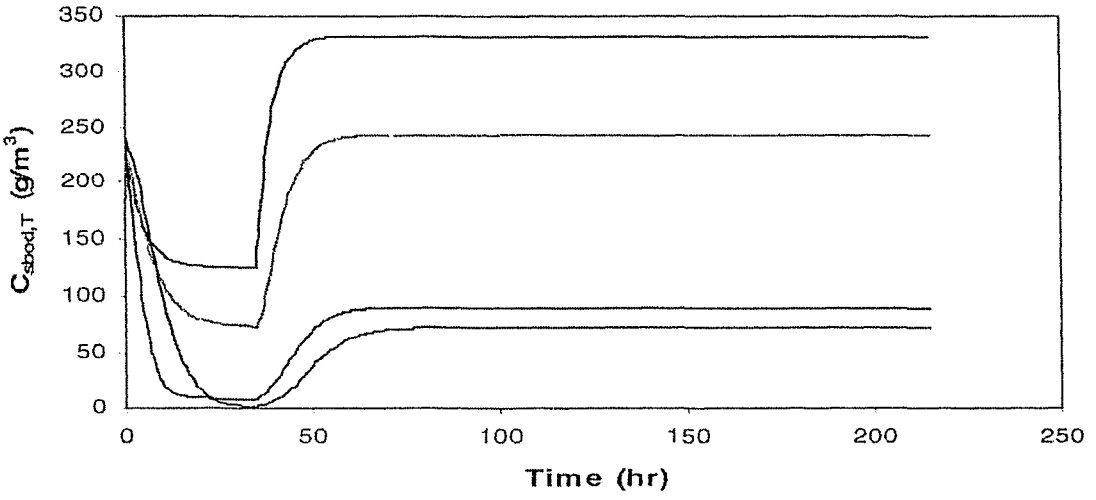

Figure 5.12 (b): Predicted $C_{O2,\,T}$ in a 4-stage RBC at Organic Loading = 12.7 g/m^2.d, for Case I [5], when the influent flow rate is increased one and half times and the concentration of the soluble BOD_5 is doubled.
Steady state concentration at the exit of RBC = 1.15×10^{-10} g/m^3

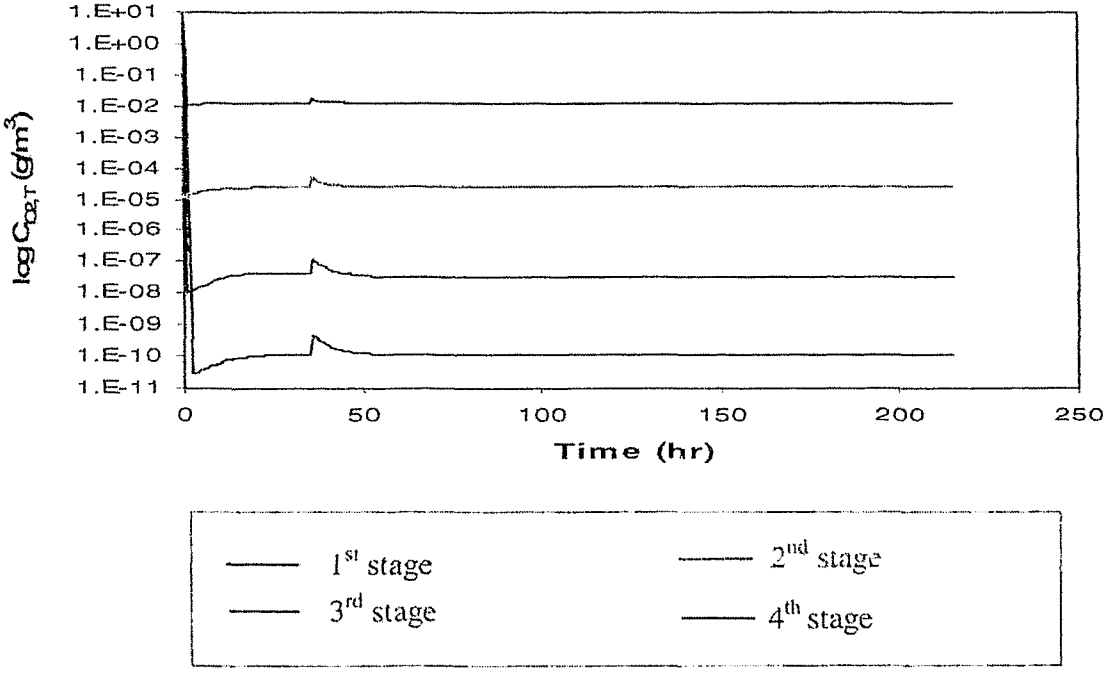

Figure 5.13 (a): Predicted $C_{sbod,\,T}$ in a 4-stage RBC at Organic Loading = 12.7 g/m^2.d, for Case I, Alvarez-Cuenca [5], when both the influent flow rate and the concentration of the soluble BOD_5 are doubled.

Steady state achieved after upset = 76 hours

Steady state concentration at the exit of RBC = 146 g/m^3

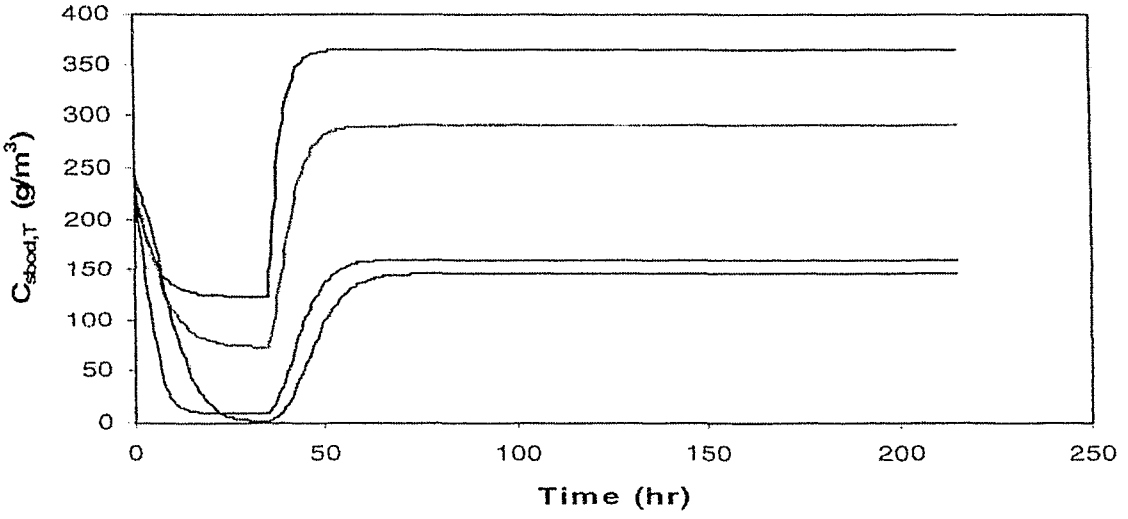

Figure 5.13 (b): Predicted $C_{O2,\,T}$ in a 4-stage RBC at Organic Loading = 12.7 g/m^2.d, for Case I [5], when both the influent flow rate and the concentration of the soluble BOD_5 are doubled.

Steady state concentration at the exit of RBC = 3.01×10^{-10} g/m^3

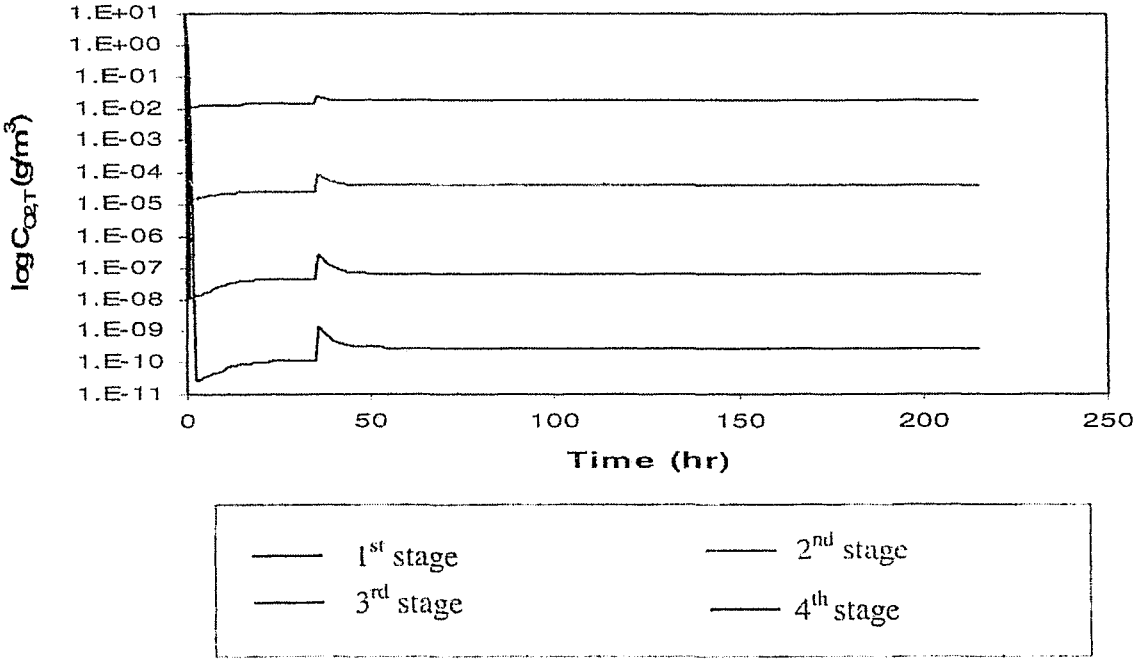

the concentration of the oxygen in the trough, in Figure 5.10 (b), shows a sharp increase in the oxygen consumption, when the upset in the flow rate is occurred, and achieves the steady state in almost 10 hours.

The rise time for Case I [5] upsets is calculated to find the time, which the four stage treating system takes to reach the steady state after the upset is occurred. It is observed that the four-stage RBC system takes 28 hours to reach the steady state when the flow rate is doubled, and the system takes 44 hours when the concentration of soluble BOD_5 is doubled in the influent stream. The rise time is 47 hours when the flow rate is increased one and a half times and the concentration of soluble BOD_5 is doubled, and 41 hours when both the flow rate and the concentration of soluble BOD_5 are doubled.

The profiles with respect to time for the consumption of the soluble BOD_5 and oxygen in the bio-film, for upsets in the system, when the influent flow and concentration of soluble BOD_5 are doubled at an organic load of 12.7 $g/m^2.d$, are provided in Figure 5.14. In the bio-film, the consumption of the substrate follows the same trend as that observed for the consumption of the substrate in the trough as shown in Figure 5.13 (a). The concentration of oxygen in the bio-film is readily consumed in each stage, as shown in Figure 5.14 (b).

Figure 5.14 (a): Predicted $C_{sbod,\ BF}$ in a 4-stage RBC at Organic Loading = 12.7 g/m^2.d, for Case I, Alvarez-Cuenca [5], when both the influent flow rate and the concentration of the soluble BOD_5 is doubled.
Steady state concentration at the exit of RBC = 146 g/m^3

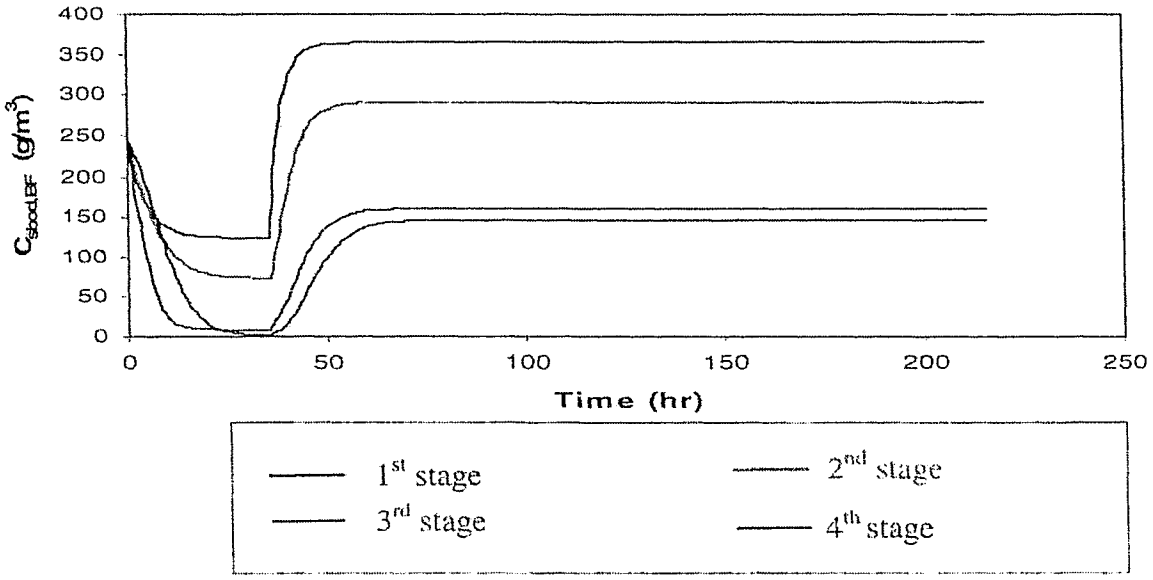

Figure 5.14 (b): Predicted $C_{O2,\ BF}$ in a 4-stage RBC at Organic Loading = 12.7 g/m^2.d, for Case I [5], when both the influent flow rate and the concentration of the soluble BOD_5 is doubled.

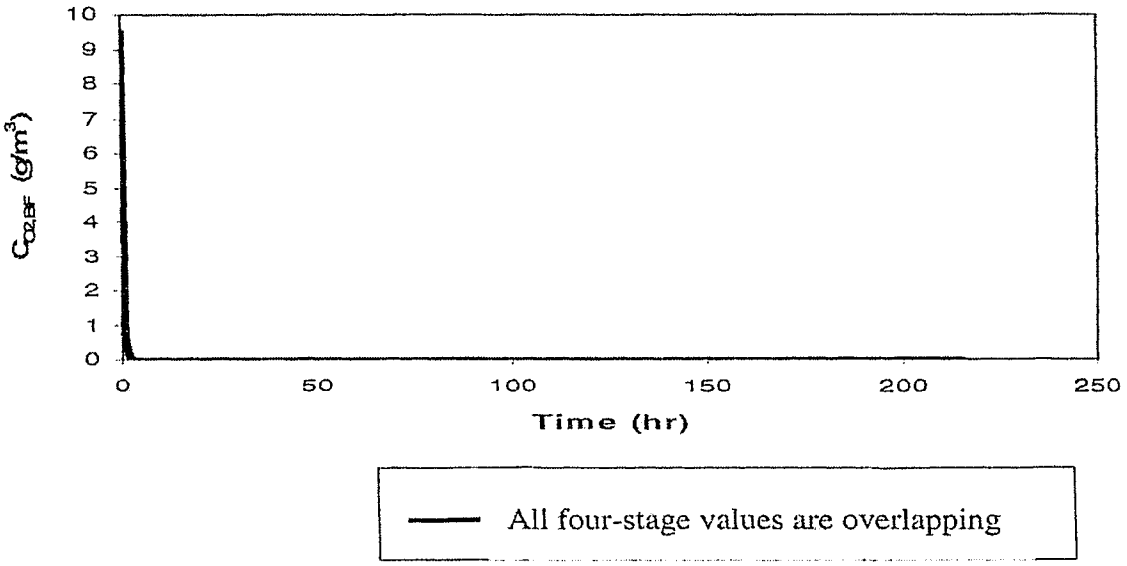

5.4 Case II

In this case study, the dynamic model is examined by applying the experimental results obtained from the treatment of industrial wastewater [37]. The laboratory scale RBC unit consisted of three stages with seven disks per stage. The characteristics of the unit are provided in Table 6.

The wastewater treated by the unit was the sewage produced by an industrial process. The process consisted of the recovery of ferrous metals, paper, organic material, plastics, etc. and of their transformations to products such as animal feed, pulp paper, plastic film, compost and steel. The industrial sewage had the average characteristics as shown in Table 6. The various parameters for this case study are provided in Table 6. The values of the parameters used in the computer program are taken from the 3-stage lab-scale study [37].

Table 7 shows the results of the soluble BOD_5 obtained at the end of each stage of biological unit for the experiments carried out at six different organic loadings [37]. The computer program with the 5^{th} order Runge-Kutta-Fehlberg method [43] using the Cash-Karp approach was run for these different organic loadings, assuming 0–2% of the rate of soluble BOD_5 consumption in the trough. Table 8 shows the simulated model results obtained for different organic loadings treated in the three stages of RBC. Table 9 shows the comparison of the simulated model and the experimental results in terms of percent BOD_5 removal.

Table 6: Lab-scale unit specifications, wastewater characteristics and model input parameters for Case II, Paolini [37]

	Parameter	Value
Lab-scale bio-disk unit specifications	No. of biological stages	3
	No. of disks per stage	7
	Disk diameter, m	0.275
	Net volume per stage, m^3	0.00871
	Total surface area of the disks per stage, m^2	0.831
Wastewater characteristics of lab-scale unit	COD, g/m^3	1840
	Soluble BOD_5, g/m^3	1640
	Ammonia (as N), g/m^3	40
	Oxidized nitrogen, g/m^3	0.0
	Total nitrogen, g/m^3	65
	Suspended solids, g/m^3	110
	pH value	6.6 – 7.0
Values of parameters used in model for the simulation [40]	Mean thickness of bio-film, m	0.0034
	Mass transfer coefficient, m/h	0.028
	Microorganism concentration, g/m^3	26400
	Saturation constant, g/m^3	202

Table 7: Experimental data for the concentration of soluble BOD_5 for Case II, Paolini [37]:

Organic load ($g/m^2.d$)	Concentration of soluble BOD_5 at 1st stage (g/m^3)	Concentration of soluble BOD_5 at 2nd stage (g/m^3)	Concentration of soluble BOD_5 at 3rd stage (g/m^3)
8.7	208	18	18
11.1	240	27	20
18.9	775	208	34
22.1	810	245	50
27.7	900	367	89
39.5	1150	680	320

Table 8: soluble BOD_5 concentration in wastewater predicted by the model for Case II, Paolini [37]:

Organic load ($g/m^2.d$)	Steady-state Concentration of soluble BOD_5 at the exit of 1st stage (g/m^3)	Steady-state Concentration of soluble BOD_5 at the exit of 2nd stage (g/m^3)	Steady-state Concentration of soluble BOD_5 at the exit of 3rd stage (g/m^3)
8.7	120	6.39	0.379
11.1	236	20.1	1.82
18.9	531	92.4	14.0
22.1	643	144	20.1
27.7	803	262	63.8
39.5	1030	543	234

Table 9: Comparison of the experimental data for the concentration of soluble BOD_5, and the simulation results of soluble BOD_5 concentration in terms of percent removal predicted by the model for Case II, Paolini [37]:

Organic load ($g/m^2.d$)	% BOD_5 removal (Experimental)	% BOD_5 removal (Model)	% Deviation = [1 – (%BOD_5 simulated / %BOD_5 Experimental)] 100
8.7	98.9	99.97	1
11.1	98.78	99.88	1
18.9	97.92	99.14	1
22.1	96.95	98.4	1
27.7	94.57	96.1	2
39.5	80.48	85.7	6

The concentration of soluble BOD_5 at the third stage increases with an increase in the organic load. The model predicted results lie within the close proximity of the values at third stage as shown in Tables 7 and 8. The results differ approximately by 20 g soluble BOD_5/m^3 from the experimental results at low organic loading in the third stage. The percent deviation of simulated model results is 1% to 6% from that of the experimental results.

The simulation results for the concentration of soluble BOD_5 and the concentration of oxygen in the trough, at different organic loadings for Case II [37] are provided in Figures 5.15 to Figures 5.20 These figures show the substrate profile (expressed as BOD_5), at different organic loadings, plotted for the three stages of the RBC. The figures show a decrease in concentration of the soluble BOD_5 and oxygen to steady state values in each stage. The comparison of the model and the experimental results is shown in Figure 5.21.

From Figures 5.15 (a)–5.16 (a), it is observed that at organic loading of (less than12 $g/m^2.d$), low substrate concentration levels (less than $5g/m^3$) are achieved in the third stage of RBC. Figures 5.17 (a)–5.20 (a) show that the concentration of the substrate, in each stage, starts to increase with higher organic loading. Figure 5.18 (a) represents the substrate profile at an organic load of $22.1g/m^2.d$. The concentration of the substrate obtained from the simulated result, at this load, is $20g/m^3$ in the third stage of the RBC. Figures 5.19 (a) and 5.20 (a) provide the profiles with respect to time at higher organic loading (greater than $22.1g/m^2.d$), showing higher levels of concentration of soluble substrate (greater than 20 g/m^3) in the third stage of the RBC.

5.4.1 Initial conditions:

The initial conditions for the three-stage lab scale RBC unit are given by

At time t = 0

$C_{sbod,T} = 1640\ g/m^3$

$C_{O2,T} = 9\ g/m^3$

$C_{sbod,BF} = 1640\ g/m^3$

$C_{O2,BF} = 9.5\ g/m^3$

The profiles with respect to time for the consumption of the oxygen in the trough, in the three stages, are shown in Figures 5.15 (b) – 5.20 (b) at different organic loadings. The trends for the oxygen consumption show a drastic decrease in oxygen concentration initially in each stage to a steady state in almost 10–80 hours.

The simulation profiles with respect to time for the consumption of the soluble BOD_5 and oxygen, in the bio-film, at an organic load of 39.5 $g/m^2.d$, are provided in Figure 5.22. In the bio-film, the consumption of the substrate follows the same trend as that observed for the consumption of the substrate in the trough as shown in Figure 5.20 (a). The concentration of oxygen in the bio-film is drastically consumed in the three stages, as shown in Figure 5.22 (b).

Figure 5.15 (a): Predicted $C_{sbod,T}$ in a 3-stage RBC at Organic Loading = 8.7 g/m^2.d for Case II, Paolini [37]
Steady state concentration at the exit of RBC = 0.379 g/m^3

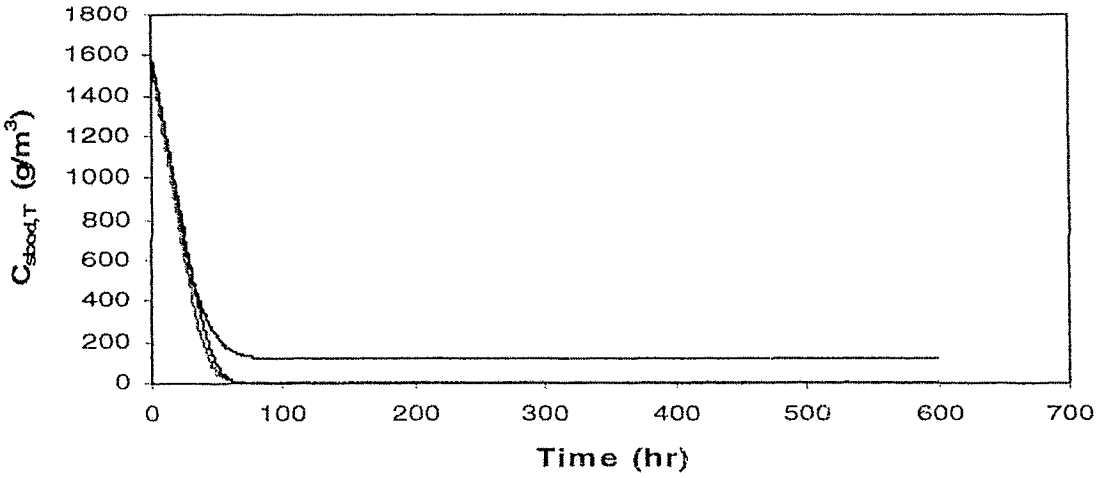

Figure 5.15 (b): Predicted $C_{O2,T}$ in a 3-stage RBC at Organic Loading = 8.7 g/m^2.d for Case II
Steady state concentration at the exit of RBC = 1.94x10^{-8} g/m^3

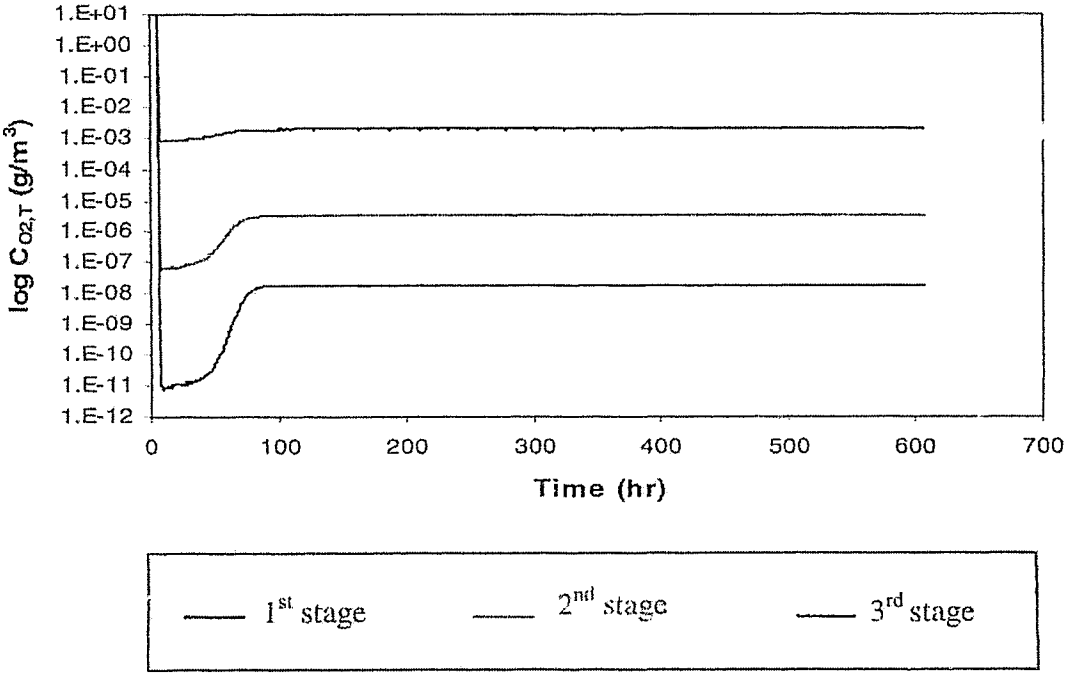

Figure 5.16 (a): Predicted $C_{sbod,T}$ in a 3-stage RBC at Organic Loading = 11.1 g/m^2.d for Case II, Paolini [37]
Steady state concentration at the exit of RBC = 1.82 g/m^3

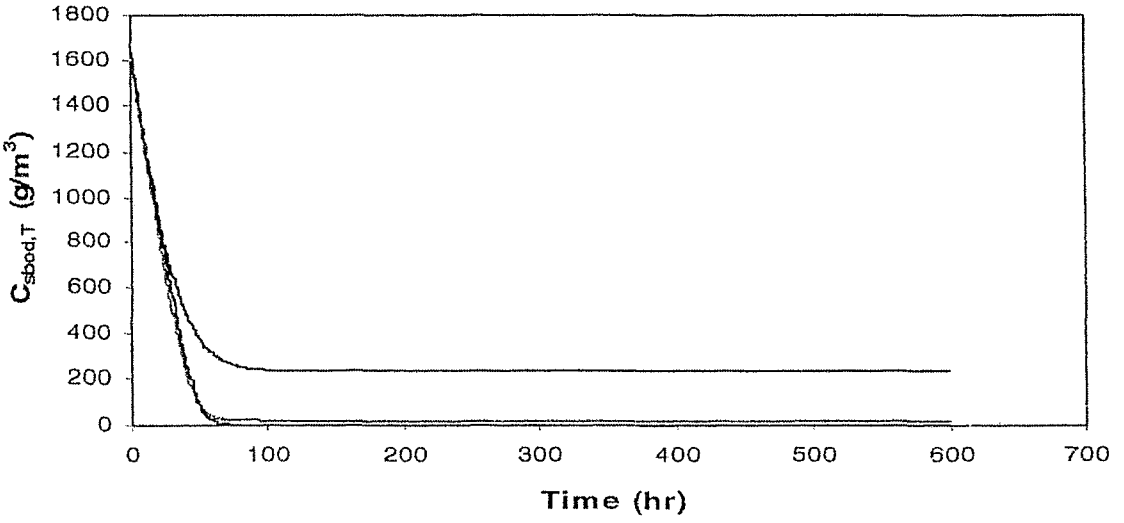

Figure 5.16 (b): Predicted $C_{O2,T}$ in a 3-stage RBC at Organic Loading = 11.1 g/m^2.d for Case II
Steady state concentration at the exit of RBC = 1.51x10^{-8} g/m^3

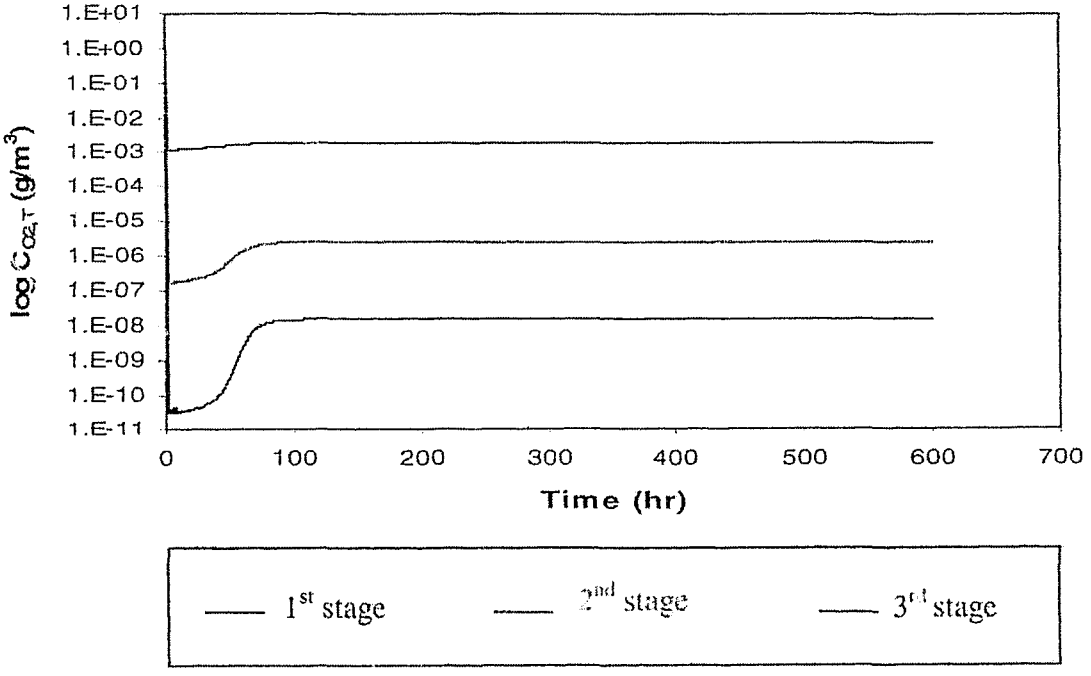

Figure 5.17 (a): Predicted $C_{sbod,T}$ in a 3-stage RBC at Organic Loading = 18.9 g/m^2.d for Case II, Paolini [37]
Steady state concentration at the exit of RBC = 14.0 g/m^3

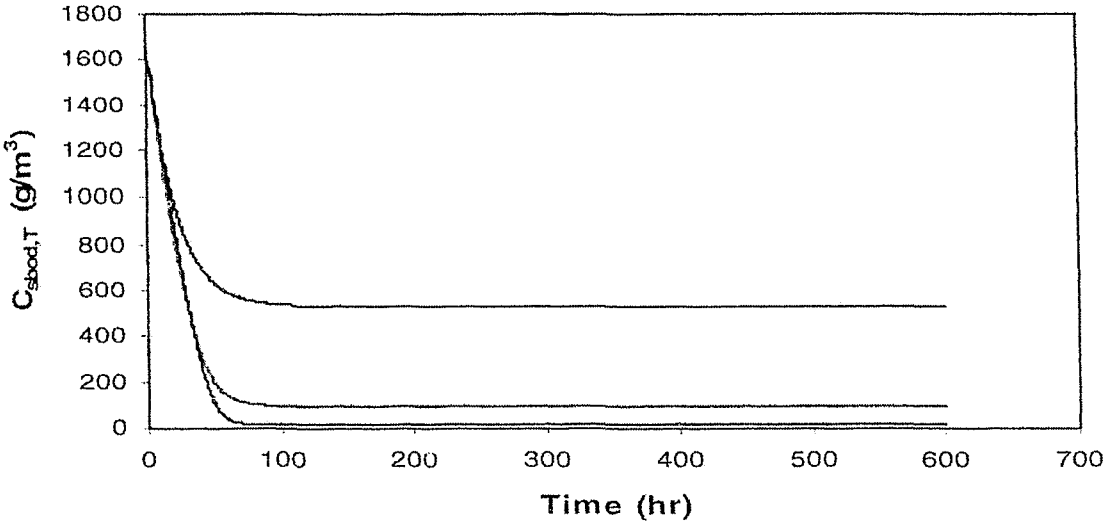

Figure 5.17 (b): Predicted $C_{O2,T}$ in a 3-stage RBC at Organic Loading = 18.9 g/m^2.d for Case II
Steady state concentration at the exit of RBC = 5.23x10^{-9} g/m^3

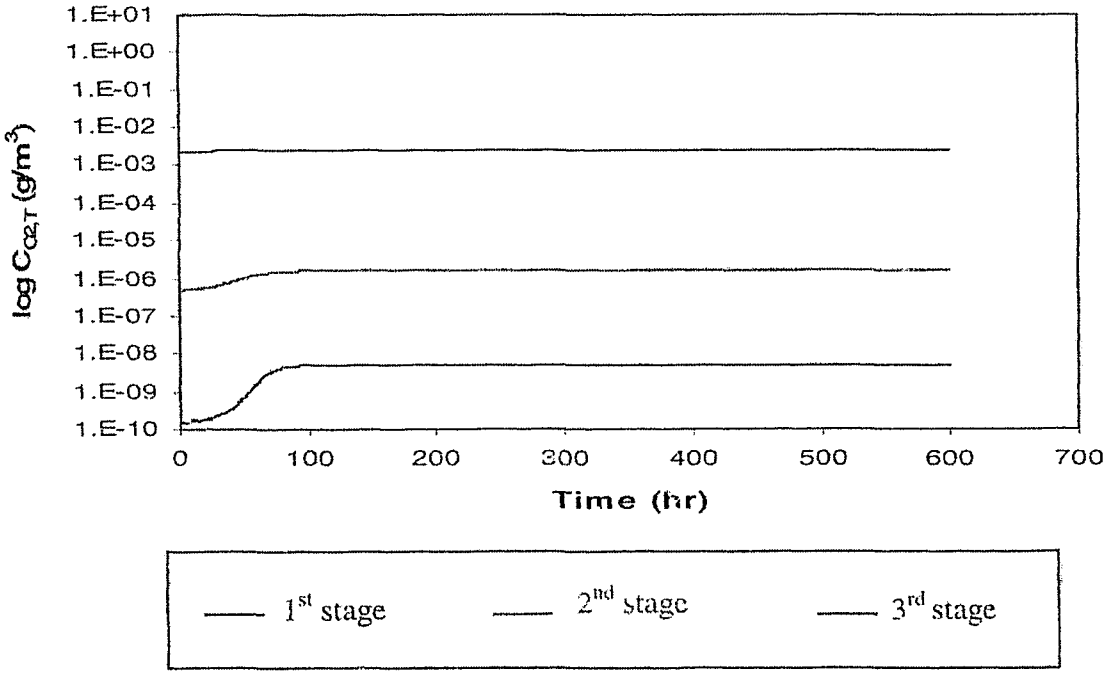

Figure 5.18 (a): Predicted $C_{sbod,T}$ in a 3-stage RBC at Organic Loading = 22.1 g/m^2.d for Case II, Paolini [37]
Steady state concentration at the exit of RBC = 20.1 g/m^3

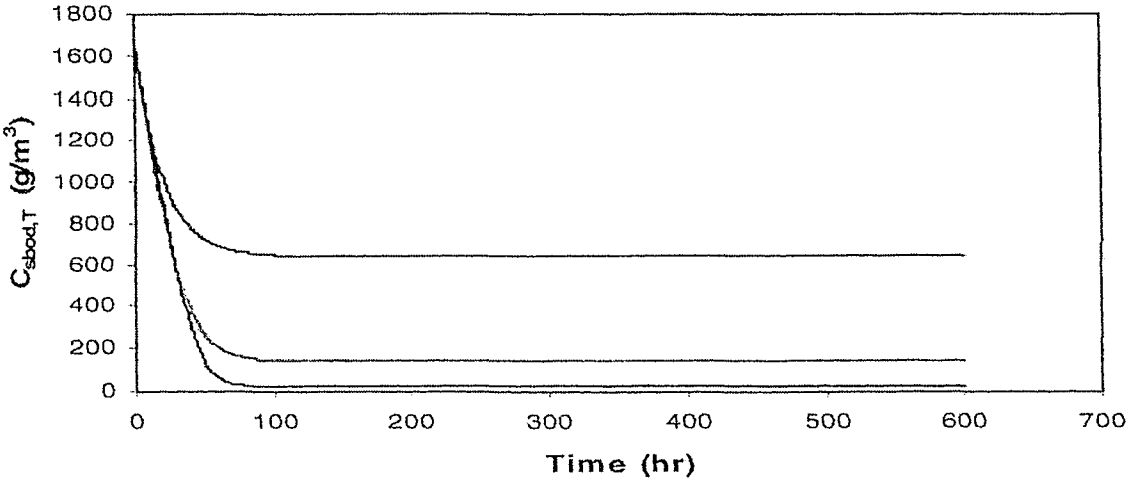

Figure 5.18 (b): Predicted $C_{O2,T}$ in a 3-stage RBC at Organic Loading = 22.1 g/m^2.d for Case II
Steady state concentration at the exit of RBC = 3.73x10^{-9} g/m^3

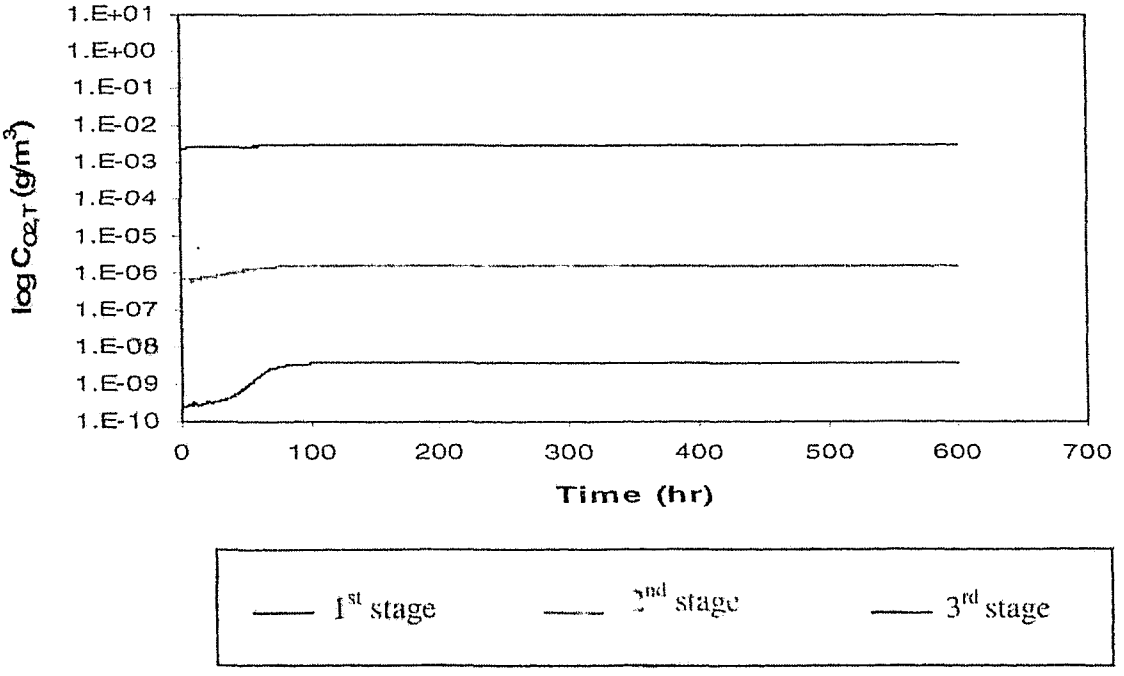

Figure 5.19 (a): Predicted $C_{sbod,T}$ in a 3-stage RBC at Organic Loading = 27.7 g/m^2.d for Case II, Paolini [37]
Steady state concentration at the exit of RBC = 63.8 g/m^3

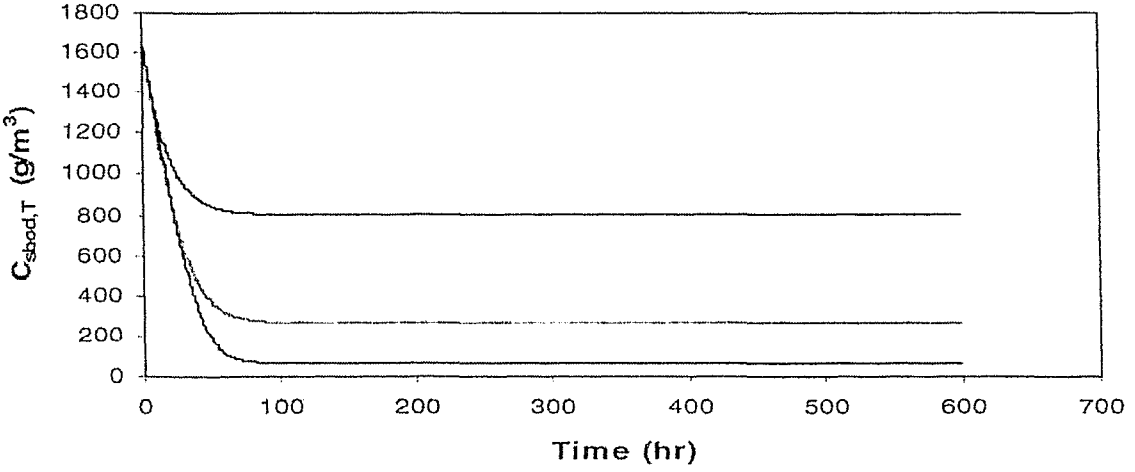

Figure 5.19 (b): Predicted $C_{O2,T}$ in a 3-stage RBC at Organic Loading = 27.7 g/m^2.d for Case II
Steady state concentration at the exit of RBC = 2.63x10^{-9} g/m^3

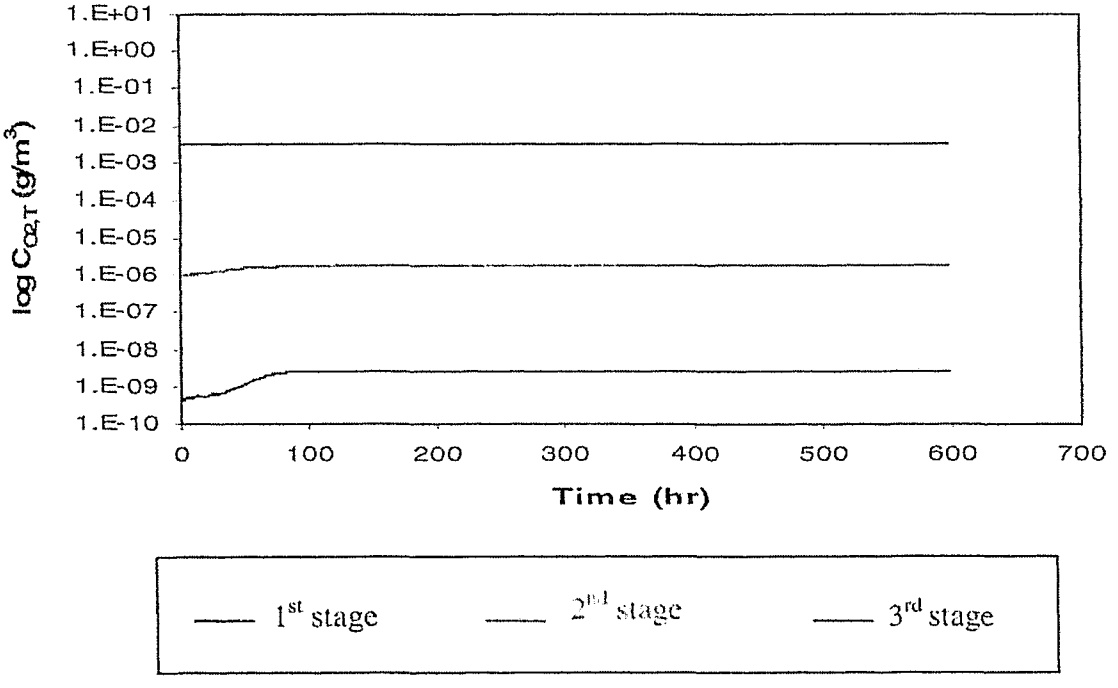

Figure 5.20 (a): Predicted $C_{sbod,T}$ in a 3-stage RBC at Organic Loading = 39.5 g/m^2.d for Case II, Paolini [37]
Steady state concentration at the exit of RBC = 234 g/m^3

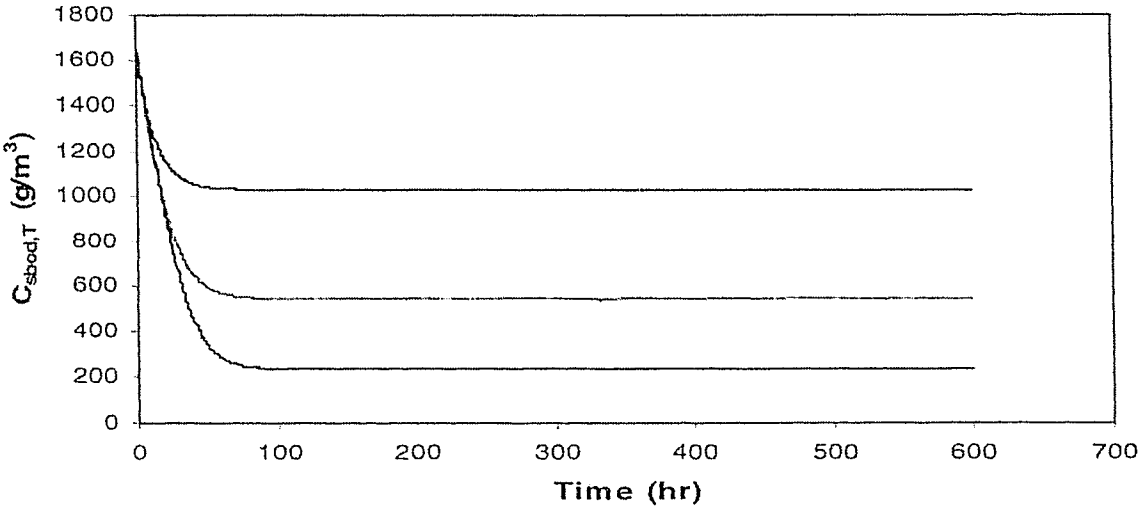

Figure 5.20 (b): Predicted $C_{O2,T}$ in a 3-stage RBC at Organic Loading = 39.5 g/m^2.d for Case II
Steady state concentration at the exit of RBC = 2.7x10^{-9} g/m^3

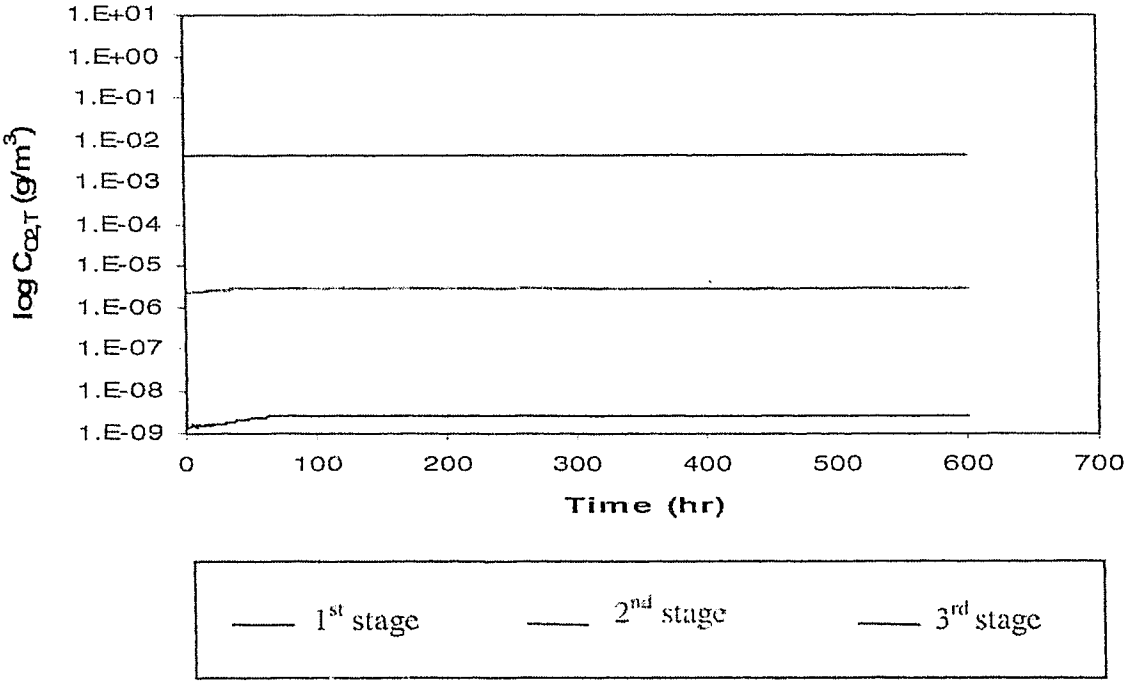

Figure 5.21: Comparison of simulated model and experimental results of a 3-stage RBC for Case II, Paolini [37]

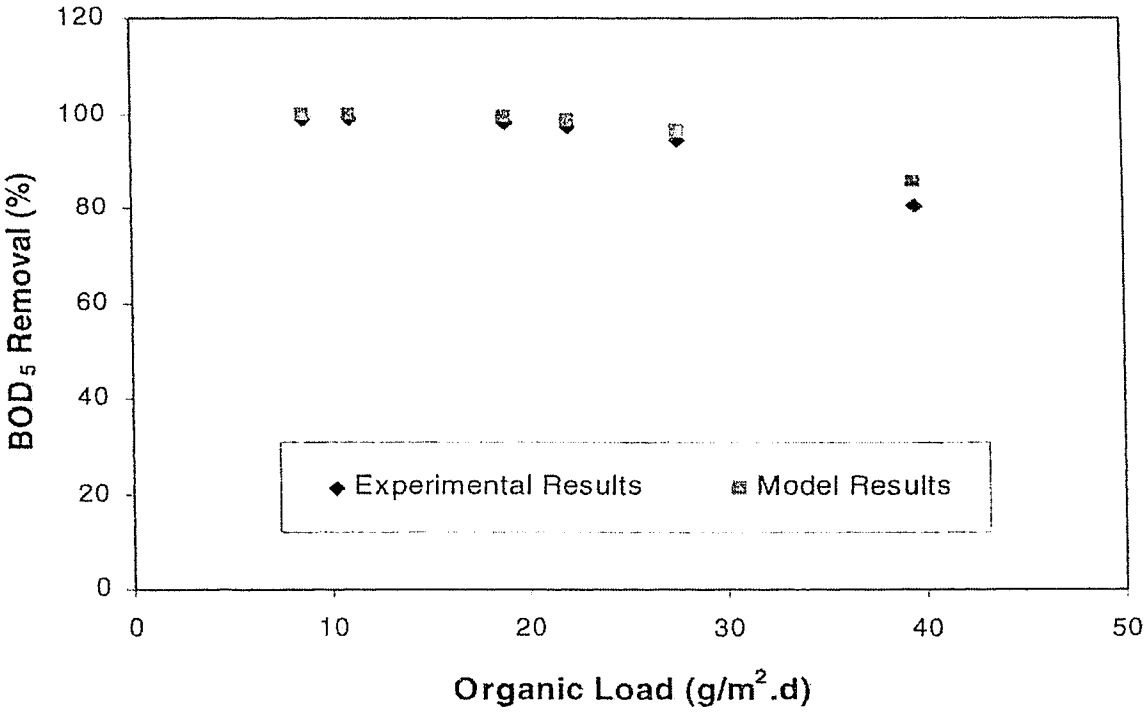

Figure 5.22 (a): Predicted $C_{sbod,\ BF}$ in a 3-stage RBC at Organic Loading = 39.5 g/m^2.d for Case II, Paolini [37]
Steady state concentration at the exit of RBC = 234 g/m^3

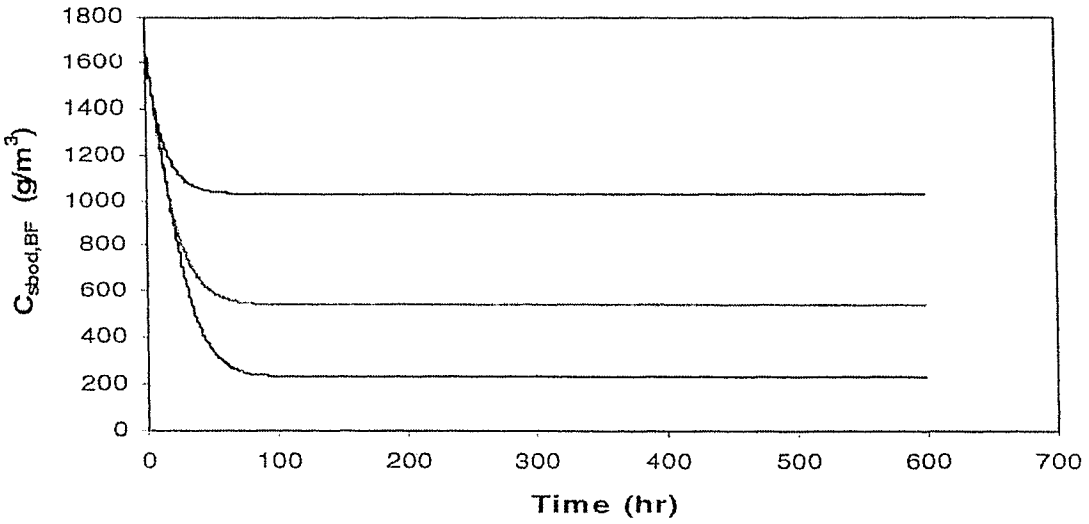

Figure 5.22 (b): Predicted $C_{O2,\ BF}$ in a 3-stage RBC at Organic Loading = 39.5 g/m^2.d for Case II

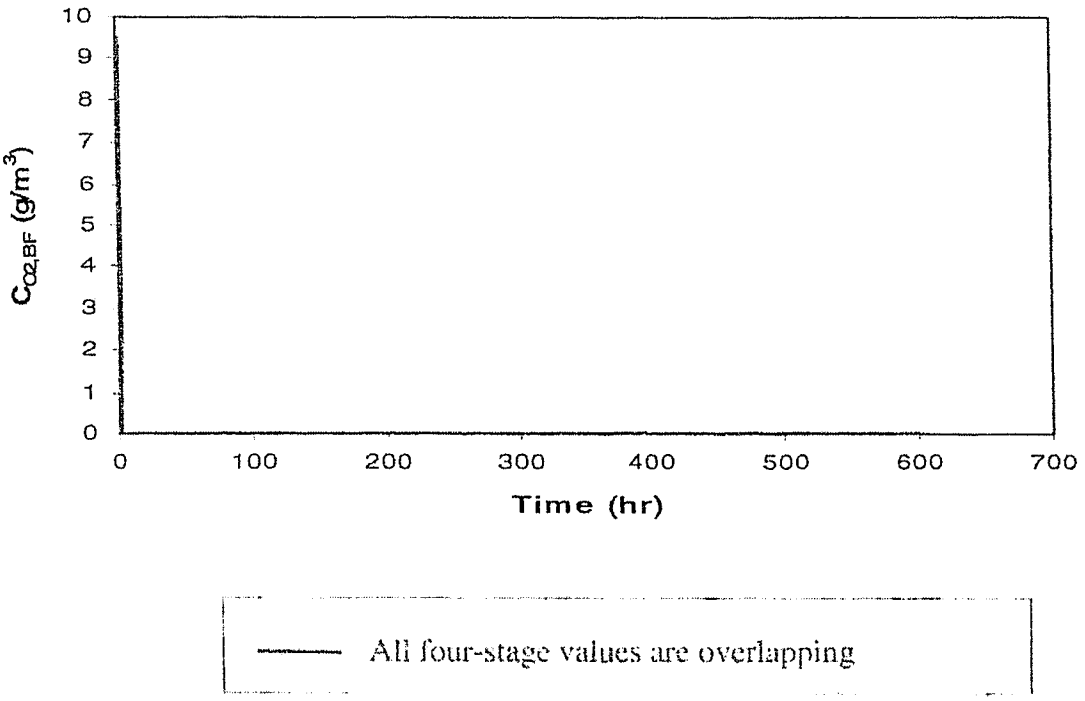

5.4.2 Effects of upsets for Case II [37]:

The simulation results of Case II [37], for the upsets in the system, show variations in the behaviour of the system. These variations incur when a change is introduced in the influent flow rate and the concentration of the soluble BOD_5 at 8.7 $g/m^2.d$ organic load. These simulation results are provided in Figures 5.23–5.26. Figure 5.26 (a) shows an increase in the concentration of the soluble substrate, in each stage, when both the influent flow rate and the concentration of soluble BOD_5 are doubled. The concentration of soluble substrate in the third stage after the second steady state achieved, is 43.9 g/m^3. This is due to the upsets in the concentration of soluble BOD_5 and the flow rate in the influent stream, when these parameters are doubled. The trend for the concentration of the oxygen in the trough provided in figure 5.26 (b) shows a sharp increase in the oxygen consumption, when both the concentration of the soluble BOD_5 and the flow rate are doubled, and the three stage treating system achieves steady state in 10–40 hours.

The rise time for the Case II [37] upsets is calculated to find the time, which the three stage treating system takes to reach the steady state after the upset is occurred. In this case, it is observed that the system takes 89 hours to reach the steady state when the flow rate is doubled, and it takes 136 hours when the concentration of soluble BOD_5 is doubled in the influent stream to the RBC. The rise time is 223 hours when the flow rate is increased one and a half times and concentration of soluble BOD_5 is doubled, and 238 hours when both the flow rate and the concentration of soluble BOD_5 are doubled.

Figure 5.23 (a): Predicted $C_{sbod,T}$ in a 3-stage RBC at Organic Loading = 8.7 g/m^2.d, for Case II, Paolini [37], when the influent flow rate is doubled.
Steady state achieved after upset = 188 hours
Steady state concentration at the exit of RBC = 4.6 g/m^3

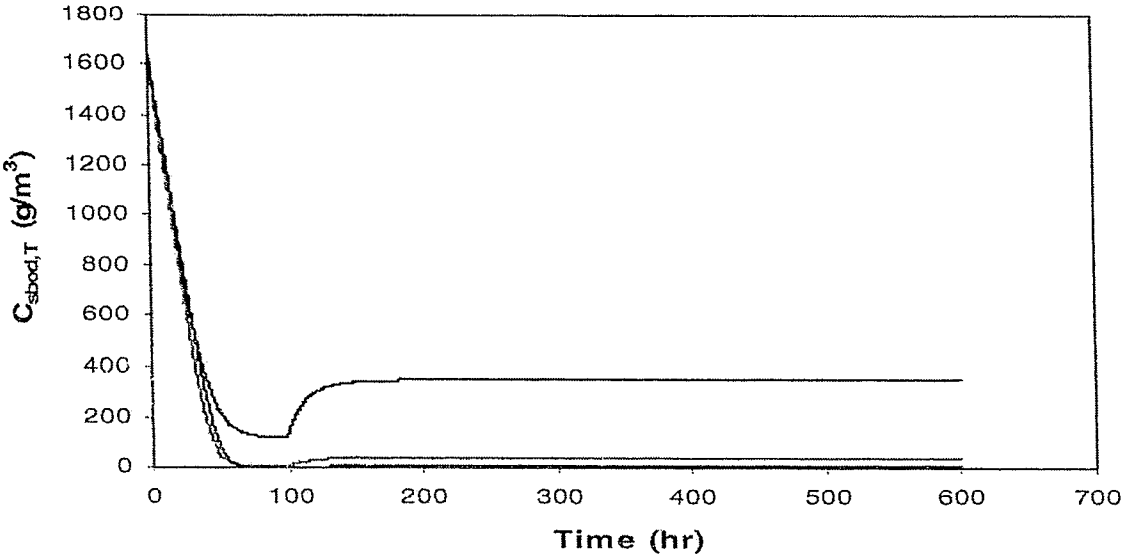

Figure 5.23 (b): Predicted $C_{O2,T}$ in a 3-stage RBC at Organic Loading = 8.7 g/m^2.d, for Case II, when the influent flow rate is doubled.
Steady state concentration at the exit of RBC = 9.96x10^{-9} g/m^3

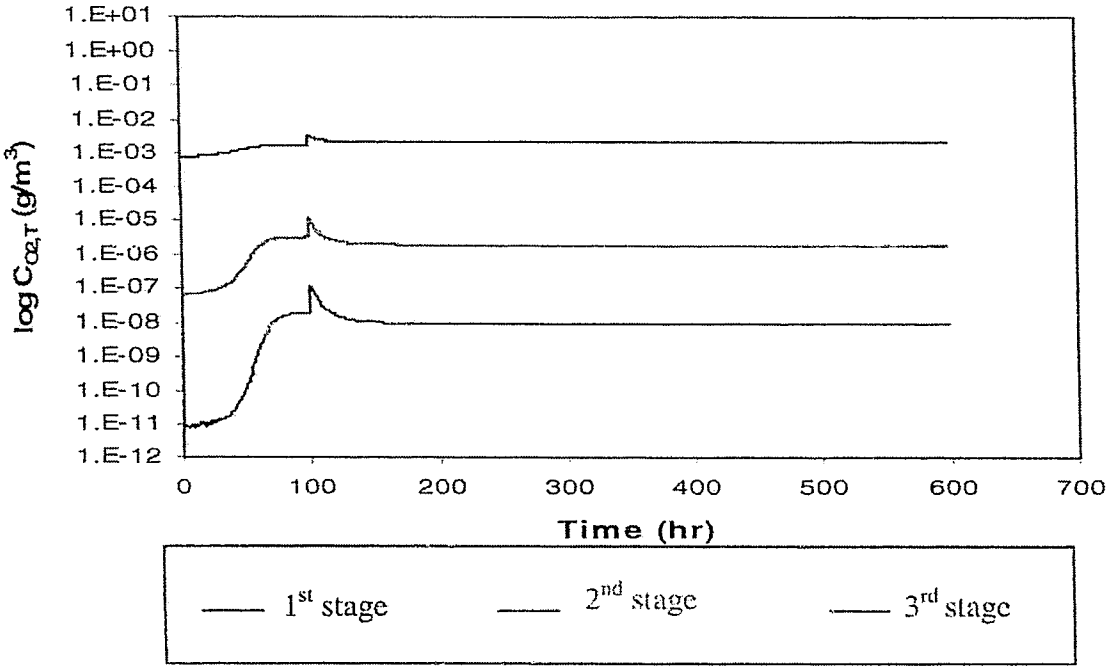

Figure 5.24 (a): Predicted $C_{sbod,T}$ in a 3-stage RBC at Organic Loading = 8.7 g/m^2.d, for Case II, Paolini [37], when the concentration of soluble BOD_5 is doubled.
Steady state achieved after upset = 235 hours
Steady state concentration at the exit of RBC = 1.58 g/m^3

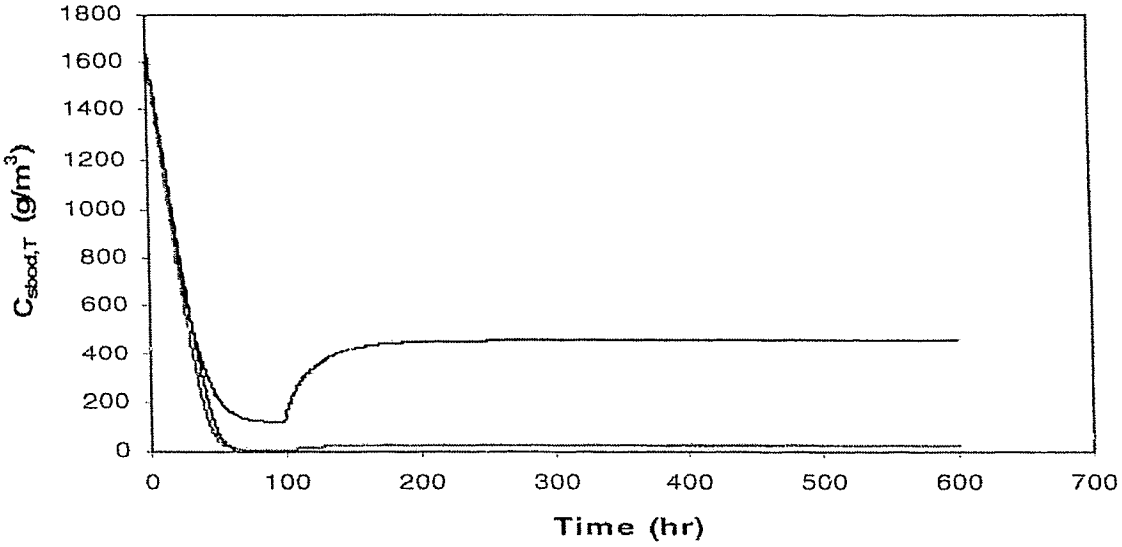

Figure 5.24 (b): Predicted $C_{O2,T}$ in a 3-stage RBC at Organic Loading = 8.7 g/m^2.d, for Case II, when the concentration of soluble BOD_5 is doubled.
Steady state concentration at the exit of RBC = 2.62x10^{-9} g/m^3

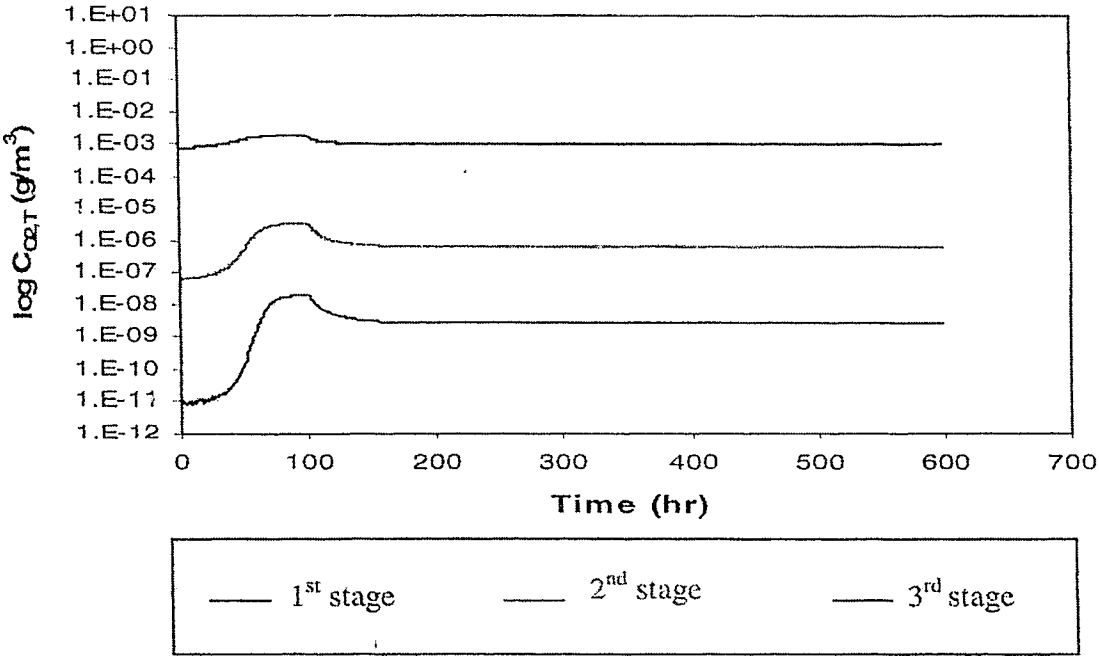

Figure 5.25 (a): Predicted $C_{sbod,T}$ in a 3-stage RBC at Organic Loading = 8.7 g/m^2.d, for Case II, Paolini[37], when the influent flow rate is increased one and half times and the concentration of the soluble BOD_5 is doubled.

Steady state achieved after upset = 322 hours

Steady state concentration at the exit of RBC = 10.4 g/m^3

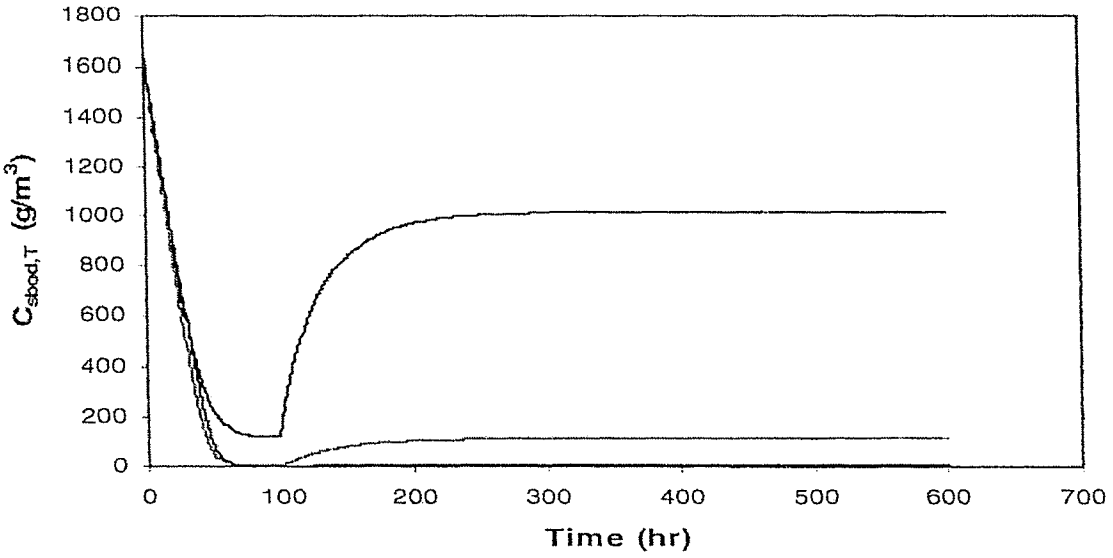

Figure 5.25 (b): Predicted $C_{O2,T}$ in a 3-stage RBC at Organic Loading = 8.7 g/m^2.d, for Case II, when the influent flow rate is increased one and half times and the concentration of the soluble BOD_5 is doubled.

Steady state concentration at the exit of RBC = 8.84x10^{-10} g/m^3

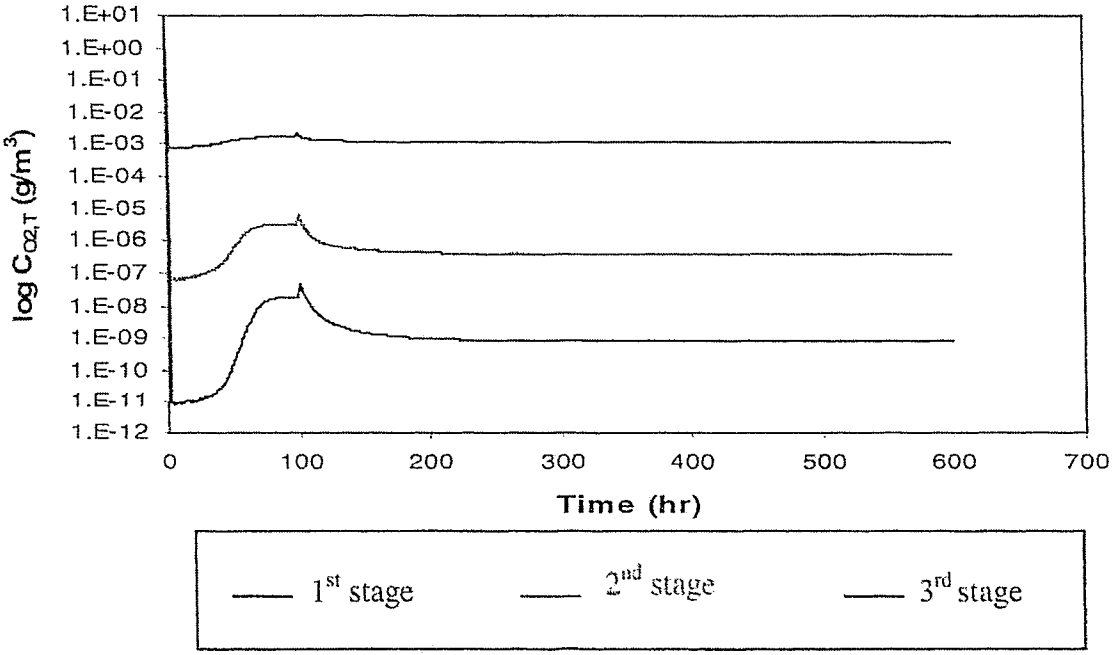

Figure 5.26 (a): Predicted $C_{sbod,T}$ in a 3-stage RBC at Organic Loading = 8.7 g/m^2.d, for Case II, Paolini [37], when both the influent flow rate and the concentration of the soluble BOD_5 is doubled.

Steady state achieved after upset = 337 hours

Steady state concentration at the exit of RBC = 44.2 g/m^3

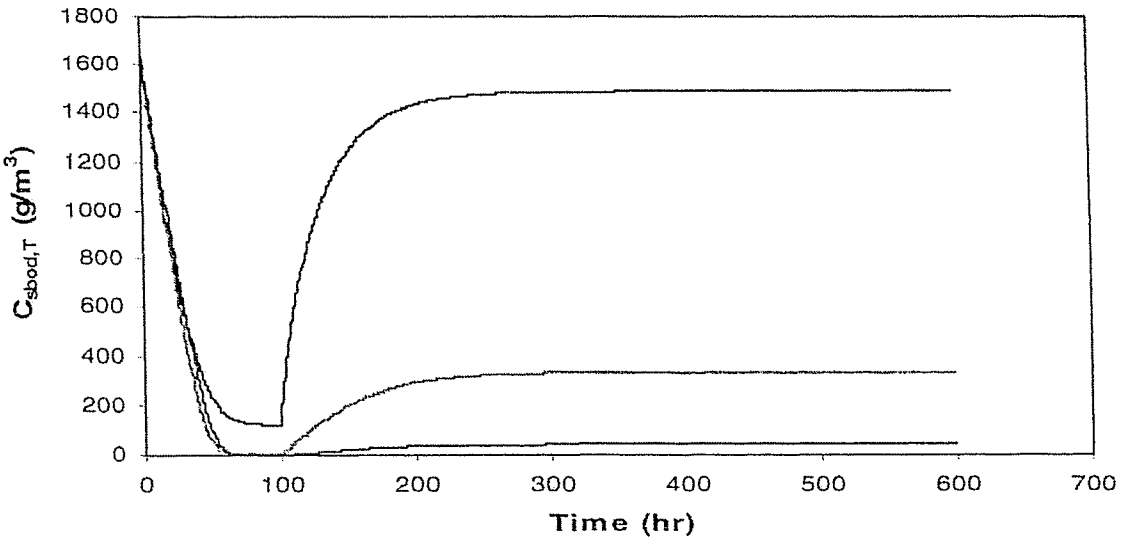

Figure 5.26 (b): Predicted $C_{O2,T}$ in a 3-stage RBC at Organic Loading = 8.7 g/m^2.d, for Case II, when both the influent flow rate and the concentration of the soluble BOD_5 is doubled.

Steady state concentration at the exit of RBC = 3.87x10^{-10} g/m^3

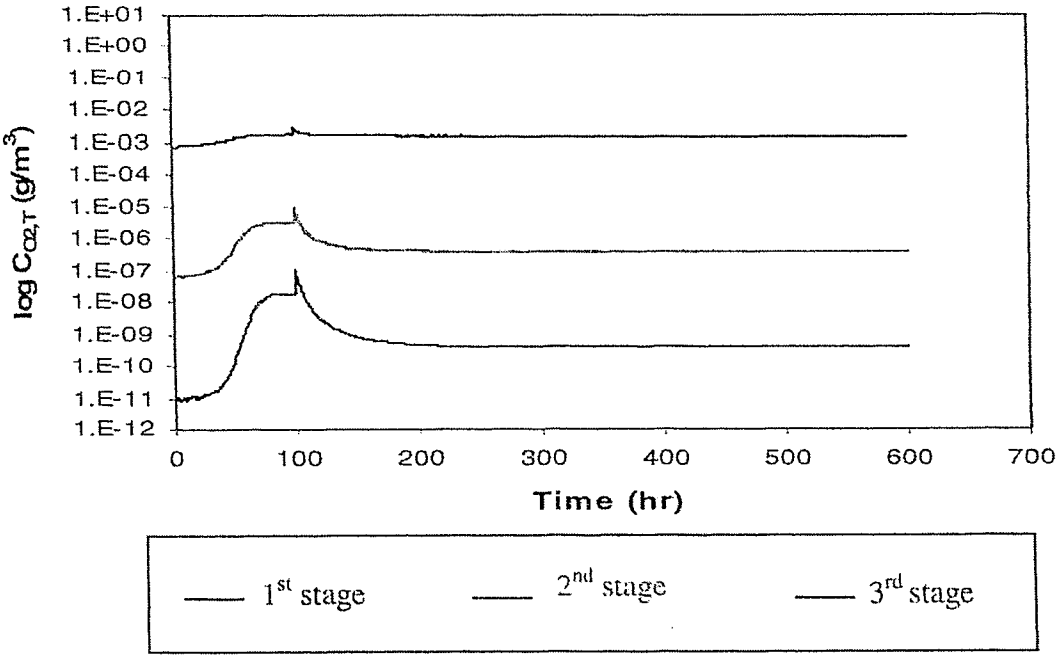

The profiles with respect to time for the consumption of the soluble BOD_5 and oxygen in the bio-film, for upsets in the system, when the influent flow is doubled at an organic load of 8.7 $g/m^2.d$, are provided in Figure 5.27. In the bio-film, the consumption of the substrate follows the same trend as that observed for the consumption of the substrate in the trough, as shown in Figure 5.23 (a). The concentration of oxygen in the bio-film is readily consumed in each stage, as shown in Figure 5.27 (b).

Figure 5.27 (a): Predicted $C_{sbod,\ BF}$ in a 3-stage RBC at Organic Loading = 8.7 g/m^2.d, for Case II, Paolini [37], when the influent flow rate is doubled.
Steady state concentration at the exit of RBC = 4.6 g/m^3

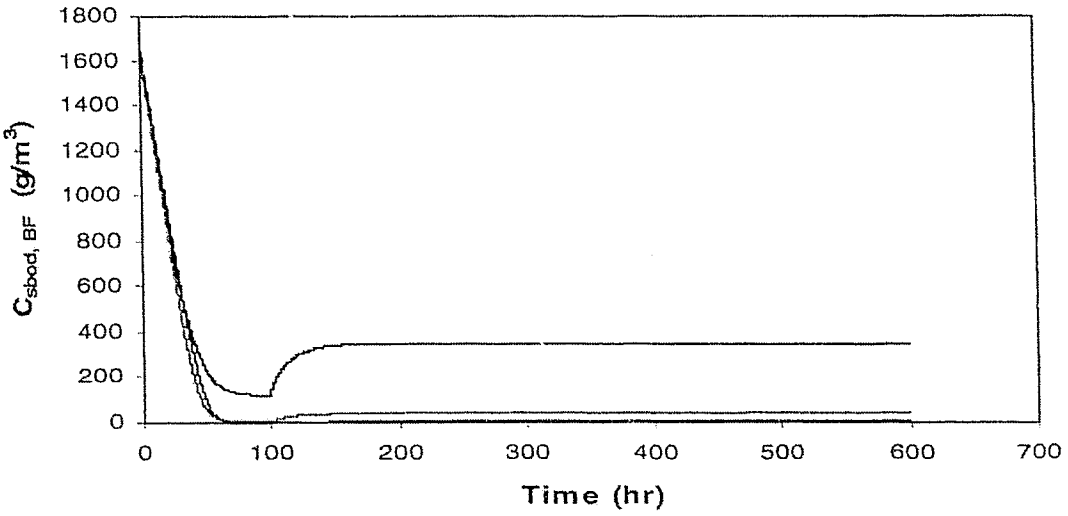

Figure 5.27 (b): Predicted $C_{O2,\ BF}$ in a 3-stage RBC at Organic Loading = 8.7 g/m^2.d, for Case II, when the influent flow rate is doubled.

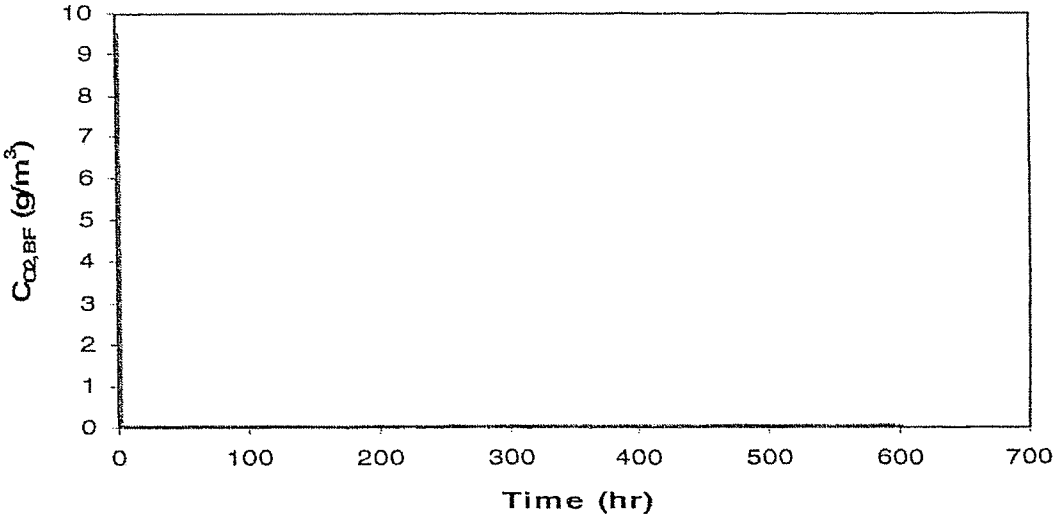

All four-stage values are overlapping

CHAPTER 6 CONCLUSION AND FUTURE WORK

6.1 Conclusion

A dynamic model to predict the concentration of soluble BOD_5 in Rotating Biological Contactor systems was simulated. The model was solved using the Runge Kutta Fehlberg adaptive step size control algorithm [43]. The results show a decrease in the concentration of soluble BOD_5 in each stage of the RBC. For Case I Alvarez-Cuenca [5], the four-stage RBC takes 35 hours to reach the steady state at an organic load of 12.7 $g/m^2.d$. For Case II Paolini [37], the three-stage RBC takes 123 hours to reach the steady state at an organic load of 11.1 $g/m^2.d$. The dynamic model results were found to be compatible with the results of two different experimental studies [5,37].

The simulated model was also applied to find the changes in behavior of the system due to variations in the upstream variables. The variables considered for both studies [5,37], were the influent flow rate, and the concentration of the soluble BOD_5 in the influent wastewater. The model simulation provides an approximation in time to achieve the steady state under conditions of upsets in the inlet flow rate, and the inlet concentration of the soluble BOD_5.

6.2 Future Work

The model has neglected the effect that rotational speed of the disk of rotating biological contactor has on the following important factors: The thickness of the liquid film carried by the disk, the rate of oxygen transfer into the liquid in the trough, the mass transfer coefficient from the liquid in the trough to the submerged bio-film, the shearing

action and its effect on sloughing, and the physical properties of the bio-film and the suspension of the solids in the trough.

The mass transfer coefficient varies considerably with the speed of rotation. Paolini et al., in their work [37], provided the relationship between mass transfer coefficient and the rotational speed as follows.

$$K_L = 0.012n + 0.016 \qquad (12)$$

In this equation, K_L is the substrate transfer coefficient into the liquid film (m/hr) and n is the rotational speed of the disk (rev/hr).

Applying this relationship into the simulated model for the lab scale RBC unit [37], the behavior of the treating unit can be examined for the consumption of the substrate, as the number of revolutions of the disk varies.

The dynamic model can also be extended to find the substrate consumption in the bio-film by considering the consumption of soluble substrate along axial and tangential directions of the bio-film attached to the disk of a rotating biological contactor.

References

1. http://www.ecotechnos.com [05-02-2004]
2. Tchobanoglous G., Burton F.L., Stensel H.D., 2003. *Wastewater Engineering, Treatment and Reuse.* 4th ed., Metcalf & Eddy Inc., Dubuque, IA: McGraw-Hill.
3. Alvarez-Cuenca, M., Smith, T, and Coelho, V.A. 1993. Rotating Biological Contactors: The Canadian Experience. *Third international conference on Waste Management in the Chemical and Petrochemical Industries, New Technologies and Practices for Waste Minimization.* Salvador, Bahia, Brazil. October 20-23.
4. WEF 2000. *Aerobic Fixed Growth Reactors, a special Edition by Aerobic Fixed Growth Reactors Task force of the WEF under the direction of Municipal subcommittee of the technical practice committee.* Alexandria, VA.
5. Alvarez-Cuenca, M., 1996. Nitrification-Denitrification Studies in Rotating Biological Contactors (RBC). Report submitted to the Ontario Ministry of the Environment and Energy. (Program ET 340). Ryerson University, Toronto.
6. Tchobanoglous G., 1991. *Wastewater Engineering, treatment, disposal, and reuse.* Metcalf & Eddy Inc., New York, McGraw-Hill.
7. Arvin, E., and Harremoes, P., 1990. Concepts and Models for Bio-film Performance. *"Water Sci. Technol."*, 22, 171.
8. Sawyer, C.N., 1973. Nitrification and Denitrification Facilities, Wastewater Treatment, U.S.EPA Technol. Transfer, Cincinnati, Ohio.
9. Brenner, R.C., 1984. Design Information on Rotating Biological Contactors. EPA-600/2-84-106, U.S. EPA, Cincinnati, Ohio.

10. Scheible, O.K., and Novak, J.J., 1980. Upgrading Primary Tanks with Rotating Biological Contactors. *Proc. 1st Natl. Symp. Rotating Biol. Contactor Technol., Vol. II, EPA-600/9-80-046b,* Champion, Pa.

11. Chou, C.C., 1978. Oxygen Transfer Capacity of Clean Media Pilot Reactors at South Shore. Autrotrol Corp. memorandum, Milwaukee, Wis.

12. Reh, C.W., 1977. An Approach to Design of RBCs for Treatment of Municipal Wastewater. *Paper presented at Am. Soc. Civ. Eng. Natl. Environ. Eng. Conf.,* Nashville, Tenn.

13. Weston, Inc., 1985. Review of Current RBC (Rotating Biological Contactor) Performance and Design Procedures. EPA-600/2-85-033, U.S. EPA, Water Eng. Res. Lab., Cincinnati, Ohio.

14. LYCO, Inc., 1992. Rotating Biological Surface (RBS) Wastewater Equipment. RBS Design Manual, Marlboro, N.J.

15. Palma Di, L, Merli C., Paris M., and Petrucci E., 2003. A Steady State Model for the Evaluation of Disk Rotational Speed influence on RBC Kinetic: Model Presentation. *"Bioresource Technology"*. 86: 193.

16. Harremoes, P., and Henze, M., 1995. Biofilters. In: *Wastewater Treatment (Biological and Chemical Processes).* Sperling, Berlin.

17. Williamson, K., and McCarty, P.L., 1976. Model of Substrate utilization by Bacterial Films. *"J. Water Pollution Control Federation"*, 48, 9.

18. Kornegay, B.H., and Andrews, J.F., 1968. Kinetics of Fixed film Biological Reactors. *"J. Water Pollution Control Federation"*, 40, R460.

19. Clark J.H., 1978. Performance of a Rotating Biological Co' ..' under Varying Wastewater Flow. *"J. Water Pollution Control Federation"*, 50, 896.

20. Spengel, D. B., and Dzombak, D. A., 1992. Bio-kinetic Modeling and Scale-up considerations for Rotating Biological Contactors. *"Water Environ. Res"*, 64, 223.

21. Watanabe, Y., 1985. Mathematical Modelling for Nitrification and Denitrification in Rotating Biological Contactors. *Mathematical models in Biological Wastewater Treatment. Jorgensen, S., and Gromiel, M. Elsevier, New York,* pp. 419.

22. Gujer, W., and Boller, M., 1990. A mathematical Model for Rotating Biological Contactors. *"Water Science and Technology"*, 22(1/2), 53.

23. Famularo, J. Mueller, J. A. and Mulligan, T., 1978. Application of Mass Transfer to Rotating Biological Contactors. *"J. Water Pollution Control Federation"*, 50, 653.

24. Williamson, K., and McCarty, P.L., 1976. Verification studies of the Bio-film Model for Bacterial substrate utilization. *"J. Water Pollution Control Federation"*, 48, 281.

25. Gujer, W., and Wanner, O., 1990. Modeling Mixed Population Bio-films. *In Bio-films.* W.G. Characklis and K. C. Marshall (Eds.), Wiley Interscience, New York, N.Y., 397.

26. Watanabe, Y., and Ishiguro, M., 1978. Denitrification Kinetics in a Submerged Rotating Biological Disk Unit. *"Progress Water Technology"*, 10(5/6), 187.

27. Watanabe, Y., Bravo, H., and Nishidome, K., 1982. Simulation of Nitrification and its Dynamics in a Rotating Biological Contactor. *"Water Science and Technology"*, 14, 811.

28. Antonie R. L. and Welch F. M., 1969. Preliminary results of a Novel Biological Process for treating Dairy Wastes, *Proc. 24th Purdue Ind. Waste Conf.*, pp.115.

29. Weng C.N and Molof A.H., 1974. Nitrification in the Biological Fixed film Rotating Disk System. *"J. Water Pollution Control Federation"*, 46, 1674.

30. Bintaja, H., Van Der Erve, J., and Boelhouwer, C., 1975. Oxygen Transfer in a Rotating Disk Treatment Plant. *"Water Research"*, 9, 1147.

31. MatsuoT., and Yamamoto, K., 1985. Mathematical Models for the Oxygen Transfer Processes in a Rotating Biological Contactor. *Mathematical Models in Biological Wastewater Treatment. Second Edition, Jorgensen, S., and Gromiel, M. Elsevier,* New York, pp. 357.

32. Zeevalkink, J., Kelderman, P., Visser, D., and Boelhouwer, C., 1979. Physical Mass Transfer in a Rotating Disk Gas-Liquid Contactor. *"Water Research"*, 13, pp.913.

33. Kornegay B.H., 1975. Modeling and Simulation of Fixed film Biological Reactors for Carbonaceous *Waste Treatment in Mathematical Modeling for Water Pollution Control Processes Edited by Kienath T.M. & Wanielista M. Ann arbor Science,* Ann Arbor, Mich., pp.271.

34. Grady, C.P., Daigger, G., and Lim, H., 1999. *Biological Wastewater Treatment. Second Edition, Revised and Expanded.* Marcel Dekker, New York.

35. Hansford, G., Andrews, J. Grieves, G., and Carr, D., 1978. A Steady State Model for the Rotating Biological Disk Reactor. *"Water Research"*, 12, 855.

36. Grady, C.P.L. Jr. and Lim, H.C., 1980. A Conceptual Model of RBC Performance. *Proceedings, First National Symposium/Workshop on Rotating Biological Contactor Technology,* E. D. Smith, R.D. Miller, and Y.C. Wu, eds. *University of Pittsburgh,* Pittsburgh, pp.829.

37. Paolini A.E., Sebastinani, E.and Variali, G., 1978. Development of Mathematical Models for the Treatment of an Industrial Wastewater by means of Biological Rotating Disk Reactors. *"Water Research"*, 13, pp.751.

38. Kornegay B.H. & Andrews J.F., 1969. Application of continuous culture theory to the trickling filter process. *Proc. 24th Purdue Ind. Waste Conf.,* pp.1398.

39. Grieves C.G., 1972. *Dynamic and steady state models for the rotating biological disk reactor,* Ph.D Thesis, Clemson University.

40. Kornegay B.H., 1969. *The characteristics and kinetics of fixed film biological reactors,* Ph.D Thesis, Clemson University.

41. Hoehn R.C., 1970. *The effects of thickness on the structure and metabolism of bacterial films,* Ph.D Thesis, University of Missouri, Columbia.

42. Piel K.M. and Gaudy A.F., 1971. Kinetic constants for aerobic growths of microbial populations selected with various single compounds and with municipal wastes as substrates, *"Appl. Microbiol"*, 21, 253.

43. Chapra S. C., Canale R. P., 2002. *Numerical Methods for Engineers With Software and Programming Applications.* 4th edition. Boston: McGraw-Hill.

APPENDICES

Appendix A

RUNGE KUTTA FEHLBERG METHOD:

The fourth and fifth-order algorithm for Runge-Kutta method with Cash-Carp approach is as follows:

The fourth-order Runge-Kutta method:

$$y_{i+1} = y_i + ah$$

where

h = step size

$$a = \frac{1}{6}(k_1 + 2k_2 + 2k_3 + k_4)$$

In this equation

$$k_1 = f(x_i, y_i)$$

$$k_2 = f(x_i + \frac{1}{2}h, y_i + \frac{1}{2}k_i h)$$

$$k_3 = f(x_i + \frac{1}{2}h, y_i + \frac{1}{2}k_2 h)$$

$$k_4 = f(x_i, y_i + k_3 h)$$

The fifth-order Runge-Kutta method:

$$y_{i+1} = y_i + ah$$

where:

h = Stepsize

$$a = \frac{1}{90}(7k_1 + 32k_3 + 12k_4 + 32k_5 + 7k_6)$$

In this equation

$$k_1 = f(x_i, y_i)$$

$$k_2 = f(x_i + \frac{1}{4}h, y_i + \frac{1}{4}k_1 h)$$

$$k_3 = f(x_i + \frac{1}{4}h, y_i + \frac{1}{8}k_1 h + \frac{1}{8}k_2 h)$$

$$k_4 = f(x_i + \frac{1}{2}h, y_i - \frac{1}{2}k_2 h + k_3 h)$$

$$k_5 = f(x_i + \frac{3}{4}h, y_i + \frac{3}{16}k_1 h + \frac{9}{16}k_4 h)$$

$$k_6 = f(x_i + h, y_i - \frac{3}{7}k_1 h + \frac{2}{7}k_2 h + \frac{12}{7}k_3 h - \frac{12}{7}k_4 h + \frac{8}{7}k_5 h)$$

The Cash-Carp Runge-Kutta method:

$y_{i+1} = y_i + ah$

h = Stepsize

$$a = (\frac{37}{378}k_1 + \frac{250}{621}k_3 + \frac{125}{594}k_4 + \frac{512}{1771}k_6)$$

for the 4^{th} order algorithm

and for the 5^{th} order algorithm

$$a = (\frac{2825}{27648}k_1 + \frac{18575}{48384}k_3 + \frac{13525}{55296}k_4 + \frac{277}{14336}k_5 + \frac{1}{4}k_6)$$

In this equation

$$k_1 = f(x_i, y_i)$$

$$k_2 = f(x_i + \frac{1}{5}h, y_i + \frac{1}{5}k_1 h)$$

$$k_3 = f(x_i + \frac{3}{10}h, y_i + \frac{3}{40}k_1 h + \frac{9}{40}k_2 h)$$

$$k_4 = f(x_i + \frac{3}{5}h, y_i + \frac{3}{10}k_1 h - \frac{9}{10}k_2 h + \frac{6}{5}k_3 h)$$

$$k_5 = f(x_i + \frac{3}{4}h, y_i - \frac{11}{54}k_1 h + \frac{5}{2}k_2 h - \frac{70}{27}k_3 h)$$

$$k_6 = f(x_i + \frac{7}{8}h, y_i + \frac{1631}{55296}k_1 h + \frac{175}{512}k_2 h + \frac{575}{13824}k_3 h + \frac{44275}{110592}k_4 h + \frac{253}{4096}k_5 h)$$

APPENDIX B

FORMULAE:

The following formula was used for the calculation of finding the flow rate of the influent wastewater stream at an organic loading.

Flow = (organic loading x disk surface area)/ soluble BOD

The mass transfer coefficient values for oxygen were calculated using the following formula and used in numerical algorithm for simulation.

k = Diffusivity / length of the biofilm

APPENDIX C

SENSITIVITY ANALYSIS

The sensitivity analysis was carried out by changing the values of the half saturation constant for soluble BOD and maximum specific growth rate of the attached biomass for the four-stage RBC pilot plant.

The values of the half saturation constant and maximum specific growth rate, at which the sensitivity analysis was carried out for the four-stage pilot plant, are provided below.

Value	1st stage	2nd stage	3rd stage	4th stage
K_s [19] Base Case	431	546	32	8
$\hat{\mu}$ [19] Base Case	0.18	0.16	0.08	0.0125
K_s (25% increased)	538.75	682.5	40	10
K_s (25% decreased)	323.25	409.5	24	6
$\hat{\mu}$ (25% increased)	0.225	0.2	0.1	0.015625
$\hat{\mu}$ (25% decreased)	0.135	0.12	0.06	0.009375

The results obtained from the numerical solution of differential equations by introducing these parameters, at an organic load of 12.7 g/m^2.d for case I study are provided in the following table.

Values of K_s and $\hat{\mu}$	Steady-state Conc of $sBOD_5$ at 1st stage (g/m^3)	Steady-state Conc of $sBOD_5$ at 2nd stage (g/m^3)	Steady-state Conc of $sBOD_5$ at 3rd stage (g/m^3)	Steady-state Conc of $sBOD_5$ at 4th stage (g/m^3)
[19] Base Case	124	73.5	8.41	2.19
K_s (25% increased)	141	90.8	13.2	4.4
K_s (25% decreased)	109	56.9	4.8	0.9
$\hat{\mu}$ (25% increased)	109	57.8	5.0	1.0
$\hat{\mu}$ (25% decreased)	144	95.7	16.4	6.5

Similarly for the three-stage lab scale RBC unit, the results obtained from the numerical solution of differential equations by introducing the different values of the parameters for half saturation constant and maximum specific growth rate, at an organic load of 11.1 $g/m^2.d$ are provided in the following table.

Values of K_s and $\hat{\mu}$	Steady-state Conc of $sBOD_5$ at 1st stage (g/m^3)	Steady-state Conc of $sBOD_5$ at 2nd stage (g/m^3)	Steady-state Conc of $sBOD_5$ at 3rd stage (g/m^3)
[37] Base Case	236	20.1	1.82
K_s (25% increased)	281	30.2	3.16
K_s (25% decreased)	187	0.80	0.80
$\hat{\mu}$ (25% increased)	180	0.85	0.85
$\hat{\mu}$ (25% decreased)	337	40.2	4.5

It is observed that the concentration of soluble BOD increases by increasing the value of Ks in each stage from the results of concentration of soluble BOD at referenced values [19], and decreases by decreasing the value of Ks. Whereas the concentration of soluble BOD decreases by increasing the value of maximum specific growth rate, in each stage, and increases by decreasing the value of maximum specific growth rate. Also, the results of concentration of soluble BOD, by changing the two parameters of half saturation constant and maximum specific growth rate, do not deviate much, in each stage.